Modulation of A-type potassium channels by stress mediators

Thesis

in partial fulfillment of the requirements for the degree of Doctor of Philosophy (Ph.D.)

submitted to the Council of the Faculty of Medicine at Friedrich Schiller University of Jena

by M.Sc. Kefan Yang
born on 26.12.1990 in Hubei, China

Modulation von A-Typ-Kaliumkanälen durch Stressmediatoren

Dissertation

zur Erlangung des akademischen Grades
Doctor of Philosophy (Ph.D.)

vorgelegt dem Rat der Medizinischen Fakultät
der Friedrich-Schiller-Universität Jena

von M.Sc. Kefan Yang
geboren am 26.12.1990 in Hubei, China

Gutachter/Reviewers:

1. Prof. Dr. Stefan H. Heinemann

   Center for Molecular Biomedicine, Department of Biophysics, Friedrich Schiller University Jena and Jena University Hospital, Jena

2. apl. Prof. Dr. Thomas Zimmer

   Institute of Physiology II, Jena University Hospital, Jena

3. Prof. Dr. Niels Decher

   Institute for Physiology and Pathophysiology, Vegetative Physiology, Philipps University of Marburg, Marburg

Tag der öffentlichen Verteidigung/Date of the public disputation: 15.09.2020

Contents

List of abbreviations

°C	– Celsius degree
3MP	– 3-mercaptopyruvate
3MST	– 3-mercaptopyruvate sulfurtransferase
4-CY	– 4-cyanobenzaldehyde
AD	– Alzheimer's disease
AP	– Action potential
ARK	– Aldo-Keto reductase
ATP	– Adenosine triphosphate
BDNF	– Brain-derived neurotrophic factor
BK_{Ca}	– Big-conductance Ca^{2+}-sensitive K^+ channel
C terminus	– COOH terminus, carboxyl-terminus
C/Cys	– Cysteine
CA1	– *Cornu ammonus* 1
Ca^{2+}	– Calcium ion
$CaCl_2$	– Calcium chloride
CARS	– Cysteinyl-tRNA synthetase
CAT	– Cysteine aminotransferase
CBS	– Cystathionine β-synthase
CD8	– Cluster of differentiation 8
Cl^-	– Chloride ion
CMV	– Cytomegalovirus promoter
CNS	– Central nervous system

CO – Carbon monoxide

CSE – Cystathionine γ-lyase

Ctrl – Control

DAO – D-amino acid oxidase

Diamide – 1,1'-azobis[N,N-dimethylformamide]

DMEM – Dulbecco's modified Eagle's medium

DNA – Deoxyribonucleic acid

DPPLs – Dipeptidyl aminopeptidase-like proteins

DRG – Dorsal root ganglion

DTNP – 2,2'-dithiobis[5-nitropyridine]

DTT – 1,4-dithiothreitol

E. coli – *Escherichia coli*

EDTA – Ethylenediaminetetraacetic acid

EGTA – Ethylene glycol-bis[2-aminoethylether]-N,N,N',N'-tetraacetic acid

FCS – Fetal calf serum

GSH – Reduced glutathione

GYY4137 – Morpholin-4-ium 4-methoxyphenyl(morpholino) phosphinodithioate

H_2O_2 – Hydrogen peroxide

H_2S – Hydrogen sulfide

H_2S_n – Hydrogen polysulfides

HEK293T – Human embryonic kidney 293T cell

HEPES – 4-[2-hydroxyethyl]-1-piperazineethanesulfonic acid

HO – Heme oxygenase

IAM – Iodoacetamide

K^+ – Potassium ion

K_{ATP} – ATP-sensitive potassium channel

KChIPs – Potassium channel interacting proteins

KCl – Potassium chloride

kDa – Kilodalton

kHz – Kilohertz

Kv – Voltage-gated potassium channel

LTP – Long-term potentiation

MBP – Maltose-binding protein

Mg-ATP – Magnesium ATP

$MgCl_2$ – Magnesium chloride

mM – Millimolar

ms – Millisecond

mV – Millivolt

MΩ – Megaohm

N terminus – NH_2 terminus, amino-terminus

nA – Nanoampere

Na^+ – Sodium ion

Na_2S_n – Sodium polysulfides

NaCl – Sodium chloride

$NADP^+$ – Nicotinamide adenine dinucleotide phosphate

NADPH – Reduced form of $NADP^+$

NaHS – Sodium hydrogen sulfide

nm – Nanometer

nM – Nanomolar

NMG – N-methyl-D-glucamine

NO – Nitric oxide

O_2 – Oxygen

PBS – Phosphate-buffered saline

PCR – Polymerase chain reaction

PIP_2 – Phosphatidylinositol 4,5-bisphosphate

PTEN – Phosphatase and tensin homolog

Rho – Rhodanese

RNA – Ribonucleic acid

RNS – Reactive nitrogen species

roGFP2 – Reduction-oxidation sensitive green fluorescent protein 2

ROS – Reactive oxygen species

RSS – Reactive sulfur species

S/Ser – Serine

SEM – Standard error of the mean

SOD – Superoxide dismutase

T1 – Tetramerization domain

TEV – Tobacco etch virus

TM – Transmembrane segment

TRPA1 – Transient receptor potential ankyrin 1 channel

TY – Tryptone yeast

WT – Wild type

μM – Micromolar

τ_{inact} – Time constant of inactivation

Summary

A-type voltage-gated potassium (Kv) channels open on membrane depolarization and undergo subsequent rapid inactivation with importance in fine-tuning of cellular excitability. To serve diverse cellular needs, the inactivation is regulated by numerous mechanisms; for example, cysteine residues in the N-terminal inactivation ball domain make the inactivation susceptible to redox state changes. Hydrogen sulfide (H_2S), which is enzymatically generated in various tissues, is increasingly recognized as an important signaling molecule, particularly in the cardiovascular and nervous systems. In aqueous solutions, H_2S is in equilibrium with more oxidized sulfur species, e.g., polysulfides, and these sulfur-containing compounds are often collectively termed reactive sulfur species (RSS). Various roles of RSS have been identified, such as regulation of neuronal excitability, but often the mechanisms are not well understood.

In this work, the H_2S donor NaHS and the polysulfide donors Na_2S_n were used to study whether and how A-type Kv channels might be regulated by RSS. Using the patch-clamp method, we found that Na_2S_n broaden single action potentials in murine dorsal root ganglion neurons and slow the inactivation of their natively expressed A-type Kv channels (e.g., Kv1.4, Kv3.4). Therefore, we studied the functional properties of recombinant Kv1.4 and Kv3.4 and mutants thereof upon heterologous expression in HEK293T cells. Polysulfides (Na_2S_n) were $>$ 1000 times more effective than NaHS in slowing down inactivation with the potency increasing with the number of sulfur atoms ($Na_2S_2 < Na_2S_3 < Na_2S_4$), indicating that spontaneously formed Na_2S_n in NaHS solutions were the active components. A cysteine residue at position 13 (C13) in the ball domain of Kv1.4, and C6, C24 in that of Kv3.4 mediated the slowing of inactivation by RSS. Mass spectrometry analysis of a recombinantly produced peptide corresponding to the ball domain of Kv1.4 revealed that RSS sulfhydrate the peptide at position C13.

A-type Kv channels can also be formed by association of non-inactivating Kvα subunits with cytoplasmic ancillary Kvβ subunits that provide inactivation ball domains and thus induce N(β)-type inactivation. N(β)-type inactivation conferred by Kvβ1.1 (C7), Kvβ1.2 (C8, C28) and Kvβ3.1 (C7, C22), containing one or two cysteine residues, was sensitive to RSS because of the named cysteine residues. Kvβ1.3, lacking a cysteine in the ball

domain, was unaffected by RSS. Interestingly, the inactivation of Kv1.1/Kvβ1.1 remained sensitive to RSS even with Kvβ1.1-C7S. A mutagenesis study revealed that C35 and C36 in the N terminus of Kv1.1 render the inactivation of the Kv1.1/Kvβ1.1 complex sensitive to RSS. Although we could not elucidate the underlying molecular mechanism, this α-subunit dependence seems specific to sulfhydration because for other cysteine-specific modifiers this phenomenon was not observed.

We furthermore showed that intracellular heme slows down inactivation of Kv3.4 and inactivation induced by Kvβ1.1, involving residues C6:C24 and C7:H10, respectively, i.e. cysteines that are also relevant for the impact of RSS. We have to postulate that there is abundant crosstalk between redox/RSS and heme/carbon monoxide signaling, and that these factors contribute to the modulation of neurotransmitter release and excitotoxicity, at least partially by means of regulating the speed and degree of A-type Kv channel inactivation.

Zusammenfassung

Spannungsgesteuerte K^+-Kanäle (Kv) vom A-Typ werden durch Membrandepolarisation geöffnet und inaktivieren danach wieder schnell, wodurch sie zur Feinregulierung der zellulären Erregbarkeit geeignet sind. Um dies unter variablen zellulären Bedingungen bewerkstelligen zu können, ist der Prozess der Inaktivierung durch zahlreiche Mechanismen reguliert. Beispielsweise wird die sogenannte N-Typ-Inaktivierung sensitiv für Änderungen im Redoxzustand durch Cysteine im N-terminalen Proteinbereich. Schwefelwasserstoff (H_2S), welcher in unterschiedlichen Geweben enzymatisch hergestellt wird, ist mittlerweile als wichtiges Signalmolekül erkannt, welches besonders im kardiovaskulären und neuronalen System von Bedeutung ist. In wässrigen Lösungen ist H_2S mit oxidierten Schwefel-Spezies, wie beispielsweise Polysulfiden, im Gleichgewicht. Diese schwefelhaltigen Verbindungen werden oft zusammenfassend als Reaktive Schwefelspezies (RSS) bezeichnet. Obwohl bekannt ist, dass RSS unterschiedliche physiologische Rollen haben, z. B. bei der Regulation der neuronalen Erregbarkeit, sind die zugrundeliegenden Mechanismen oft unverstanden.

In dieser Arbeit wurde untersucht, ob und wie die Donoren für H_2S (NaHS) und für Polysulfide (Na_2S_n) Kv-Kanäle vom A-Typ beeinflussen. Unter Anwendung der Patch-Clamp-Methode fanden wir, dass Na_2S_n einzelne Aktionspotentiale in Neuronen von Hinterwurzelganglien der Maus verbreitern und die Inaktivierung von nativ exprimierten A-Typ-Kanälen (z. B., Kv1.4, Kv3.4) verlangsamen. Daher untersuchten wir die funktionellen Eigenschaften von rekombinanten Kv1.4 und Kv3.4 und Mutanten davon nach heterologer Expression in HEK293T-Zellen. Polysulfide (Na_2S_n) verlangsamten die Inaktivierung der Kanäle $>$ 1000-mal effektiver als NaHS, wobei die Effektivität mit der Anzahl der Schwefelatome zunahm ($Na_2S_2 < Na_2S_3 < Na_2S_4$); dies deutet darauf hin, dass Na_2S_n die eigentlich aktiven Komponenten in aus NaHS hergestellten wässrigen Lösungen sind. Cysteinreste an der Position 13 (C13) in der Balldomäne von Kv1.4 und C6 und C24 in der von Kv3.4 waren für den Einfluss von RSS auf die Inaktivierungsgeschwindigkeit verantwortlich. Massenspektrometische Analysen von rekombinantem Protein der entsprechenden Balldomäne aus Kv1.4 ergaben, dass das Peptid durch RSS an Position C13 sulfhydriert wird.

A-Typ-Kanäle können auch durch die Assoziation von nicht-inaktivierenden Kvα-Unter-

einheiten mit zytoplasmatischen Kvβ-Untereinheiten mit N-terminaler Balldomäne entstehen. Diese N(β)-Typ-Inaktivierung, war auch sensitiv gegenüber RSS, wenn deren Balldomänen Cysteine enthielten: Kvβ1.1 (C7), Kvβ1.2 (C8, C28), Kvβ3.1 (C7, C22). Die Inaktivierung durch Kvβ1.3, welches kein Cystein in der Balldomäne vorweist, wurde durch RSS nicht verändert. Interessanterweise blieb die Inaktivierung des Kv1.1/Kvβ1.1-Komplex sensitiv gegenüber RSS, selbst wenn das kritische Cystein in Kvβ1.1 entfernt war (C7S). Ein umfangreicher Mutageneseansatz zeigte, dass C35/C36 im N-Terminus der α-Untereinheit Kv1.1 die RSS-Sensitivität des Kv1.1/Kvβ1.1-Komplexes bewirkt. Obwohl der Mechanismus nicht aufgeklärt werden konnte, scheint diese Abhängigkeit von der α-Untereinheit für Sulfhydrierung spezifisch zu sein, denn ein ähnliches Phänomen wurde mit anderen Cystein-spezifischen Agenzien nicht gefunden.

Wir zeigten außerdem, dass intrazelläres Häm, ähnlich wie für Kv1.4 die Inaktivierung von sowohl Kv3.4 als N(β)-Inaktivierung durch Kvβ1.1 verlangsamt, wobei die Reste C6:C24 bzw. C7:H10 beteiligt waren, also dieselben Cysteine, die auch für die Wirkung von RSS wichtig sind. Wir müssen also von einer komplexen gegenseitigen Beeinflussung der Stress-Signalachsen „Redox/RSS“ und „Häm/Kohlenstoffmonoxid“ ausgehen. Zusammen können diese Faktoren zur Modulation der Neurotransmitterfreisetzung bzw. der Erregungstoxizität mittels der Modulation der Geschwindigkeit und des Ausmaßes der Inaktivierung von A-Typ-Kaliumkanälen beitragen.

1 Introduction

1.1 Ion channels

Ion channels are membrane-spanning pore-forming proteins that connect the cytosol to the cell exterior. These proteins allow inorganic ions to diffuse rapidly across the plasma membrane down their electrochemical gradients at rates up to 100 million ions per second when the ion-conducting pore is open (Aidley and Stanfield, 1996). A wide range of biological processes are controlled by the ion fluxes through various ion channels, for example electrical excitability in muscle cells, electrical signaling in neuronal and cardiac cells, hormone secretion, cell proliferation and migration, cell volume regulation (Aidley and Stanfield, 1996; Hille, 2001; Szabo et al., 2010; Ashcroft and Rorsman, 2013; Comes et al., 2015; Jeevaratnam et al., 2018).

1.1.1 Voltage-gated potassium (Kv) channels

Ion channels can be categorized according to their ionic selectivity, such as potassium (K^+), sodium (Na^+), calcium (Ca^{2+}), and chloride (Cl^-) channels (Yu and Catterall, 2004). Among the ion channel groups thus far identified, the group of K^+ channels represents the most diverse one (Rudy, 1988; Pongs, 1992; Coetzee et al., 1999; Yu and Catterall, 2004). Based on the mode of activation, the number of transmembrane (TM) segments and ion conducting pore(s) of K^+ channels, they can be divided into four structural types: inwardly rectifying 1-pore 2-TM (K_{ir}), 2-pore 4-TM (K_{2P}), Ca^{2+}-activated 6-TM or 7-TM, and voltage-gated 1-pore 6-TM (Kv) (Shieh et al., 2000; Wulff et al., 2009).

1.1.1.1 Kv channel physiological functions

Kv channels are broadly distributed in the nervous system and other tissues, their open probabilities are dependent on the membrane potential, i.e., such channels are typically

closed at resting potentials (–90 mV to –70 mV) and they open when the membrane depolarizes (Sahoo et al., 2014). The opening of Kv channels results in an efflux of K^+, which can serve to repolarize or even hyperpolarize the membrane (Wulff et al., 2009). Therefore, in excitable cells, like neurons and cardiac myocytes, Kv channels are involved in regulating the waveforms and firing patterns of action potentials (APs); they also play important roles in cell-volume regulation, proliferation and migration (Hille, 2001; Wulff et al., 2009; Sahoo et al., 2014).

1.1.1.2 Nomenclature and structure of Kv channels

To fulfill different physiological roles, there are a large number of Kv channels, which are encoded by 40 genes in mammalian genomes and each gene encodes a corresponding protein (α subunit). Kv channels can be divided into 12 subfamilies (Kv1 to Kv12) (Coetzee et al., 1999; Gutman et al., 2005; Sahoo et al., 2014; Ranjan et al., 2019) as shown in Table 1.

Table 1: Kv channels

Protein	Gene	Group
Kv1.1	Kcna1	*Shaker*
Kv1.2	Kcna2	
Kv1.3	Kcna3	
Kv1.4	Kcna4	
Kv1.5	Kcna5	
Kv1.6	Kcna6	
Kv1.7	Kcna7	
Kv1.8	Kcna10	
Kv2.1-2.2	Kcnb1-2	*Shab*

Protein	Gene	Group
Kv3.1	Kcnc1	*Shaw*
Kv3.2	Kcnc2	
Kv3.3	Kcnc3	
Kv3.4	Kcnc4	
Kv4.1-4.3	Kcnd1-3	*Shal*
Kv5.1	Kcnf1	Modifiers
Kv6.1-6.4	Kcng1-4	
Kv8.1-8.2	Kcnv1-2	
Kv9.1-9.3	Kcns1-3	

Protein	Gene	Group
Kv7.1-7.5	Kcnq1-5	KCNQ
Kv10.1	Kcnh1	EAG
Kv10.2	Kcnh5	
Kv11.1	Kcnh2	ERG
Kv11.2	Kcnh6	
Kv11.3	Kcnh7	
Kv12.1	Kcnh8	ELK
Kv12.2	Kcnh3	
Kv12.3	Kcnh4	

Rapidly inactivating A-type Kv channels are highlighted in red.

Based on the relatedness of genes, K^+ channels in *Shaker* (Kcna), *Shab* (Kcnb), *Shaw* (Kcnc) and *Shal* (Kcnd) groups belong to the "Kv family" (Sahoo et al., 2014). Because Kv5 (Kcnf), Kv6 (Kcng), Kv8 (Kcnv) and Kv9 (Kcns) channels can modulate Kv family members, they are included in this family as so-called "Modifiers" (Bocksteins and Snyders, 2012; Sahoo et al., 2014). Further Kv channel families are KCNQ (Kv7, Kcnq) and EAG (Kv10-Kv12, Kcnh).

Similar to the first cloned Kv channel — the *Drosophila Shaker* channel (Papazian et al., 1987), all mammalian Kv channels are composed of four α subunits (Figure 1A). Each α subunit contains six transmembrane segments (S1-S6) and a membrane-associated

P-loop between S5 and S6 (Figure 1B). The sequences of four S5-P-S6 segments line the ion conduction pore. S4 segments, harboring positively charged arginine or lysine residues, act as voltage sensor domains: alteration of the transmembrane electric field results in a movement of the positive charges and, hence, generates a protein conformational change leading to the opening of the gate (Long et al., 2005a,b).

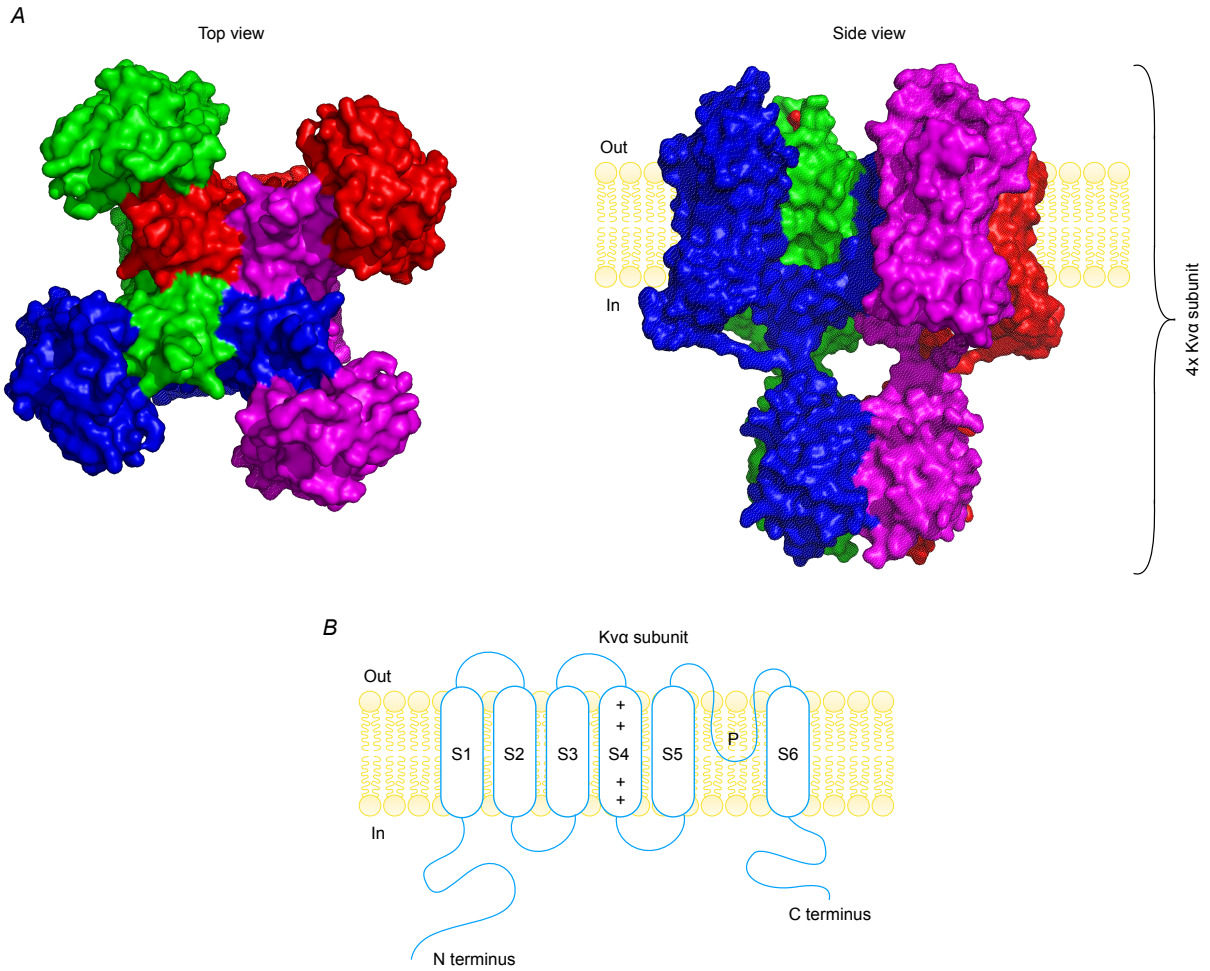

Figure 1: Structure of a Kvα channel

A. Structure of four Kv1.2/Kv2.1 (Kcna2/Kcnb1) chimeric α subunits (structural data from PDB 2R9R, Long et al. (2005b), and Sahoo et al. (2014)), viewing from the top (left) and side (right). ***B***. α subunit topological model, comprising a cytosolic NH_2 (N) and COOH (C) terminus, membrane-delimited six transmembrane segments (S1-S6) as well as a P-loop. S4 harbors positively charged residues and serves as a voltage sensor. Not drawn to scale.

1.1.1.3 Regulation of Kv channels

Associations with auxiliary protein subunits, for instance, Kvβ subunits, K^+ channel interacting proteins (KChIPs), transmembrane dipeptidyl aminopeptidase-like proteins (DPPLs), modify Kv channel gating, assembling, trafficking to and from the plasma membrane, and targeting to different cellular compartments (Gutman et al., 2005; Pongs and Schwarz,

2010; Sahoo et al., 2014).

Cytosolic Kvβ subunits bind to N termini of Kv1α subunits (Long et al., 2005a) and increase the inactivation rate of some Kv1 channels (Heinemann et al., 1994, 1995, 1996; Rettig et al., 1994). Such as Kvβ1.1 induced rapid inactivation to Kv1.5 (Figure 2A). Moreover, Kvβ subunits influence the surface expression of Kv1 channels (Shi et al., 1996; Pongs and Schwarz, 2010). For example, Kv1.2 surface expression is efficiently increased by coexpressing with Kvβ2 (Shi et al., 1996). *Shal* group Kv4 channels (Kv4.1-Kv4.3) are mainly expressed in somatodendritic compartments (Birnbaum et al., 2004; Jerng et al., 2004a; Shah et al., 2010; Carrasquillo and Nerbonne, 2014). KChIPs and DPPLs may either separately or jointly modulate gating properties of Kv4 channels, especially in the subthreshold potential range of action potential firing, by interacting with Kv4 channels to form protein complexes (Dougherty and Covarrubias, 2006; Dougherty et al., 2008; Maffie and Rudy, 2008).

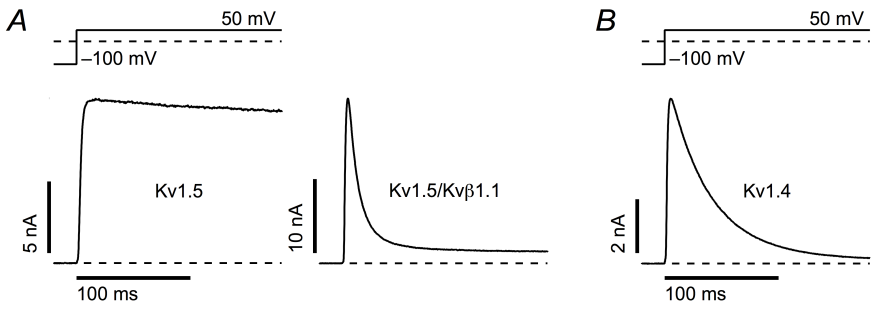

Figure 2: Current traces of Kv1.5, Kv1.5/Kvβ1.1 and Kv1.4 channels

Whole-cell current traces of Kv1.5 channels expressed alone or with Kvβ1.1 (***A***), and Kv1.4 channels (***B***) expressed in HEK293T cells and measured at a depolarizing voltage of 50 mV from a holding potential of –100 mV (top) for indicated time course.

In addition to this "mix-and-match" of Kvα and ancillary subunits, Kv channel properties can be modified by post-translational protein modifications, such as N-glycosylation, phosphorylation, oxidative modification and ubiquitination (Wulff et al., 2009; Sahoo et al., 2014; Capera et al., 2019). For example, inactivation of Kv3.4 is susceptible to phosphorylation and oxidation of residues in the N terminus of the protein (Covarrubias et al., 1994; Duprat et al., 1995; Stephens and Robertson, 1995; Beck et al., 1998; Antz et al., 1999; Ritter et al., 2012, 2015a; Kaczmarek and Zhang, 2017; Muqeem et al., 2018; Zemel et al., 2018). Kv2.1 channels, no matter natively expressed in hippocampal neurons or recombinantly expressed in HEK293 cells, are inhibited by the endogenous signaling molecule carbon monoxide (CO) (Dallas et al., 2011).

1.1.2 Non-inactivating delayed rectifier Kv channels

Kv channels open or activate upon membrane depolarization, some channels enter an inactivated state at maintained depolarizing potential. With respect to the kinetics of inactivation, Kv channels can be divided into slow- or non-inactivating delayed rectifier and rapidly inactivating A-type channels.

The majority of cloned Kv channels, e.g., Kv1.5 from the Kv1 subfamily (Figure 2A), activates after membrane depolarization and inactivates little or slowly after heterologous expression and is therefore classified as delayed rectifier Kv channels (Jan and Jan, 1990; Pongs, 1992; Gutman et al., 2005). This type of channels participates in repolarization of action potential and attenuation of cellular excitability (Connor and Stevens, 1971; Willis et al., 2018).

1.1.3 A-type Kv channels

A-type K^+ currents were initially characterized in vertebrate neurons (Hagiwara et al., 1961; Connor and Stevens, 1971; Neher, 1971; Thompson, 1977; Llinas, 1988; Rudy, 1988). The name "A-type" was originally derived from the typical profile of these currents that rapidly activate at sub-threshold voltages followed by fast inactivation, e.g., Kv1.4 (Figure 2B). Inhibition by 4-aminopyridine and insensitivity to extracellular tetraethylammonium ions are considered to be pharmacological hallmarks of A-type Kv channels (Thompson, 1977).

1.1.3.1 Physiological functions of A-type Kv channels

A-type Kv channels are abundantly expressed in neuronal, cardiac and smooth muscle cells (Connor and Stevens, 1971; Dixon et al., 1996; Hoffman et al., 1997; Coetzee et al., 1999; Amberg et al., 2003).

In the nervous system, A-type Kv channels have been examined extensively and are thought to regulate firing frequency since they modulate the rate of recovery from the refractory period (Connor and Stevens, 1971; Tierney and Harris-Warrick, 1992; Bouskila and Dudek, 1995; Liss et al., 2001). A-type Kv channels are usually silent at resting membrane potentials due to pronounced steady-state inactivation in many neurons (Bouskila and Dudek, 1995). However, A-type Kv channels transiently activate in these cells during

the decay of the afterhyperpolarizations phase of the APs, when the membrane potential becomes sufficiently negative to remove inactivation, tending to reduce the excitatory effect of depolarizing membrane currents (Connor and Stevens, 1971; Ruppersberg et al., 1991a). In this manner, A-type K^+ currents prolong the period between APs and control the neuronal firing frequency by means of inactivation (Rudy, 1988; Amberg et al., 2003; Cai et al., 2007).

A-type K^+ currents are also present in atrial and ventricular myocytes and are referred to as "transient outward" current (I_{to}) in these cells. In contrast to neuronal A-type K^+ currents, I_{to} currents are available at resting membrane potentials and predominantly responsible for the initial repolarization of the cardiac AP (Apkon and Nerbonne, 1991; Barry and Nerbonne, 1996; Nerbonne, 2000). Pharmacological blockade of I_{to} with 4-aminopyridine causes an increase in AP amplitude and duration (Firek and Giles, 1995). The physiological function of A-type Kv channels in smooth muscles may be related to the maintenance of membrane potential and regulation of excitability (Amberg et al., 2003).

1.1.3.2 Inactivation kinetics of A-type Kv channels

Inactivation of A-type Kv channels is mediated by fast and slow processes (Hoshi et al., 1990, 1991). The fast component of inactivation has become known as N-type inactivation as it is initiated by the N-terminal protein structure (Hoshi et al., 1990) whereas the slow component is named C-type for its relation to the pore structure (Hoshi et al., 1991).

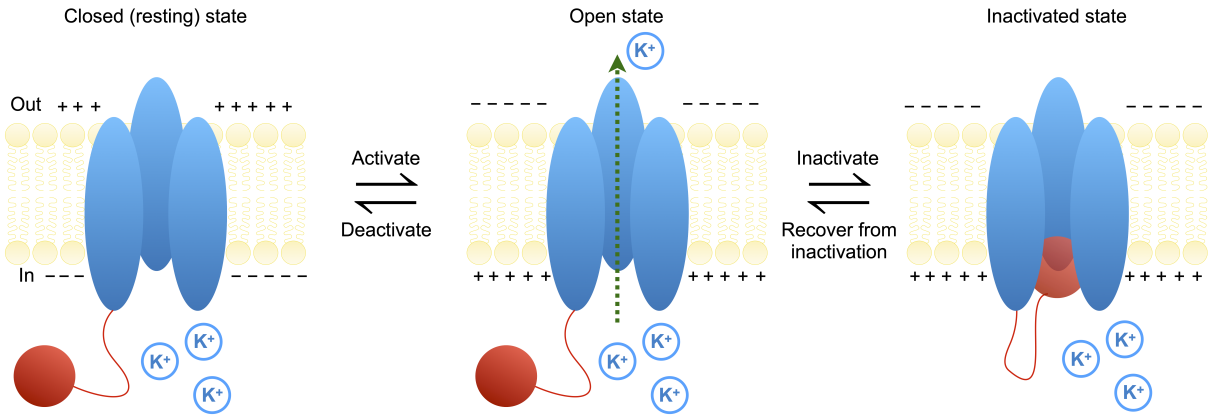

Figure 3: The "ball-and-chain" model for the N-type inactivation of Kv channels

At resting membrane voltage, the channel is closed and the N-terminal ball domains do not obstruct the permeation pathway (left). Upon depolarization, the channel enters an open conducting state (middle) and subsequently a non-conducting inactivated state with one N-type inactivating ball binding to its receptor in the inner pore (right). Only three of the four α subunits and one "ball" domain are shown for clarity; graphs are not drawn to scale. Modified after Kurata and Fedida (2006).

The N-type inactivation can be well explained by the "ball-and-chain" model: inactiva-

tion is produced by one of the four cytosolic N termini; it obstructs the pore of the open channel (Figure 3). The intrinsically disordered N-terminal protein can be divided into a positively charged distal "ball" segment that actually blocks the hydrophobic central cavity/vestibule of the inner pore and a flexible "chain" that provides mobility to the "ball" and determines the kinetics of inactivation. Moreover, mutational or acute enzymatic removal of the N terminus eliminates N-type inactivation, while the inactivation can be restored by intracellularly applying a solution of synthetic peptide with the same amino acid sequences as the N terminus (Hoshi et al., 1990; Antz and Fakler, 1998).

1.1.3.3 Post-translational protein modification of A-type Kv channels

A wealth of modulators affects A-type Kv channels through post-translational protein modification. It is assumed that fine-tuning the inactivation properties of these channels is required to meet specific cellular needs.

A-type Kv channels in both neuronal and cardiac cells can be modulated by phosphorylation. Usually, phosphorylation of serine residues in the N-terminal ball domain of these channels results in altered N-type inactivation through rearranging the inactivating ball domain (Covarrubias et al., 1994; Antz et al., 1999). Oxidation of cysteine residues in the N-terminal ball domain slows down or eliminates the inactivation. One explanation is that N-terminal ball domain is "immobilized" by forming a disulfide bridge with another protein-based thiol group (Ruppersberg et al., 1991b; Rettig et al., 1994; Duprat et al., 1995; Sahoo et al., 2014).

In addition to phosphorylation and oxidation, other common post-transcriptional modifications, like N-glycosylation and palmitoylation, have been shown to influence biochemical properties, current densities and subcellular localization of such channels (Santacruz-Toloza et al., 1994; Takimoto et al., 2002; Cai et al., 2007). For instance, palmitoylation of specific cysteines in KChIP3 is required for efficient plasma membrane localization and up-regulation of functional expression of Kv4.3 channels (Takimoto et al., 2002).

1.1.4 A-type Kv channels in dorsal root ganglion (DRG) neurons

DRG neurons convey the somatosensory information from peripheral organs, such as the skin, muscles, joint capsules and viscera, to the central nervous system (Kandel et al., 2013). A diverse group of ion channels expressed in DRG neurons transduce physical,

thermal or chemical stimuli into electrical signals that are conducted along axons and finally result in neurotransmitter release (Rasband et al., 2001; Salzer et al., 2019). For example, transient receptor potential channels (TRPs) initiate temperature sensation in DRG neurons (Bandell et al., 2004).

Early studies reported that A-type Kv channels (such as Kv1.4, Kv3.4, and Kv4.1, Kv4.3) were predominately expressed in DRG neurons and that APs shape in these cells was modified after manipulating the function of A-type Kv channels (Kostyuk et al., 1981; Pearce and Duchen, 1994; Gold et al., 1996; Ritter et al., 2012, 2015b; Zemel et al., 2018), suggesting physiological roles of A-type K^+ currents in regulating neuronal excitability. Consistently, A-type Kv currents in DRG neurons are reduced in multiple chronic pain models (Everill and Kocsis, 1999; Stewart et al., 2003; Takeda et al., 2006; Xu et al., 2006; Zhang et al., 2007a, 2019).

1.1.4.1 Kv1.4 channel

In DRG neurons, the expression of Kv1.4 channel (Kcna4) was identified in the neuronal soma and axon using immunohistochemistry, immunoblotting, western blot and polymerase chain reaction (PCR) (Ishikawa et al., 1999; Rasband et al., 2001; Yang et al., 2004; Qian et al., 2009; Cao et al., 2010; Duan et al., 2012), and a great reduction in Kv1.4 expression was found after nerve injury (Rasband et al., 2001).

The biophysical properties and expression of Kv1.4 are susceptible to a number of signaling processes. For example, inactivation of Kv1.4 can be regulated by phosphorylation: on the one hand, Ca^{2+}/calmodulin-dependent phosphorylation cascades lead to slower inactivation kinetics of Kv1.4; on the other hand, calcineurin reverses this effect by dephosphorylation (Roeper et al., 1997). Thus, Kv1.4 inactivation is susceptible to the changes of intracellular Ca^{2+}, providing a mechanism of regulating critical frequency for presynaptic spike broadening and synaptic plasticity induction (Roeper et al., 1997). A-type K^+ current density in DRG neurons is decreased and Kv1.4 expression is downregulated after exposure to transforming growth factor β 1 (TGFβ1), resulting in depolarization of the resting membrane potential and broadening of the AP (Zhu et al., 2012). This may explain the modulation of sensory neuronal function in chronic inflammation by TGFβ1 (Zhu et al., 2012).

Additionally, a cysteine residue at position 13 (C13) has been shown to be involved in oxidation-dependent regulation of Kv1.4 inactivation (Ruppersberg et al., 1991b) (Figure 4). When Kv1.4 channels were expressed in *Xenopus* oocytes, the inactivation was fast in

the cell-attached configuration with reducing cytosol; however, upon patch excision, the inactivation was largely slowed due to exposing the cytosolic side of the patch to ambient oxygen-saturated recording solution. After pushing the patch back into the reducing cytosol, the fast inactivation was obtained (Ruppersberg et al., 1991b; Sahoo et al., 2014). The sensitivity of Kv1.4 to the intracellular oxidation was rendered by the C13S mutant. A cysteine in the same position also forms the binding motif $CXXHX_{16}H$ in the N terminus of Kv1.4 for free heme. Once heme binds to the motif, the inactivation is impaired due to the conformational change of the inactivating ball domain (Sahoo et al., 2013).

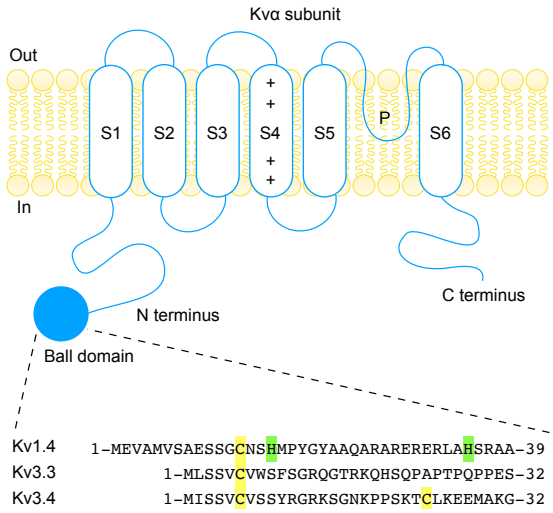

Figure 4: N-terminal ball domain in an A-type Kv α subunit

Top. The N termini of A-type Kv channel α subunits (blue filled circle) harbor "ball" domains responsible for N-type inactivation. ***Bottom***. N-terminal sequences of rat Kv1.4, rat Kv3.3, and rat Kv3.4 are aligned (Sahoo et al., 2014); cysteine (yellow) and histidine (green) residues are highlighted. Residue numbers are indicated based on respective sequences from the UniProt database.

1.1.4.2 Kv3.4 channel

Immunohistochemical analysis revealed that Kv3.4 channels (Kcnc4) express in the axon, soma and presynaptic terminals of DRG neurons (Chien et al., 2007; Ritter et al., 2015b; Zemel et al., 2017; Muqeem et al., 2018).

Kv3.4 channels contribute to nociceptor AP repolarization and AP duration (Ritter et al., 2012, 2015a; Liu et al., 2017). Dysfunction of Kv3.4 activity has large effects on nociceptor excitability (Zemel et al., 2018). For instance, knock-down or inhibition of Kv3.4 channels in DRG neurons induces AP broadening, while phosphorylation of these channels leads to AP shortening (Ritter et al., 2012, 2015b; Muqeem et al., 2018; Zemel et al., 2018). Similarly to Kv1.4, oxidation of a cysteine residue at position 6 in the N-terminal inactivation ball domain of Kv3.4 removes inactivation (Stephens and Robertson,

1995) (Figure 4), which may be explained by forming a disulfide bond between the ball and another part of the channel (Stephens and Robertson, 1995).

1.1.4.3 Kv4 channels

All three Kv4 channels' (Kv4.1-Kv4.3) mRNA isoforms (Kcnd1-3) are present in DRG preparations with differential expression (Kim et al., 2002; Winkelman, 2005; Zemel et al., 2018). In all sizes of DRG neurons, Kv4.1 mRNA has been detected. In small size DRG neurons, Kv4.2 mRNA is absent, while Kv4.3 mRNA is mainly found in this type of DRG neurons (Phuket, 2009; Matsuyoshi et al., 2012; Yunoki et al., 2014).

In contrast to N-type inactivating Kv1.4 and Kv3.4 channels, Kv4 channels, although having N-terminal inactivating ball domains, do not undergo N-type inactivation in their native configuration. However, N-terminal inactivating ball domains of Kv4 channels act as binding domains for KChIPs (An et al., 2000; Bahring et al., 2001; Pioletti et al., 2006; Wang et al., 2007; Covarrubias et al., 2008; Jerng and Pfaffinger, 2014). The Kv4/KChIPs complex undergoes rapid inactivation via a distinct mechanism which may involve the failure of the voltage sensors to actively open the activation gate (Bahring and Covarrubias, 2011). In some cases, N-type inactivation of Kv4 channels can be introduced by interacting with the cytoplasmic N termini of DPPLs (Dougherty and Covarrubias, 2006; Amarillo et al., 2008; Jerng et al., 2004b, 2009; Kaulin et al., 2009; Nadin and Pfaffinger, 2010).

1.1.5 Kvβ-mediated N-type inactivation

In vivo, Kv channels often appear as heteromultimeric complexes coassembled with ancillary β subunits. For example, purified Kv channels from bovine brain were implicated as tightly associated octameric structures in a stoichiometry of four α and four β subunits (4Kvα/4Kvβ) (Parcej et al., 1992; Scott et al., 1990, 1994) (Figure 5A).

Each α and β subunit in a Kvα/Kvβ complex is associated by a contact loop, which supplies the docking surface for Kvβ subunit (Li et al., 1992; Parcej et al., 1992; Shen et al., 1993; Sewing et al., 1996; Gulbis et al., 2000; Parcej and Eckhardt-Strelau, 2003; Sokolova et al., 2003; Long et al., 2005b; Pongs and Schwarz, 2010). The contact loop engages only a few amino acids of Kvα tetramerization domain (T1), these amino acids are highly conserved among members of the Kv1α subfamily (Sewing et al., 1996). Therefore, the conserved contact loop provides a molecular explanation to the specificity of Kv1α and

Kvβ subunit interactions (Gulbis et al., 2000).

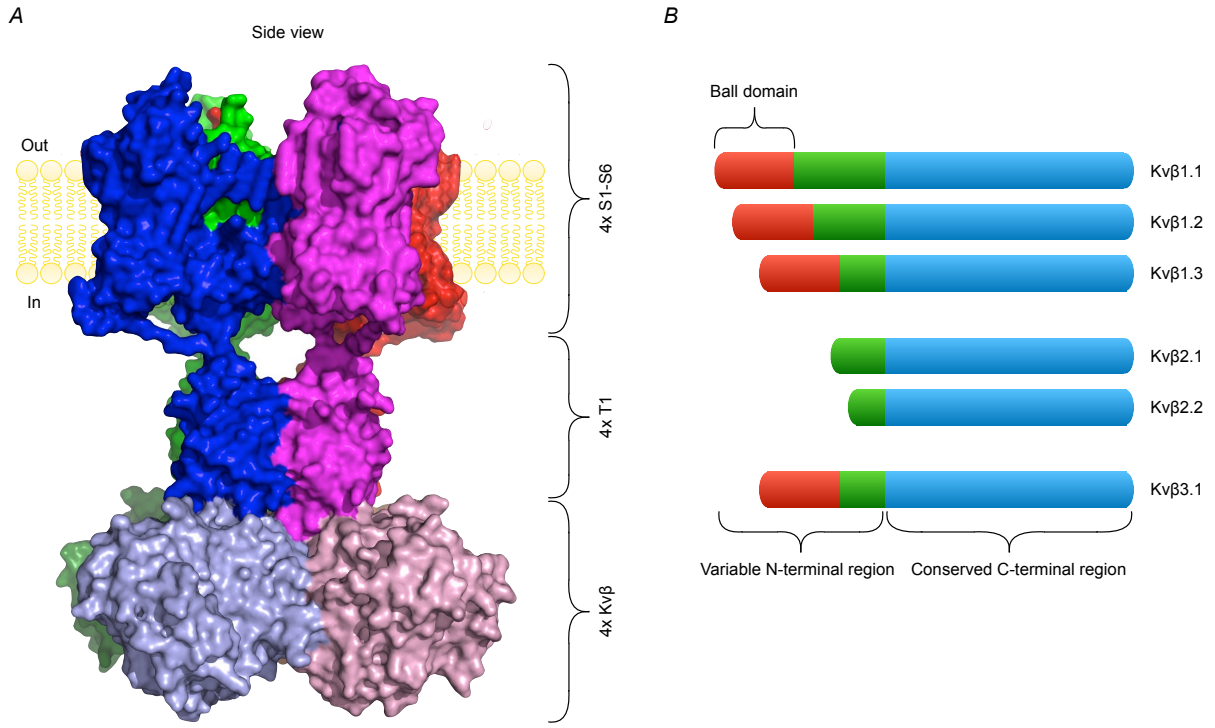

Figure 5: Structure of a Kvα/Kvβ channel complex and Kvβ protein family

A. Structure of four α subunits as in Figure 1A coassembled with four Kvβ2 (Kcnab2) subunits through four tetramerization (T1) domains (structural data from PDB 2R9R, Long et al. (2005b), and Sahoo et al. (2014)). ***B***. Bar diagram of Kvβ protein family members (Pongs and Schwarz, 2010) with conserved C-terminal regions (blue), and variable N-terminal regions, including the N-type inactivation ball domains (red); not drawn to scale.

In mammalian genomes, there are three Kvβ genes: Kcnab1-3. Alignment of the Kvβ protein family unmasks variable N termini followed by a highly conserved core domain (about 330 residues long) (Figure 5B) (Pongs and Schwarz, 2010). The conserved core domains have been shown to function as aldo-keto reductases that use NADPH (reduced nicotinamide adenine dinucleotide phosphate) as a cofactor (McCormack and McCormack, 1994; Weng et al., 2006; Pan et al., 2008a; Tipparaju et al., 2008). In addition to the core domains, Kvβ1 and Kvβ3 have N-terminal inactivating ball domains (about 70 residues long). Some of these Kvβ N-terminal inactivating ball domains can interact with Kv1α subunits, and thereby introduce N(β)-type inactivation to non-inactivating delayed rectifier Kv channels by the "ball-and-chain" mechanism (Rettig et al., 1994; Heinemann et al., 1995; Morales et al., 1995; Zhou et al., 2001).

In the family of Kv1 channel α subunits, only Kv1.4, as highlighted in Table 1 is capable of generating A-type K^+ currents on its own (Figure 2B). However, Kvβ1 and Kvβ3 harboring N-terminal "ball" domains substantially contribute to the fine-tuning of A-type Kv channel inactivation and thereby regulate electrical excitability. For instance, C7 in Kvβ1.1 (Rettig et al., 1994), C7 and C22 in Kvβ3 (Heinemann et al., 1996) render the Kv

channels (e.g., Kv1.1 and Kv1.5) sensitive to intracellular redox milieu changes like Kv1.4 and Kv3.4 channels (Ruppersberg et al., 1991b; Rettig et al., 1994; Stephens et al., 1996b,a; Sahoo et al., 2014) (Figure 6).

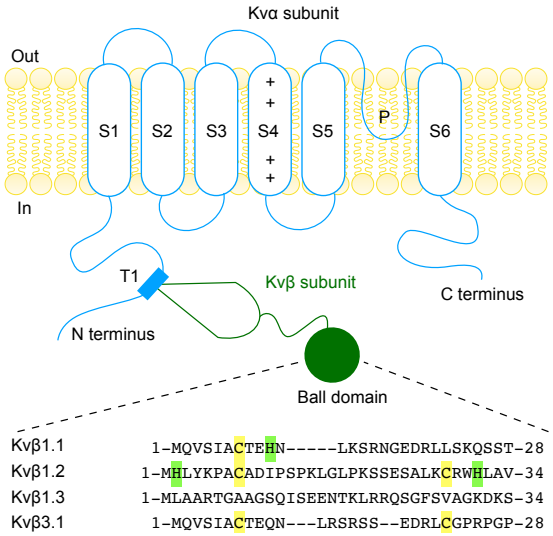

Figure 6: N-terminal ball domain in an A-type Kv α subunit

As in Figure 4, α subunit topological models of a delayed rectifier channel coassembled with an auxiliary Kvβ subunit at the tetramerization site (T1) (top), N-terminal sequences of human Kvβ subunits are aligned (bottom).

Kvβ2, instead, has a shorter N terminus (Figure 5B), accelerates Kv1.4 N-type inactivation (McCormack et al., 1995), but it does not induce inactivation when coexpressed with non-inactivating delayed rectifier Kv1 channels (Heinemann et al., 1996). To explore the expression and assembly of Kvβ2 with Kv1α subunits, chimeric Kvβ2 subunits N(Kvβ1.1) · C(Kvβ2) and N(Kvβ3) · C(Kvβ2) were generated by splicing N-terminal inactivating domains of Kvβ1.1 or Kvβ3 to the N terminus of Kvβ2. Both chimeric Kvβ2 subunits induced N-type inactivation of Kv1.1 and Kv1.5, suggesting the expression of Kvβ2 and the association of Kvβ2 with these Kv1α subunits (Heinemann et al., 1996).

Moreover, the degree and kinetics of N(β)-type inactivation are dependent on the phosphorylation state (Covarrubias et al., 1994; Kwak et al., 1999), lipid composition (Oliver et al., 2004), and the level of free intracellular Ca^{2+} (Jow et al., 2004; Decher et al., 2008; Swain et al., 2015). Also, because the core domains of Kvβ subunits use NADPH as a cofactor, oxidation of the Kvβ-bound NADPH inhibits N(β)-type inactivation by restraining the N-terminal inactivating ball domains (Pan et al., 2011).

1.2 Reactive sulfur species (RSS)

Hydrogen sulfide (H_2S) is a colorless, flammable gas with the smell of rotten eggs, it has been known for its toxicity and environmental hazard over centuries (Wang, 2012; Wallace and Wang, 2015; Filipovic et al., 2018). However, H_2S has crucial effects on cell signaling processes that are particularly relevant to its wide range of physiological functions (Li et al., 2011; Wang, 2012; Wallace and Wang, 2015; Filipovic et al., 2018). Therefore, H_2S is regarded as the third member of biologically active gaseous transmitters after nitric oxide (NO) and carbon monoxide (CO) (Wang, 2002, 2003, 2014).

H_2S has a pKa_1 of about 7 at 25 °C (Chen and Morris, 1972; Li and Lancaster, 2013; Iciek et al., 2015) and, thus, in aqueous solutions it is in equilibrium with more oxidized sulfur species, such as hydropersulfides (HSSH), polysulfides (H_2S_n) and thiosulfate ($S_2O_3^{2-}$) (Miranda and Wink, 2014; Cuevasanta et al., 2017). In parallel to the extensively studied reactive oxygen species (ROS) and reactive nitrogen species (RNS), these sulfur-containing agents can react (e.g., oxidize or reduce) with other molecules under physiological conditions, and are often collectively categorized as "reactive sulfur species" (RSS) (Iciek et al., 2015; Mishanina et al., 2015).

1.2.1 Biosynthesis of hydrogen sulfide (H_2S)

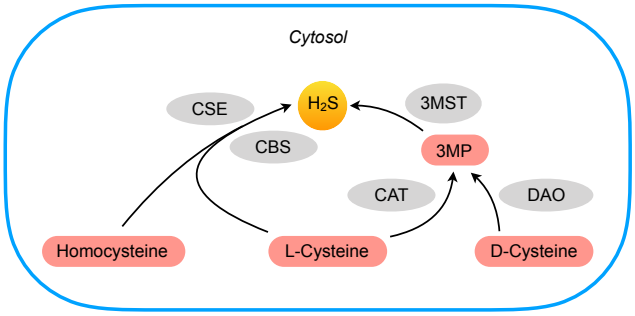

Figure 7: Biosynthesis of H_2S

H_2S is produced from homocysteine, L-Cysteine alone or L-Cysteine along with homocysteine via enzymes cystathionine γ-lyase (CSE) and cystathionine β-synthase (CBS) (Wang, 2012; Kimura, 2015; Wallace and Wang, 2015; Filipovic et al., 2018). L-Cysteine and D-Cysteine can also be metabolized to 3-mercaptopyruvate (3MP) by cysteine aminotransferase (CAT) and D-amino acid oxidase (DAO), respectively (Kimura, 2015). Afterwards, 3-MP is metabolized to H_2S by 3-mercaptopyruvate sulfurtransferase (3MST).

In mammalian cells, using homocysteine, L-cysteine, D-cysteine and their derivatives as the substrates, H_2S is generated mostly through three enzymatic pathways of cystathionine γ-lyase (CSE), cystathionine β-synthase (CBS) and 3-mercaptopyruvate sulfurtransferase (3MST) (Wang, 2012; Kimura, 2015; Wallace and Wang, 2015; Filipovic et al., 2018) (Fig-

ure 7). For example, in the cardiovascular system, the production of H_2S is predominantly regulated by CSE whereas CBS is the enzyme mostly responsible for H_2S production in the nervous system (Wang, 2012; Wallace and Wang, 2015; Filipovic et al., 2018).

1.2.2 Endogenous H_2S level and its physiological functions

Depending on the analytical methods, a range of endogenous physiological H_2S levels in various tissues and cells, from nanomolar concentrations to more than 1 mM, has been reported (Furne et al., 2008; Shen et al., 2012; McCook et al., 2014; Zhang et al., 2014; Filipovic et al., 2018). The broad distribution of H_2S, such as in nervous and cardiovascular systems, underlies the wide scope of their physiological effects (Li et al., 2011; Wang, 2012; Kabil et al., 2014; Filipovic et al., 2018).

In the nervous system, H_2S functions as a signaling molecule by modulating neurotransmission and neuromodulation (Wang, 2012). For example, levels of H_2S were reported to be severely diminished in the brains of Alzheimer's disease patients in comparison to those of the healthy individuals (Eto et al., 2002; Giuliani et al., 2013). Pretreatment with the H_2S donor NaHS improved learning and memory deficits in a rat model of Alzheimer's disease (Xuan et al., 2012a). Markedly decreased production of H_2S was also reported in Huntington's disease (Paul et al., 2014; Sbodio et al., 2016). Numerous roles of H_2S have been identified in the cardiovascular system, including attenuating myocardial ischemia reperfusion injury, promoting angiogenesis, relaxing smooth muscle cells and regulating blood pressure (Elrod et al., 2007; Elsey et al., 2010; Predmore and Lefer, 2010; Szabo and Papapetropoulos, 2011; Shen et al., 2015).

1.3 Effects of RSS on ion channels

H_2S is freely permeable through plasma membranes and one major group of target proteins is membrane ion channels (Chen et al., 2002; Wilkinson and Kemp, 2011; Gamper and Ooi, 2015). Regulation of different ion channels underpins various systemic responses to H_2S in the nervous and cardiovascular systems (Tang et al., 2010; Li et al., 2011; Peers et al., 2012). For example, H_2S functions as a neuromodulator in the brain by enhancing N-methyl-D-aspartate receptor-mediated responses and strengthening hippocampal long-term potentiation (Abe and Kimura, 1996); through persulfidation of one cysteine residue (C43) in the Kir6.1 subunit of K_{ATP} channels, H_2S activates the channel in vascular smooth

muscle cells, lowers blood pressure, and protects the heart from ischemia/reperfusion injury (Zhao et al., 2001; Zhang et al., 2007b; Mustafa et al., 2011).

The transient receptor potential ankyrin 1 (TRPA1) channel, which is a member of the TRP family of ion channels and widely expressed in neuronal cells (e.g., sensory DRG neurons) (Bautista et al., 2005), transduces a variety of stimuli to the central nervous system, including chemical, thermal and mechanical irritants (Nilius et al., 2012). In both cultured DRG neurons and heterologous cell expression systems (e.g., HEK293), H_2S (from donor NaHS) activated TRPA1 channels to induce Ca^{2+} influx by targeting two cysteine residues (C422 and C622) in the N terminus of the channel (Streng et al., 2008; Ogawa et al., 2012). However, polysulfide (from the donor Na_2S_3) affected the channels much more potently (approximately 1000 times) than that of NaHS (Kimura et al., 2013), suggesting polysulfides, which can be generated from NaHS, may actually activate TRPA1 channels (Streng et al., 2008; Nagy and Winterbourn, 2010; Toohey, 2011; Ogawa et al., 2012).

1.4 Interaction of heme with ion channels

Heme (Fe^{2+}-protoporphyrin-IX, ferroprotoporphyrin) is a metallic organic compound consisting of an iron atom (ferrous iron, Fe^{2+}) in the center and a protoporphyrin-IX ring, where iron is coordinated with the protoporphyrin-IX ring through its four nitrogen atoms (Sahoo et al., 2013; Burton et al., 2016). When the central ferrous iron in heme is oxidized to its ferric state (Fe^{3+}), the complex is named hemin (Fe^{3+}-protoporphyrin-IX, ferriprotoporphyrin). Heme is known as an essential protein prosthetic group, and heme-containing proteins play vital roles in diverse biological functions, such as oxygen transport, electron transfer, and gas sensing and transport (Tsiftsoglou et al., 2006; Hanna et al., 2017; Donegan et al., 2019).

Additionally, heme can act as a nongenomic modulator of ion channel functions, such as big-conductance Ca^{2+}-sensitive K^+ (BK_{Ca}) channel (Tang et al., 2003; Horrigan et al., 2005; Jaggar et al., 2005), epithelial Na^+ channel (Wang et al., 2009), A-type Kv1.4 channel (Sahoo et al., 2013), and K_{ATP} channel (Burton et al., 2016). In all three K^+ channels, heme modulates channel activity through interacting with a flexible region of the cytoplasmic channel domain. In the case of BK_{Ca} channels, heme binds to the C-terminal CXXCH motif (Tang et al., 2003; Jaggar et al., 2005); for Kv1.4 channels, heme binds to the $CXXHX_{18}H$ motif in the N terminus (Sahoo et al., 2013); and for K_{ATP} channels, heme is suggested to bind to the similar $CXXHX_{16}H$ motif in the cytoplasmic sulfonylurea receptor 2A domain

(Burton et al., 2016). Thus, there may be similarities in the modes of heme binding across different K^+ channels. As RSS and heme share biological targets (e.g., cysteine residues) in ion channels and have the ability to interact chemically with each other (Pietri et al., 2011; Donegan et al., 2019), it is therefore expected that RSS signaling interplays with that of heme.

1.5 Objectives

A-type Kv channels are major regulators of neuronal excitability that have been mainly characterized in the nervous systems (Zemel et al., 2018). Fine-tuned regulations of N-type inactivation of these channels, such as oxidation (Ruppersberg et al., 1991b; Rettig et al., 1994; Duprat et al., 1995; Stephens et al., 1996a; Hsieh, 2008), phosphorylation (Covarrubias et al., 1994; Drain et al., 1994; Antz et al., 1999; Kwak et al., 1999; Birnbaum et al., 2004; Cai et al., 2005; Ritter et al., 2012) and heme (Sahoo et al., 2013), are effective ways of modifying cells to meet specific requirements.

The endogenously produced gaseous messenger H_2S utilizing the donor NaHS has various impacts on cellular excitability, including changes in AP characteristics (Feng et al., 2013) and Ca^{2+} entry (Streng et al., 2008; Ogawa et al., 2012). Functional properties of multiple ion channels (e.g., K_{ATP} and BK_{Ca}) are diversely regulated by applying NaHS (Tang et al., 2010), suggesting direct or indirect effects of H_2S on these channels. For instance, cysteine residues in targeted channel proteins may be modified by H_2S through persulfide formation (sulfhydration) (Paul and Snyder, 2012; Cuevasanta et al., 2017); cellular levels of various reactive species may also be altered by H_2S (Li et al., 2011; Sun et al., 2012; Spassov et al., 2017).

With the existence of cysteine residues in the N-terminal inactivating ball domains of A-type Kv channels (e.g., Kv1.4 and Kv3.4), and many Kvβ subunits that induce N-type inactivation of non-inactivating delayed rectifier Kv1 channels, we hypothesize that inactivation of these channels may be modulated by sulfide species, as well as by other stress mediators, such as glutathionylation inducing reagent diamide (1,1'-azobis[N,N-dimethylformamide]) and cysteine-specific modifier DTNP (2,2'-dithiobis[5-nitropyridine]), and heme.

In the first part of this work, the effects of sulfide species on the electrical activity and native A-type Kv channels of DRG neurons were investigated. Their donors NaHS/Na_2S_n affected the APs and markedly impaired the N-type inactivation of native A-type Kv channels in DRG neurons as well as the heterologously expressed Kv1.4 and Kv3.4 channels

in HEK293T cells. Furthermore, similar experiments were performed on Kvβ-induced N-type inactivation of non-inactivating delayed rectifier Kv1 channels. In addition, the molecular loci required for the interaction of Kv3.4 and Kv1.4/Kvβ1 with hemin were analyzed.

2 Materials and methods

2.1 Materials

2.1.1 Bacterial strain and cell line

2.1.1.1 *E.coli* strain

XL1-Blue competent cells (Stratagene, Darmstadt, Germany)

2.1.1.2 Cell line

HEK293T cells (Human embryonic kidney 293T cells, Center for Applied Microbiology and Research, Porton Down, Salisbury, UK)

2.1.2 Plasmid and vector

Plasmid vector pcDNA3 was used for transient cytomegalovirus (CMV) promoter-driven expression in mammalian cells (Invitrogen, Darmstadt, Germany). All the mutants were generated by site-directed mutagenesis and later verified by DNA sequencing, and they are termed by amino acid residues substitution (e.g., C13S of Kv1.4, means cysteine at position 13 is substituted by serine), which are listed in Table 2.

Table 2: List of DNA constructs and mutants

Protein (Gene)	UniProt database accession no.	Mutant (s)
α subunits Kv family		
rat Kv1.1 (Kcna1)	P10499	C35A, C36A, C35A:C36A
human Kv1.2 (Kcna2)	P16389	C435S
rat Kv1.4 (Kcna4)	P15385	C13S, H16R, C13S:H16R
human Kv1.5 (Kcna5)	P22460	-
rat Kv3.4 (Kcnc4)	Q63734	C6S, C24S, C6S:C24S
β subunits Kv family		
human Kvβ1.1 (Kcnab1)	Q14722-2	C7S, E349K, C7S:E349K, C7S:H10A
human Kvβ1.2 (Kcnab1)	Q14722-3	C8S, C28S, C8S:C28S
human Kvβ1.3 (Kcnab1)	Q14722-1	A8C
human Kvβ2.1 (Kcnab2)	Q13303	-
human Kvβ3.1 (Kcnab3)	O43448	C7S, C22S, C7S:C22S

2.1.3 Chemicals and reagents

Unless otherwise stated, all chemicals were used to prepare solutions used in high-grade obtained from Sigma-Aldrich (Taufkirchen, Germany) and Carl Roth (Karlsruhe, Germany). Cell culture materials were from Life Technologies (Darmstadt, Germany).

2.1.3.1 NaHS and polysulfides

Sodium hydrogen sulfide (NaHS) was obtained from Cayman Chemical (Ann Arbor, MI, USA). Sodium polysulfide set, including sodium disulfide (Na_2S_2), sodium trisulfide (Na_2S_3), and sodium tetrasulfide (Na_2S_4), was obtained from Dojindo Molecular Technologies (Kumamoto, Japan). High-concentration stocks of NaHS (500 mM) and sodium polysulfides (100 mM) were prepared in respective electrophysiological recording bath solutions, and then diluted to the desired concentrations right before application. Stock solutions of NaHS and polysulfides were used within one hour of preparation, except for the NaHS "aging" experiments.

2.1.3.2 Hemin

Hemin (Fe^{3+}-protoporphyrin-IX) was purchased from Sigma-Aldrich. Stock solution of hemin at 1 mM was prepared daily by dissolving hemin powder in 30 mM NaOH for 30 min and then votexed, and stored at 4 °C in the dark. Working solutions (40 nM, 200 nM, 500 nM or 1 μM) of hemin were prepared from stock solution immediately before use.

2.1.3.3 Other reagents and chemicals

Reduced glutathione (GSH), 1,4-Dithiothreitol (DTT), hydrogen peroxide solution (H_2O_2, 30% w/w in H_2O), 1,1'-azobis[N,N-dimethylformamide] (diamide) and 2,2'-dithiobis[5-nitropyridine] (DTNP) were from Sigma-Aldrich.

2.1.4 Molecular biology buffer and solution

Tryptone yeast (TY) medium for *E.coli* growth

Ingredients	Mass (g)
Tryptone/peptone	10
Yeast extract	5
NaCl	5
Add H_2O to 1 l, autoclave, pH 7.0	
Add 15 g agar to 1 l for agar plates, pH 7.0	

Phosphate-buffered saline (PBS) for cell washing

Ingredients	Concentration (mM)
$Na_2HPO_4 \cdot 7H_2O$	4.3
KH_2PO_4	1.4
NaCl	137
KCl	2.7
	pH 7.4

2.1.5 Electrophysiological recording solutions

Bath and pipette solutions for different electrophysiological recording configurations are listed below, and before experimental use, all solutions were filtered using 0.2 μm non-pyrogenic sterile-R filters (Filtropur S 0.2, SARSTEDT AG & Co. KG, Nümbrecht, Germany). Unless otherwise stated, experiments in the results part were performed using bath and pipette solutions at pH 7.4.

2.1.5.1 Whole-cell patch-clamp recording

For Kv1.4 and Kv1.4/Kvβ

Bath solution		Pipette solution	
Ingredients	Concentration (mM)	Ingredients	Concentration (mM)
NMG	148	NMG	120
KCl	10	KCl	20
$CaCl_2$	1.5	$MgCl_2$	1
$MgCl_2$	1	EGTA	10
HEPES	10	HEPES	10
pH 6.9, 7.4 or 7.9 with HCl		pH 6.9, 7.4 or 7.9 with HCl	

For Kv3.4

Bath solution		Pipette solution	
Ingredients	Concentration (mM)	Ingredients	Concentration (mM)
NMG	148	NMG	120
KCl	4	KCl	20
$CaCl_2$	1.5	$MgCl_2$	1
$MgCl_2$	1	EGTA	10
HEPES	10	HEPES	10
pH 7.4 with HCl		pH 7.4 with HCl	

For Kvα/β

Bath solution		Pipette solution	
Ingredients	Concentration (mM)	Ingredients	Concentration (mM)
NMG	148	KCl	140
KCl	4	$MgCl_2$	1
$CaCl_2$	1.5	EGTA	10
$MgCl_2$	1	HEPES	10
HEPES	10		
pH 7.4 with HCl		pH 7.4 with KOH	

For DRG neurons action potential

Bath solution		Pipette solution	
Ingredients	Concentration (mM)	Ingredients	Concentration (mM)
NaCl	140	KCl	140
KCl	3	Mg-ATP	3
$CaCl_2$	2	EGTA	0.5
$MgCl_2$	2	HEPES	5
HEPES	10		
pH 7.3 with NaOH		pH 7.3 with KOH	

2.1.5.2 Cell-attached patch-clamp recording (identical bath and pipette solutions)

For Kv3.4

Ingredients	Concentration (mM)
NMG	148
KCl	4
$CaCl_2$	1.5
$MgCl_2$	1
HEPES	10
pH 7.4 with HCl	

For DRG neurons A-type channels

Ingredients	Concentration (mM)
NMG	148
KCl	10
$CaCl_2$	1.5
$MgCl_2$	1
HEPES	10
pH 6.9 with HCl	

2.1.5.3 Inside-out patch-clamp recording

For Kv1.4, Kv1.4/Kvβ and Kv3.4

Bath solution	
Ingredients	Concentration (mM)
KCl	140
EGTA	10
HEPES	10
Reduced GSH	0.2
pH 7.9 with KOH	

Pipette solution	
Ingredients	Concentration (mM)
NMG	148
KCl	10
$CaCl_2$	1.5
$MgCl_2$	1
HEPES	10
pH 7.9 with HCl	

2.2 Methods

2.2.1 Plasmid transformation, amplification and purification

1 μg of the desired plasmid was mixed with 50 μl *E. coli* strain XL1-Blue competent cells and kept on ice for 40 minutes, then 25 μl mixed cells were spread on a TY 1.5% agar plate with 100 μg/ml ampicillin and incubated at 37 °C overnight (16-18 h) to allow colonies to form. Subsequently, a single picked colony was inoculated in 100 ml TY medium with 100 μg/ml ampicillin, and it was amplified in a 37 °C, 180 rpm shaking incubator overnight. The amplified plasmid was extracted and purified with PureYield^{TM} Plasmid Midiprep System (Promega, Mannheim, Germany) according to the technical manual of the supplier, then the concentration of purified plasmid was determined by GeneQuant^{TM} 1300 UV/Visible Spectrophotometer (GE Healthcare, Munich, Germany).

2.2.2 Cell culture and transfection

2.2.2.1 Culture of HEK293T cells

To facilitate the correlation of Kv channel function with the expressed channel gene, a suitable heterogeneous expression system is required. Because HEK293T cells are quick to reproduce, easy to maintain and amenable to transfect, they have been widely used as an expression tool for K^+ channels (Thomas and Smart, 2005).

HEK293T cells (Center for Applied Microbiology and Research, Porton Down, Salisbury, UK) were cultured in 50 ml 25 cm^2 cell culture flasks (Greiner-Bio-One GmbH,

Frickenhausen, Germany) filled with 7 ml complete cell culture medium composed of 45% Dulbecco's modified Eagle's medium (DMEM) and 45% Ham's F-12 Nutrient Mixture, supplemented with 10% fetal calf serum (FCS) in a humid 37 °C incubator with 5% CO_2. The cells were subcultured every 2 to 3 days when grown to 70-80% of the surface of the culture flask.

To subculture the cells, the culture medium was removed and discarded, and the cells were washed with 5 ml PBS buffer and then trypsinized by incubation with 0.3 ml 0.05% Trypsin-EDTA (ethylenediaminetetraacetic acid) solution for 30 s to 1 min. This reaction was stopped with 3 ml complete cell culture medium, and the cells were detached and dissociated by pipetting up and down the medium several times. Cell suspensions in the volume of 0.1 ml, 0.2 ml and 0.5 ml were transferred to three new 50 ml 25 cm^2 cell culture flasks filled with 7 ml complete cell culture medium separately.

To seed cells, the volume of 0.3-0.5 ml cell suspension was diluted in 25 ml complete cell culture medium. For each well of the 24-well cell culture plate (Greiner-Bio-One GmbH) with glass cover slip (12 mm diameter, 0.17 mm thickness, Menzel-Gläser, Braunschweig, Germany) at the bottom of each well, 1 ml diluted cell suspension was seeded for electrophysiological measurements; the volume of 2 ml diluted cell suspension was seeded in the hollow petri dish (35 mm diameter), with glass cover slips (25 mm diameter, 0.17 mm thickness, Menzel-Gläser) sticking to the bottom by silicone elastomer (RTV615, KVD, Bad Wimpfen, Germany), for fluorescence measurements.

2.2.2.2 Transfection

HEK293T cells were transiently transfected with plasmid DNA using Roti®-Fect transfection kit (Carl Roth, Karlsruhe, Germany) the day after seeding (16-24 h), when the cells were about 50% confluent. Roti®-Fect is a liposome formulation composed of a polycationic lipid and a neutral colipid. It condenses DNA to compact structures (Roti®-Fect/nucleic acid-complexes) and ensures high efficient uptake into HEK293T cells.

For the cells of each well in the 24-well cell culture plate, 0.1-0.75 μg plasmid and 0.7 μl Roti®-Fect transfection reagent were mixed in 70 μl of DMEM-F12 (1:1) medium and incubated at room temperature for 20-30 minutes and then added to the well. For the cells in petri dish, 2 μg roGFP2 (the redox-sensitive green fluorescent protein 2) fluorescent protein and 2 μl Roti®-Fect were mixed in 200 μl DEMEM-F12 medium. Transfected cells were incubated at 37 °C with 5% CO_2 for 1-2 days before electrophysiological or fluorescence measurements were performed.

Cells not transfected with fluorescent proteins were co-transfected with 0.1 μg human-CD8 (cluster of differentiation 8) plasmid per well, and on the day of electrophysiological recording, 0.5 μl anti-CD8-coated superparamagnetic Dynabeads® (4.5 μm diameter; from Invitrogen, Life Technologies, Norway) were used for visual identification of transfected cells in each well. These beads are coated with a primary monoclonal antibody specific for the CD8 membrane antigen mainly expressed on human cytotoxic T cells, thus, the positively transfected cells can be identified.

2.2.3 Preparation of DRG neurons

DRG neurons were prepared from 6-20 weeks old wild-type C57BL/6J mice as described previously (Dib-Hajj et al., 2009). Animal care and experimental procedures were according to protocols in accordance with the guidelines established by the animal welfare committee of Jena University Hospital (registration number UKJ:TWZ18-2017).

The respective mouse was anesthetized with CO_2 and killed by cervical dislocation. Then the spinal cord was removed and longitudinally bisected. After removal of grey and white matter, DRG neurons from all accessible levels of the spinal cord were extracted and stored in ice-cold buffer containing (in mM) 137 NaCl, 5.3 KCl, 5.3 $MgCl_2$, 3 $CaCl_2$, 25 sorbitol, and 10 HEPES, pH 7.2 with NaOH. DRG neurons were detached and isolated by a combination of enzymatic treatment with Liberase™ purified enzyme blends TH (high thermolysin concentration) and papain (30 U/ml, final concentration) for 20 min, and TM (medium thermolysin concentration) and accutase for 10 min (both TH and TM were from Roche Life Science, Mannheim, Germany; both papain and accutase were from Sigma) at 37 °C and then mechanical trituration. Subsequently, neurons were suspended in DRG medium (86% DMEM, 10% FCS, 4% penicillin/streptomycin) and seeded on glass coverslips, which were coated with poly-L-lysine (Sigma) and filled in 24-well cell culture plate. Cells were cultivated in a humidified 37 °C incubator with 5% CO_2 for up to 48 h for electrophysiological recordings.

2.2.4 Patch-clamp technique

2.2.4.1 Preparation of patch-clamp pipettes

Patch pipettes were fabricated from borosilicate glass with filament (BioMedical Instruments, Zöllnitz, Germany), with outer diameter of 1.5 mm, inner diameter of 0.86 mm

and length of 80 mm. The recording pipettes were pulled using a Flaming/Brown type micropipette puller (Model P-97, Sutter Instrument Co., Novato, CA, USA) and coated with dental wax (Patterson Dental, Mendota Heights, MN, USA), fire-polished to reduce their capacitance. Pipette resistances of 0.9-2.0 MΩ were obtained in electrophysiological recording solutions.

2.2.4.2 Application pipettes

Fine-tipped glass application pipettes were also pulled with the puller mentioned above, but without coating or fire-polishing. The H_2S donor NaHS, polysulfide donors Na_2S_n, and other chemicals were locally applied with the glass application pipette in close proximity to the cell under consideration (Figure 8A).

Plastic pipettes were used for application of hemin, such as 200 nM hemin, 1 ml triple concentration (600 nM) of it was added to 2 ml bath solution in the recording chamber (35 mm diameter petri dish, Thermo Scientific, Germany) to reach the final concentration (200 nM).

2.2.4.3 Electrophysiological voltage-clamp measurements

Ionic currents through ion channels in the plasma membrane were recorded using the patch-clamp recording technique (Neher and Sakmann, 1976; Hamill et al., 1981) at room temperature (20-24 °C), which allows high current resolution, direct membrane patch voltage control and is the method of choice when measuring the activity of ion channels (Figure 8A).

The particular patch-clamp setup was equipped with the following instruments: (1) inverted microscope (IM, Zeiss, Oberkochen, Germany), lamp power supply and video camera for cell visualization; (2) anti-vibration table, surrounded by Faraday cage, which isolates the system from electrical noise; (3) the patch-clamp amplifier (EPC-9) was controlled and data were acquired by the patch-clamp software PatchMaster (both HEKA Elektronik, Lambrecht, Germany); (4) micromanipulator (Luigs & Neumann, Ratingen, Germany) for holding the amplifier headstage with recording electrode in connection with the recording pipette holder and the pipette; (5) temperature control system including a Peltier element underneath the bath chamber and a temperature control unit (Meyer and Heinemann, 1997); (6) pressure control system for the establishment of recording modes and studied chemicals application (MPCU-3, Lorenz Messgerätebau, Katlenburg-Lindau,

Germany); (7) an agar bridge (U-shape glass pipette with 1 M KCl in 1% agar) connected the bath solution and the ground electrode, to protect ground electrode from contacting with bath solution. For various study purposes, three patch-clamp recording modes: cell-attached, whole-cell and inside-out (Figure 8B) were used.

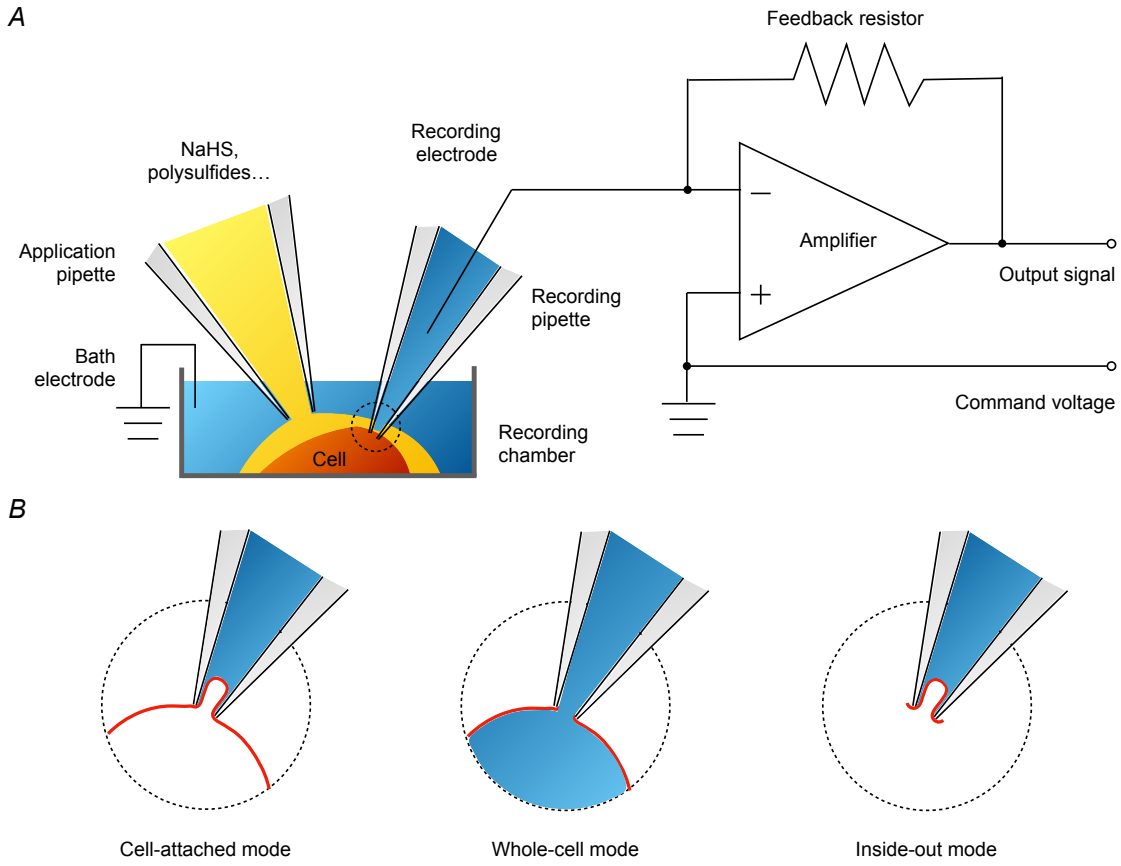

Figure 8: Patch-clamp recording technique

A. A silver recording electrode, coated with silver chloride, in a glass recording pipette with pipette solution (blue) was electrically contacted with the cell examined (red). In the voltage-clamp mode, the amplifier automatically adjusts the membrane voltage to the command voltage. Current flowing through the pipette is measured as the voltage drop across the feedback resistor. Application of studied chemicals in bath solution (yellow) was performed with an application pipette with about 2 cm H_2O pressure or with a plastic pipette. ***B***. Three patch-clamp recording modes: cell-attached, whole-cell and inside-out are illustrated as zoom-in schematic diagrams from the dashed circle in ***A***. Graphs are modified after Sakmann and Neher (1984); Clare (2010); not drawn to scale.

If not otherwise stated, the currents of specific channels transiently expressed in HEK-293T cells were measured repeatedly at a depolarization voltage of 50 mV, or were recorded in response to membrane depolarization to 60 mV from –60 mV in increasing steps of 20 mV from a holding voltage of –100 mV. The series resistance was electronically compensated up to 85% and all voltages were corrected for the liquid junction potential (Neher, 1992). Leak and capacitive currents were corrected using a p/6 method. Depending on the kinetics of recovery from inactivation, test pulses were typically applied every 15 s if not mentioned otherwise.

2.2.4.4 Action potential recording of mouse DRG neurons

Action potentials (APs) were recorded from small- to medium-sized DRG neurons in the current-clamp mode with an EPC-10 double patch-clamp amplifier (HEKA). Patch pipettes of 1.5-3.0 MΩ resistances were used. Using a low-frequency voltage clamp, a modified current-clamp mode, cells were set at a holding potential around −75 mV to warrant stability. Single APs were evoked within 5-8 ms by proper 10 ms current injections. The time interval for repetitive stimulations was 10 s.

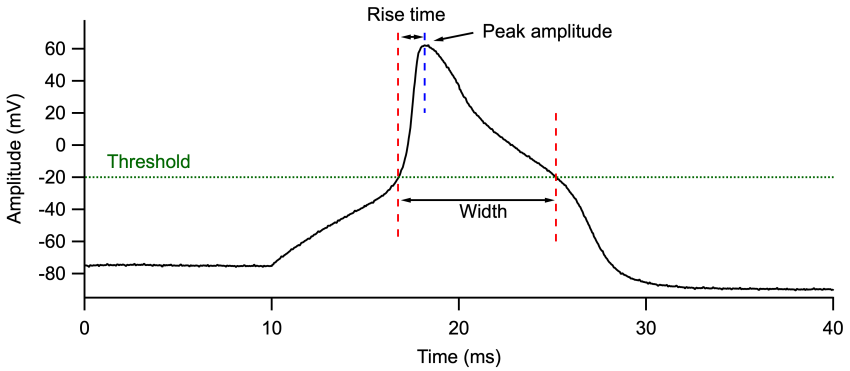

Figure 9: Mouse DRG neuron single action potential

The action potential shape is defined by width (duration of the action potential between two threshold crossings), rise time (duration from the first threshold crossing to the peak of the action potential) and peak amplitude. The threshold for detection of the action potential is set at –20 mV (green dotted line). The depicted action potential was evoked by injecting 50 pA current at 10 ms for 10 ms.

The shapes of evoked single APs were characterized by three parameters: (1) AP width, which was measured as the time interval between two threshold (at –20 mV, green dotted line in Figure 9) crossings; this threshold was chosen to eliminate the slow initial rise in AP, which is largely determined by the size of injected current and the capacitance of the cell; (2) AP rise time, which was measured from the first crossing of a threshold to the maximum amplitude; (3) Peak amplitude of the AP.

2.2.5 Fluorescence measurement

The redox-sensitive green fluorescent protein 2 (roGFP2) is a genetically engineered fluorescent redox reporter, which was developed by introducing two surface-exposed cysteine residues into the β-barrel structure of eGFP (wild-type GFP with mutation C48S and S65T) at position 147 and 204 (S147C and Q204C; Figure 10A, left) (Dooley et al., 2004). Importantly, roGFP2 has two different redox-dependent excitation peaks near 400 nm and 470 nm. While cysteine oxidation results in a disulfide bridge formation between S147C

and Q204C (Figure 10A, right), leading to an increase of the excitation peak near 400 nm and a decrease of excitation peak near 470 nm (Figure 10B). Consequently, the ratio between excitation at 400 nm and 470 nm (F400/F470) can be used as an indicator of the relative amount of oxidized/reduced roGFP2.

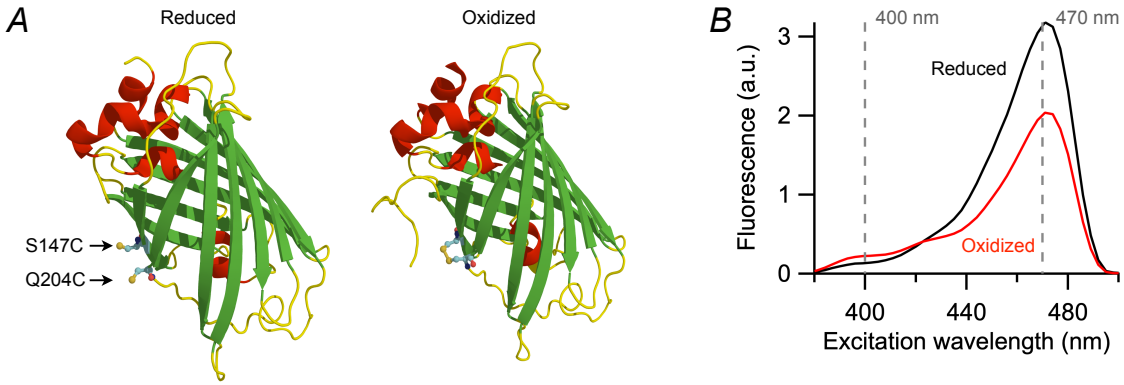

Figure 10: Redox-sensitive green fluorescent protein 2 (roGFP2)

A. Structure of roGFP2 (PDB code 1JC0). Under reduced condition, cysteine residues at position 147 and 204 (S147C and Q204C) remain apart (left); these two cysteine residues form a disulfide bridge in response to oxidation (right). ***B***. Excitation spectra of roGFP2 before (black) and after (red) oxidation. The formation of a disulfide bridge in roGFP2 leads to an increase in the excitation peak near 400 nm and a decrease of the excitation peak near 470 nm. The fluorescence intensity was measured in arbitrary units (a.u.).

The impact of polysulfide (Na_2S_4) and diamide on intracellular cysteine residues was evaluated using roGFP2. After HEK293T cells were transfected with roGFP2 for 1-2 days, fluorescence intensities of these cells were measured before and after Na_2S_4 or diamide application at pH 7.4 with a ProgRes MF cool camera (JenOptik, Jena, Germany), which was operated by PatchMaster/SmartLux software (HEKA) using a 40x oil immersion objective with excitation light at 400 nm and 470 nm ($\pm$ 8 nm) from a PolyChrome V light source (TILL Photonics, Gräfelfing, Germany). The fluorescence ratio F400/F470 was taken as readout for the redox state of HEK293T cell in response to Na_2S_4 or diamide.

2.2.6 Biochemical analysis and mass spectrometry

The protein consisting of the first 61 amino acid residues of the N-terminal inactivating ball domain of rat Kv1.4 channels (Pep61) was purified as described previously (Sahoo et al., 2013). In brief, the gene encoding Pep61 and its mutant C13S were inserted into NcoI/NotI sites of the pETM41 expression vector (EMBL), providing N-terminal His6 and maltose-binding protein (MBP) tags, and tobacco etch virus (TEV) cleavage sites. Pep61 was expressed in BL21 (DE3) pRIL *E. coli* cells. The His6-tag protein was purified in the presence of 5 mM DTT using a HisTrap FF crude affinity column (GE Healthcare). MBP/His6-tag was cleaved with TEV at 20 °C overnight and uncleaved protein, the TEV

protease together with the MBP/His6 tag was removed using an additional HisTrap FF crude affinity column. Monomeric peptide was separated from the dimeric form by Superdex Peptide (10/300 GL) (GE Healthcare).

Purified protein with two additional amino acid residues (glycine and alanine) resulting from the cleavage was incubated in 20 mM Tris, 150 mM NaCl (pH 7.4) with 200 μM Na_2S_4 at room temperature for 30 min. If applicable, samples were subsequently incubated with 5 mM DTT to remove Na_2S_4 modification. Na_2S_4 was removed using a 3 kDa cut-off filter and samples were treated with 15 mM iodoacetamide (IAM) at room temperature for 30 min in the dark. After removal of residual IAM, protein was cleaved with trypsin (mass spectrometry grade) by incubating overnight at 25 °C. Desalting was performed using C18 stage tips (Merck Millipore). Subsequently, the total mass of the resulting peptides was measured using MALDI-MS (Bruker Daltonics Ultraflex TOF/TOF).

2.2.7 Data analysis

Electrophysiological patch-clamp data were analyzed using FitMaster (HEKA Elektronik), IgorPro (WaveMetrics, Lake Oswego, OR, USA) and Microsoft Excel (Microsoft Corporation, Redmound, WA, USA) software programs. Data traces shown were digitally low-pass filtered at 1 kHz. Data were presented in the results part as means ± SEM (standard error of the mean) with n in parentheses (unless otherwise stated) representing the number of independent measurements.

2.2.7.1 Inactivation index

Inactivation index gave the estimate ratio of channels that do not inactivate after opening, which was expressed in equation (1):

$$Inactivation\ index = I_{mid}/I_{peak} \tag{1}$$

I_{peak} is the peak current amplitude, and I_{mid} stands for the averaged current amplitude measured after the onset of depolarization in the range of 25 ± 0.75 ms for cell-attached recordings of Kv3.4; 50 ± 1.5 ms for inside-out recordings of Kv1.4, Kv3.4 and Kv1.4/Kvβ1; 100 ± 3 ms for whole-cell recordings of Kv3.4 and Kvα/Kvβ; 200 ± 6 ms for whole-cell recordings of Kv1.4 and Kv1.4/Kvβ1, or cell-attached recordings of DRG neurons A-type channels. Inactivation index value of 0 represents complete inactivation, while the value of

1 represents no inactivation.

2.2.7.2 Time constant of inactivation

Time constant of inactivation (τ_{inact}) was estimated by fitting current traces, which were elicited by depolarization to 50 mV from a holding membrane voltage of –100 mV, according to Hodgkin-Huxley formalisms (equations (2), (3), (4)) with four activation gates and one inactivation gate (Hodgkin and Huxley, 1952).

$$m(t) = 1 - e^{-t/\tau_{act}} \tag{2}$$

$$h(t) = h_{\infty} + (1 - h_{\infty})e^{-t/\tau_{inact}} \tag{3}$$

$$I(t) = I(0)m(t)^4h(t)^1 \tag{4}$$

The time constant for activation gates is τ_{act} in equation (2); time constant for inactivation gates is τ_{inact}, and h_{∞} denotes the steady-state non-inactivating fraction of current in equation (3); I(0) stands for peak current at time zero of depolarization in equation (4).

3 Results

3.1 Modulation of N-type inactivation in α subunit Kv channels by stress mediators

3.1.1 Modulation of action potentials and A-type Kv channels in DRG neurons

To investigate the regulation of electrical signaling in DRG neurons by stress mediators, the physiologically generated cellular messenger polysulfide (Kimura et al., 2013) was selected. Single APs were evoked from DRG neurons with 10-ms current injection in the current-clamp mode; the current amplitude was chosen about 10 pA above the threshold for AP generation (Figure 11A). Extracellular application of the polysulfide donor Na_2S_4 at 50 μM concentration for 300 s consistently increased the AP width by about 15% (Figure 11B) whereas AP rise time and peak amplitude were not changed compared to normal bath solution application (Figure 11C, D).

Since A-type Kv channels play vital roles in defining the AP shape (Ritter et al., 2012; Zemel et al., 2018), the effect of Na_2S_4 on native A-type Kv channels was also examined. In DRG neurons, native A-type K^+ currents were recorded in the cell-attached configuration where the cytoplasmic milieu remains largely undisturbed. In the particular case illustrated in Figure 12A, inactivation of A-type K^+ current at 100 mV was slowed down considerably after pre-incubation of the cells with 50 μM Na_2S_4 for 16 min; the slow-down effect on inactivation was observed after pre-incubation of the cells with Na_2S_4 for 2 min and remained constant up to pre-incubation for 38 min (Figure 12B). The modulation of native A-type Kv channel inactivation from DRG neurons by Na_2S_4 could possibly explain the effect of Na_2S_4 on AP shape (Figure 11).

The data shown above indicate that the AP shape and the inactivation of native A-type Kv channels of DRG neurons, most likely Kv1.4 and Kv3.4, can be modified by the

polysulfide Na_2S_4. However, the regulation of specific A-type Kv channels by H_2S, polysulfides and other stress mediators and the underlying molecular mechanisms remained to be investigated. Therefore, the effects of these stress mediators on A-type K^+ currents mediated by Kv1.4 and Kv3.4 were subsequently studied in a heterologous expression system — HEK293T cells.

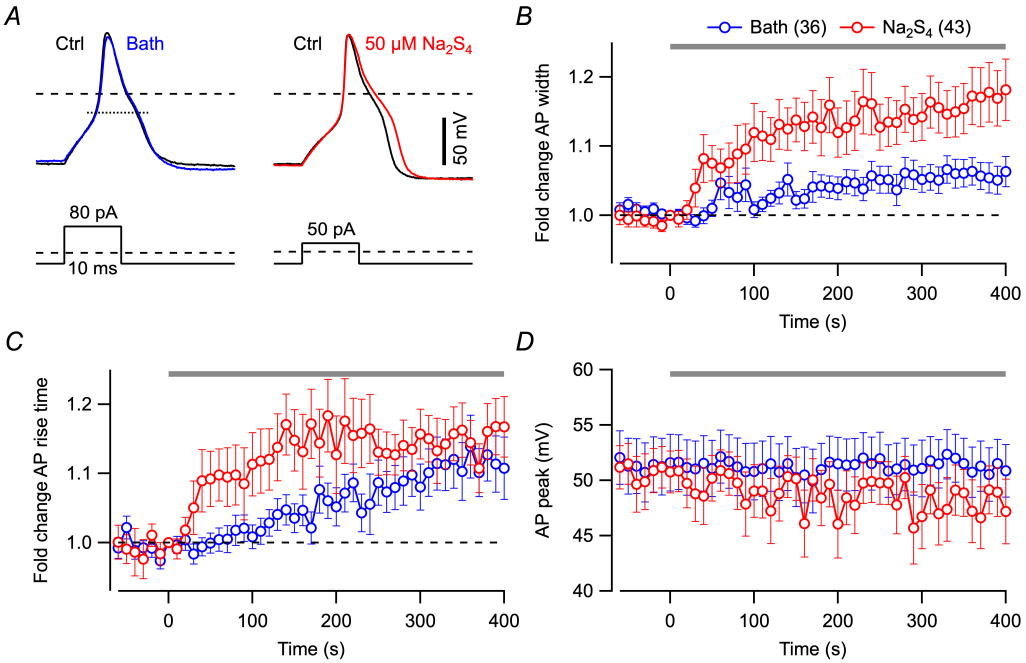

Figure 11: Effect of polysulfide on evoked APs in mouse DRG neurons

A. Superposition of representative APs evoked with the indicated current injections (bottom) before (black) and 300 s after extracellular application of normal bath solution (left, blue) or 50 μM Na_2S_4 (right, red) for DRG neurons from wild-type C57BL/6J mice. The threshold used to measure the AP width (the interval between threshold crossings) is indicated with dotted line at –20 mV in the left panel. Dashed lines indicate 0 mV (top) and 0 pA (bottom). Fold change of AP width (***B***), fold change of AP rise time (***C***), and AP peak voltage (***D***) as a function of time for normal bath solution (blue circles) or 50 μM Na_2S_4 (red circles) application, indicated by the horizontal bar from time zero to 400 s. Data are means ± SEM with individual experiment numbers n in parentheses (in ***B***, but same numbers for ***C*** and ***D***). Straight lines connect the data points. The means of AP width fold changes between 100 s and 400 s after application of normal bath solution and 50 μM Na_2S_4 are different according to a two-sided Student's t-test with P value 0.008, while there are no statistical differences for AP rise time fold change and peak voltage.

3.1.2 Effects of NaHS on Kv1.4 N-type inactivation

To examine whether the N-type inactivation of Kv1.4 channels can be acutely regulated by H_2S, rat Kv1.4 channels (rat Kcna4) were heterologously expressed in HEK293T cells. Because H_2S is toxic and difficult to handle, the widely used H_2S donor NaHS (Abe and Kimura, 1996; Peers et al., 2012; Feng et al., 2013) was employed rather than applying H_2S gas. The ionic currents through all Kv1.4 channels in the plasma membrane of HEK293T cells were assayed in the whole-cell patch-clamp recording mode. Because H_2S as well as

its donor NaHS are membrane permeable (Kimura, 2015), the compounds were applied to the extracellular side of the cells examined.

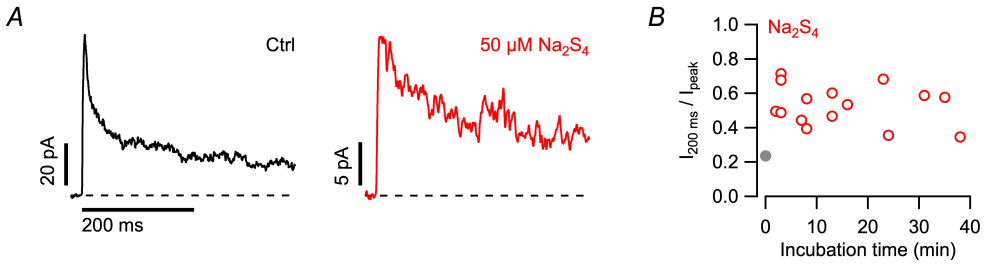

Figure 12: Modulation of native A-type Kv channels from DRG neurons by polysulfide

A. Cell-attached current traces from DRG neurons with depolarization to 100 mV from a holding potential of –100 mV, under control conditions (left) and after incubating with 50 μM Na_2S_4 for 16 min (right). ***B***. Inactivation indices ($I_{200\ ms}/I_{peak}$) for cell-attached current traces as a function of 50 μM Na_2S_4 incubation time for DRG neurons. The gray data point represents control recordings: mean ± SEM (n = 7).

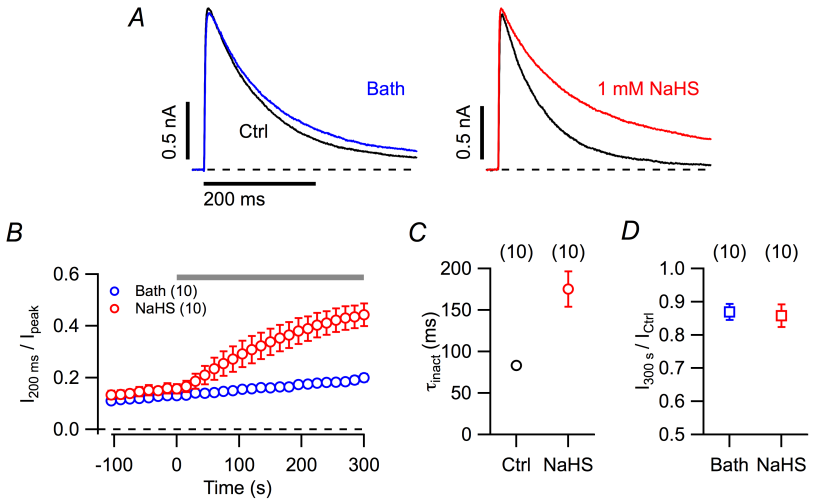

Figure 13: NaHS slows down N-type inactivation of Kv1.4

A. Whole-cell current traces of Kv1.4 channels before (black) and 300 s after application of normal bath solution (left, blue) or 1 mM NaHS freshly prepared in bath solution (right, red). ***B***. Time course of inactivation indices ($I_{200\ ms}/I_{peak}$). Either normal bath solution (blue circles) or 1 mM NaHS (red circles) was applied from time zero to 300 s. ***C***. Time constant of inactivation (τ_{inact}) before (black) and 300 s after application of 1 mM NaHS (red). ***D***. Peak current amplitude change, which was indicated by the ratio between peak current amplitude after 300 s application ($I_{300\ s}$) of normal bath solution (blue) or 1 mM NaHS (red), and peak current amplitude before application (I_{Ctrl}).

With both bath and pipette solutions adjusted to physiological pH 7.4, Kv1.4 channels were activated and then rapidly inactivated by repeatedly depolarizing to 50 mV for 400 ms from a holding potential of –100 mV (Figure 13A). Under this condition, channel inactivation had a mean time constant (τ_{inact}) of 83.3 ± 1.9 ms (n = 10) (Figure 13C). With 1 mM NaHS extracellularly applied at time zero, the inactivation of Kv1.4 was consistently slowed down as indicated by the increase of inactivation index ($I_{200\ ms}/I_{peak}$) (Figure 13B, red circles). After 300 s, the τ_{inact} increased more than twofold to 175 ± 21 ms (n = 10) (Figure 13C). Probably because of the existence of a cysteine residue (C13) in

the N-terminal ball domain of Kv1.4, which can be oxidized after cytosol mixing with the oxygen ambient pipette solution (Ruppersberg et al., 1991b), a slow and consistent loss of inactivation was noticed under the condition of no application or only with normal bath solution applied (Figure 13B, blue circles).

These results clearly demonstrated that NaHS impairs the transition of Kv1.4 channels from the open state (O) to the inactivated state (I) by slowing down the inactivation time constant. The recovery transition from the inactivated state back to the open state (I→O) upon NaHS application was investigated indirectly. For application of both normal bath solution and 1 mM NaHS, the peak current was reduced by about 10% after 300 s (Figure 13D). The peak current remained stable after NaHS application, which suggested the effect of NaHS on inactivation recovery was not notable, indicating that recovery from inactivation was resistant to NaHS application.

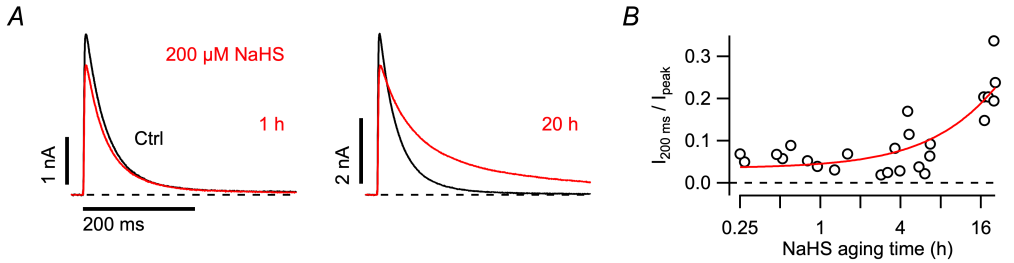

Figure 14: Effects of "fresh" and "aged" NaHS on Kv1.4 inactivation

A. Whole-cell current traces of Kv1.4 channels before (black) and 150 s after application of 200 μM NaHS (red), which was diluted from 500 mM stock concentration of NaHS prepared and stored in normal bath solution for 1 h (left, red) or 20 h (right, red) before the experiments were performed. ***B***. Inactivation indices after application of 200 μM NaHS for 150 s as a function of NaHS "aging" time. As in ***A***, 200 μM NaHS was diluted from 500 mM NaHS prepared for indicated times. The fit with the continuous curve shows the potency of 200 μM NaHS on Kv1.4 inactivation increased with NaHS "aging" time. Experiments were performed at pH 6.9.

In order to explore whether the slow-down effect on inactivation of Kv1.4 by NaHS is concentration dependent, similar experiments were performed with 200 μM NaHS. For better clarity of the effect at lower concentration, a more stable and accelerated inactivation is needed. Because Kv1.4 N-type inactivation depends on the intracellular pH, the N-type inactivation is more stable and faster at pH 6.9 (Padanilam et al., 2002), so both bath and pipette solutions were adjusted to pH 6.9. NaHS at 200 μM had a variable impact on Kv1.4 inactivation, ranging from nearly no effect to a marked slowing of inactivation (Figure 14A). The difference among these recordings was the time duration between preparing stock 500 mM concentration of NaHS in the normal bath solution and the application of diluted 200 μM NaHS. Therefore, systematic experiments were performed with 200 μM NaHS from various "aged" 500 mM NaHS solutions, i.e., high concentration of 500 mM NaHS was prepared in normal bath solution and stored in a closed 1.5-ml reaction tube for

variable durations. The inactivation index $I_{200\ ms}/I_{peak}$ upon 150 s application of 200 μM NaHS, the potency of slowing down inactivation of Kv1.4, was increased with NaHS "aging" time (Figure 14B).

3.1.3 Impact of polysulfides on N-type inactivation of Kv1.4

The potency of slowing down Kv1.4 channel inactivation by NaHS increased with "aging", suggesting that polysulfides (Na_2S_n, with sulfur atoms number n = 2-7) spontaneously generated in NaHS solutions are the active modulators of Kv1.4 function (also see Greiner et al. (2013); Kimura et al. (2013)). Therefore, the donors of polysulfides in sodium salts (Na_2S_2, Na_2S_3 and Na_2S_4) were evaluated for their potential to affect the inactivation of Kv1.4 channels.

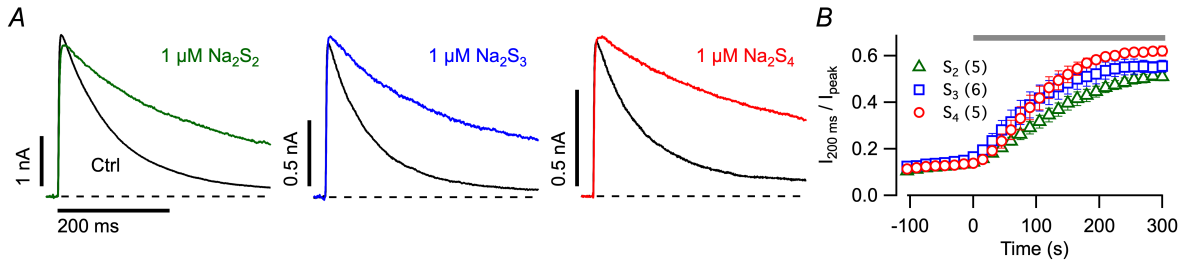

Figure 15: Impact of polysulfides on Kv1.4 inactivation

A. Whole-cell current traces of Kv1.4 channels before (black) and 300 s after application of 1 μM of polysulfide donors Na_2S_2 (green), Na_2S_3 (blue), and Na_2S_4 (red). ***B***. Time course of inactivation indices for the indicated polysulfides, applied at 1 μM concentration at time zero.

Polysulfides at the concentration of 1 μM effectively slowed down Kv1.4 channels inactivation, with the potency increasing with the number of sulfur atoms (Na_2S_4 > Na_2S_3 > Na_2S_2, Figure 15). Probably because the larger number of sulfur atoms in polysulfide is, the more readily for it to receive electrons from active cysteine and transfer its sulfur atoms to cysteine (Kimura, 2015). Therefore, cysteine residues in Kv1.4 can be modified more easily.

Tenfold lower or higher concentration of Na_2S_4, the most potent one among these tested polysulfides in impairing Kv1.4 channels function, was also applied. Even at 100 nM, Na_2S_4 notably slowed down Kv1.4 channel inactivation after 300 s (Figure 16A). The inactivation index after both 1 μM and 10 μM Na_2S_4 application saturated at about 0.6, corresponding to the remaining slow-inactivation (C-type) of Kv1.4 channels (Heinemann et al., 1996; Sahoo et al., 2013). On the one hand this indicated that C-type inactivation is resistant to polysulfides, on the other it also shows that N-type inactivation is completely abolished by the respective treatment with polysulfides.

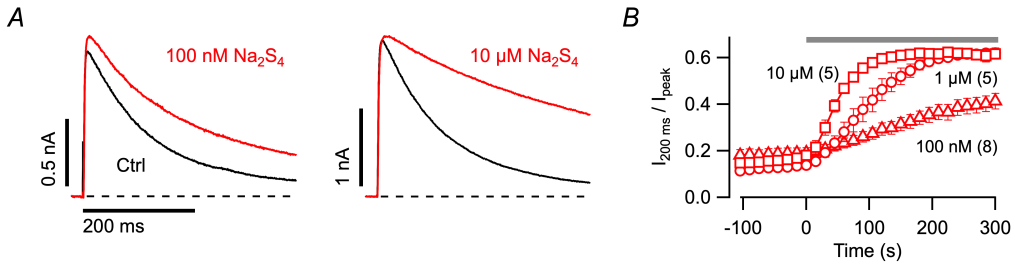

Figure 16: Effects of different concentrations of Na_2S_4 on Kv1.4 inactivation

A. Whole-cell current traces of Kv1.4 channels before (black) and 300 s after extracellular application of Na_2S_4 at concentrations of 100 nM (left, red) and 10 μM (right, red). ***B***. Time course of inactivation indices for different concentrations of Na_2S_4. Straight lines connect the data points.

As shown in Figure 17, after Kv1.4 channel inactivation was largely impaired by application of 10 μM Na_2S_4, the effect remained stable upon washing with normal bath solution. But the inactivation was restored after subsequent application of the reducing agent DTT at 5 mM, suggesting that the oxidation-sensitive cysteine residue (C13) in the N terminus of Kv1.4 channel was first modified by Na_2S_4 and then the effect was eliminated by DTT.

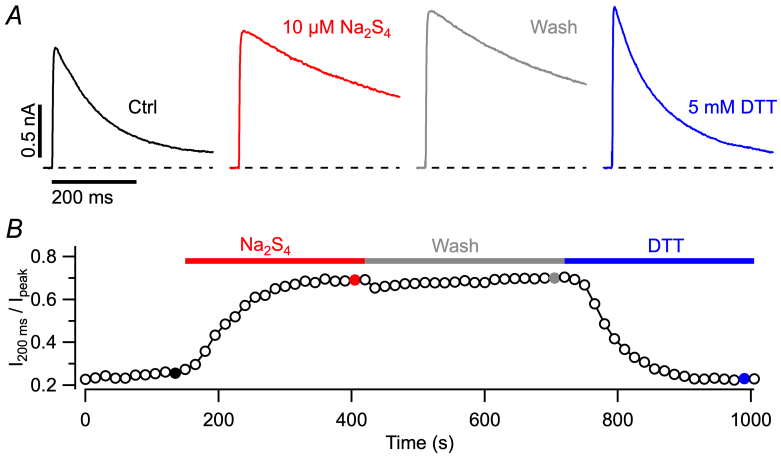

Figure 17: Restoration of Kv1.4 inactivation by DTT

A. Whole-cell current traces of Kv1.4 channels before (black) and 255 s after application of 10 μM Na_2S_4 (red), subsequent wash with normal bath solution (gray), followed by bath solution with 5 mM DTT (blue). ***B***. Time course of inactivation indices for the indicated applications. The highlighted filled data points correspond to the current traces shown in ***A***.

To further characterize the type of cysteine protein modification in the channel's N-terminal domain by polysulfide, a recombinant peptide encoding the first 61 residues of Kv1.4 (Pep61) was produced and purified as described before (Sahoo et al., 2013) and then Pep61 incubated with polysulfide was analyzed with mass spectroscopy. During the sample preparation, iodoacetamide (IAM) was used to alkylate cysteine residues to irreversibly prevent the reformation of disulfide bonds between free thiol groups (Gundry et al., 2009).

After incubating Pep61 with 200 μM Na_2S_4, a strong peak with 32 Da mass increase was observed (Figure 18A, red). This increase demonstrated the addition of one sulfur

atom to Pep61; peaks with 64 Da, 96 Da, or 128 Da mass increase showing the add-on of more sulfur atoms were very weak (Figure 18A, red). Possibly because of the limitation of sample preparation with IAM or the instability of polythiols, S-polythiolated Pep61 (e.g., pep-S(-S-S-S-AM), or pep-S(-S-S-S-S-AM)) was not readily detected. Consistent with the re-establishment of inactivation by DTT (Figure 17), the main peak was eliminated by this reducing agent (Figure 18A, blue). The mass of a mutant Pep61, harboring the C13S alteration, did not change with Na_2S_4 incubation (Figure 18B). This data evidently demonstrated the persulfidation (S-sulfhydration) of C13 by Na_2S_4 in Pep61. Mass spectrometry analysis was performed by Dr. Ina Coburger from Friedrich Schiller University Jena.

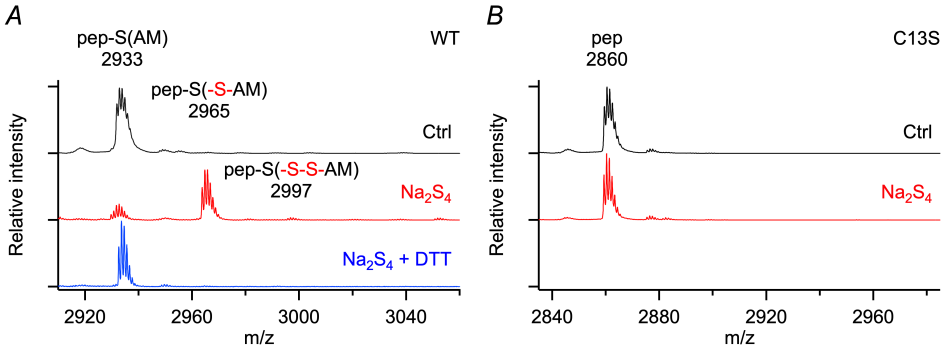

Figure 18: Mass spectroscopy of Kv1.4 N-terminal recombinant peptide

Representative MALDI MS spectra for recombinant peptides encoding the first 61 residues of Kv1.4 N terminus (***A***) and the corresponding mutant C13S (***B***) before (black) and after incubation with 200 μM Na_2S_4 (red). Wild-type (WT) peptide was sulfhydrated (strong signal with 32 Da mass increase and some indication of 64 Da increase in ***A***, red) in contrast to the C13S mutant (***B***, red). Application of 5 mM DTT removed the persulfide (***A***, blue). Peptide was alkylated with iodoacetamide (IAM) and proteolytically digested with trypsin to yield control cysteine-containing peptide (pep-S(AM) or pep-S(-S-AM)) when previously sulfhydrated. The C13S mutant does not contain the AM moiety. "m/z" refers to the ratio of mass (in Dalton) to unitary charge.

3.1.4 Mutants in the ball domain of Kv1.4

To confirm whether C13 of the Kv1.4 channel α subunit mediated the slowing of inactivation by NaHS and Na_2S_4, mutant C13S was generated in an expression vector for mammalian cells. Since the N-terminal histidine residue (H16) contributed to heme/hemin binding to Kv1.4 (Sahoo et al., 2013) and it was also identified as critical site for pH effect on Kv1.4 inactivation (Padanilam et al., 2002), the single histidine mutant H16R as well as the combined mutant with C13S (C13S:H16R) were generated. In comparison with the former wild-type (WT) data, the experiments were performed at pH 7.4, and 1 mM NaHS or 10 μM Na_2S_4 were applied.

In contrast to Kv1.4, the inactivation of its mutant C13S was not slowed down by NaHS or Na_2S_4 (Figure 19A, left). However, the mutant H16R was still sensitive to NaHS and

Na_2S_4 (Figure 19A, middle), but the effect was smaller in comparison to that of Kv1.4 (Figure 19B). For the double mutant C13S:H16R, neither NaHS nor Na_2S_4 increased the inactivation (Figure 19A, right). Notably, when mutant C13S was alone or in combination with H16R (C13S:H16R), the sensitivity of Kv1.4 inactivation to NaHS and Na_2S_4 was completely abolished. This observation suggested that the impairing effects on Kv1.4 inactivation by NaHS and Na_2S_4 were directly mediated by C13 in the N-terminal ball domain of the channel. In addition, both mutants, C13S and C13S:H16R, underwent a slow and consistent inactivation loss under control condition, but this trend was stopped and even accelerated upon NaHS and Na_2S_4 application (Figure 19B). It is likely that other cysteine residues of these mutants play a minor role in the regulation of inactivation by NaHS and Na_2S_4.

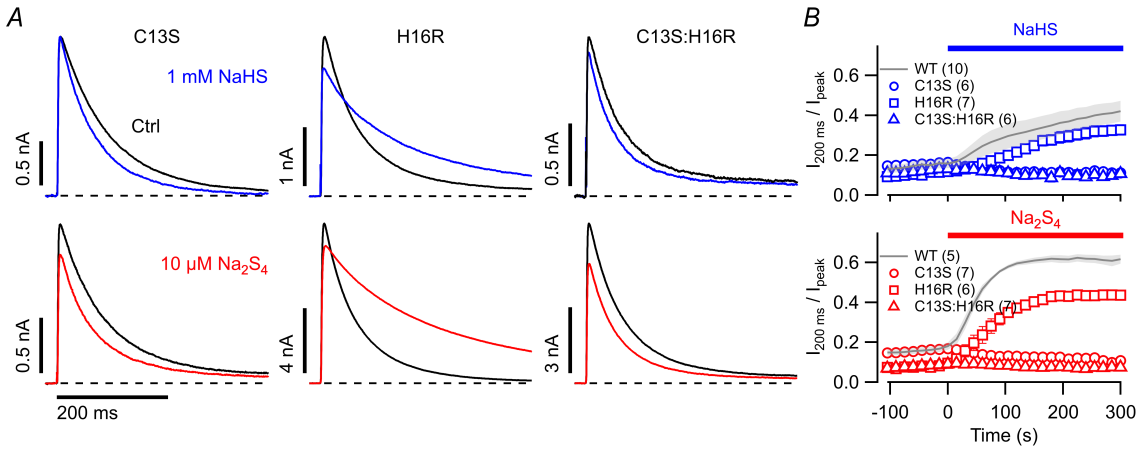

Figure 19: Effects of NaHS and Na_2S_4 on inactivation of Kv1.4 N-terminal mutants

A. Whole-cell current traces of Kv1.4 mutants C13S (left), H16R (middle), and C13S:H16R (right) before (black) and 300 s after application of 1 mM NaHS (top, blue) and 10 μM Na_2S_4 (bottom, red). ***B***. Time course of inactivation indices with application of NaHS (top) and Na_2S_4 (bottom) for WT and indicated mutants. The reference WT data were previously shown in Figure 13B and 16B.

Because inactivation of Kv1.4 mutant C13S:H16R was insensitive to NaHS and Na_2S_4 (Figure 19), this mutant was also used to study whether other functional aspects of Kv1.4 channels can be modified by polysulfide. As shown in Figure 20, neither the reversal potential nor the voltage dependence of activation were apparently changed after 7.5 min treatment with 10 μM Na_2S_4.

3.1.5 Regulation of Kv1.4 N-type inactivation by glutathionylation

So far, the inactivation of Kv1.4 has been shown to be sensitive to H_2S and polysulfides by modifying the cysteine residue (C13) in the channel's N-terminal inactivation ball domain.

Under physiological conditions, a millimolar concentration of reduced GSH (glutathione) exists in mammalian cells to maintain the reducing conditions of the cytosol (Griffith, 1999). Therefore, the effect of the cysteine glutathionylation inducing agent diamide on Kv1.4 N-type inactivation was studied. Upon the application of 10 μM diamide, the inactivation of Kv1.4 channel was slowed down (Figure 21). This data is compatible with previous reports of cysteine-specific modifiers (e.g., DTNP (2,2'-dithio-bis[5-nitropyridine])) modulate Kv1.4 N-type inactivation (Stephens et al., 1996b; Hsieh, 2008).

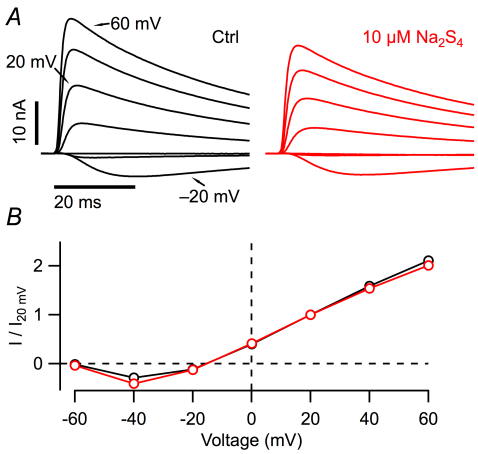

Figure 20: Impact of Na_2S_4 on the current-voltage relationship of Kv1.4-C13S:H16R

A. Whole-cell current traces of Kv1.4 channels mutant C13S:H16R, which were recorded in response to membrane depolarization to 60 mV from –60 mV in steps of 20 mV before (black) and 7.5 min after application of 10 μM Na_2S_4 (red). Current traces at depolarizing voltages –20 mV, 20 mV and 60 mV were labeled with arrow lines. ***B***. Maximal current amplitudes were normalized to that at 20 mV depolarizing voltage, from experiments as in ***A***, as a function of membrane depolarizing voltage before (black circles) and 7.5 min after Na_2S_4 application (red circles). Straight lines connect the data points, n = 7.

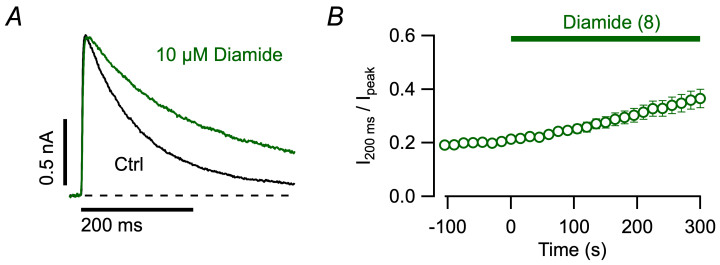

Figure 21: Diamide slowed down Kv1.4 inactivation

A. Whole-cell current traces of Kv1.4 channels before (black) and 300 s after application of 10 μM diamide (green). ***B***. Time course of inactivation indices.

3.1.6 Impact of RSS on Kv3.4 N-type inactivation

The Kv3.4 channel, encoded by Kcnc4 gene, is another A-type Kv channel and prominently expressed in DRG neurons. Upon oxidation of cysteine (Ruppersberg et al., 1991b; Stephens and Robertson, 1995) or phosphorylation of serine residues (Covarrubias et al., 1994; Beck et al., 1998) in the N termini of Kv3.4, the N-type inactivating channel can be converted to non-inactivating delayed rectifier type. The results of Kv1.4 showed that cysteine residue (C13) in the ball domain is necessary for the sensitivity of the channel to H_2S, polysulfides, and diamide. It was quite likely that Kv3.4, with cysteine residues (C6

and C24) in its N-terminal ball domain, can be modified by these stress mediators as well. Therefore, similar experiments were performed for Kv3.4 channels.

The rat Kv3.4 channels were exogenously expressed in HEK293T cells and their function was evaluated by means of the whole-cell patch-clamp. After depolarizing to 50 mV from –100 mV holding potential for 200 ms, Kv3.4 channels were activated and then rapidly inactivated with a mean inactivation time constant τ_{inact} of 18.8 ± 1.9 ms (n = 8) (Figure 22A, top), which was about fourfold faster than that of Kv1.4 (83.3 ± 1.9 ms, n = 10; Figure 13) at the same pH value.

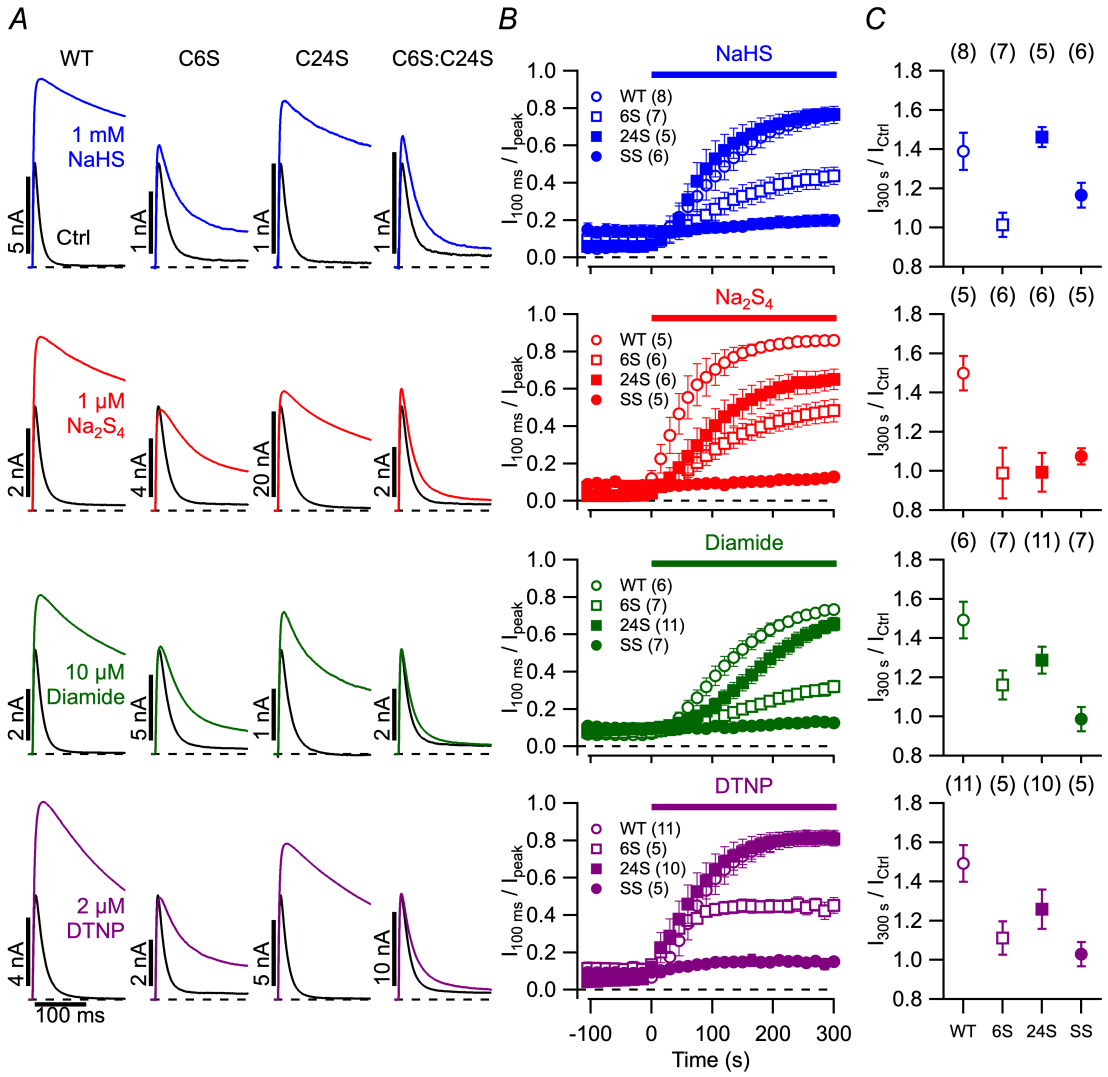

Figure 22: Effects of different stress mediators on N-type inactivation of Kv3.4

A. Whole-cell current traces of Kv3.4 channels before (black) and 300 s after application with 1 mM NaHS (blue, top), 1 μM Na_2S_4 (red, second row), 10 μM diamide (green, third row), and 2 μM DTNP (purple, bottom) for Kv3.4 (WT) (first column) and cysteine mutants C6S (6S), C24S (24S) and C6S:C24S (SS) (rest columns). Time course of inactivation indices for WT and different mutants (***B***), and peak current amplitude changes (***C***).

During the 300 s time course of 1 mM NaHS or 1 μM Na_2S_4 administration, the inacti-

vation of Kv3.4 was substantially impaired, increasing the inactivation index ($I_{100\ ms}/I_{peak}$) from 0.07 ± 0.01 to 0.76 ± 0.05 (n = 8) (Figure 22B, top) for NaHS, and from 0.06 ± 0.02 to 0.86 ± 0.02 (n = 5) (Figure 22B, second row) for Na_2S_4. These end inactivation indices are much larger than those of Kv1.4 ($I_{200\ ms}/I_{peak}$) at 0.44 ± 0.04 (n = 10) (Figure 13B, red) for NaHS, and 0.62 ± 0.02 (n = 5) (Figure 15B, red) for Na_2S_4. Most likely because N-type inactivation in Kv3.4 is much more prominent than C-type inactivation, NaHS and Na_2S_4 resulted in nearly complete loss of N-type inactivation; for Kv1.4 there existed a mixture of N-type and C-type inactivation, and only N-type inactivation in Kv1.4 was regulated by NaHS and Na_2S_4. In addition to the inactivation being nearly fully removed, the peak amplitude of Kv3.4 at 50 mV was drastically increased upon NaHS and Na_2S_4 application (Figure 22C, top and second rows). In similar experiments the peak amplitude of Kv1.4 was stable after NaHS (Figure 13D) and Na_2S_4 (Figure 15A) application. The increase of Kv3.4 peak amplitude by NaHS and Na_2S_4 suggests that N-type inactivation of this channel is the rate-limiting step of ionic current flow (Aldrich et al., 1983).

When the inactivation of Kv3.4 was impaired by 1 μM Na_2S_4 (Figure 23A, red), the effect continued to exist even when the substance was removed by washing, but the inactivation was nearly completely repaired upon washing with DTT containing solution. It is very likely that two cysteine residues C6 and C24 in Kv3.4 N terminus firstly mediated the sensitivity to RSS, and then DTT eliminated the effect.

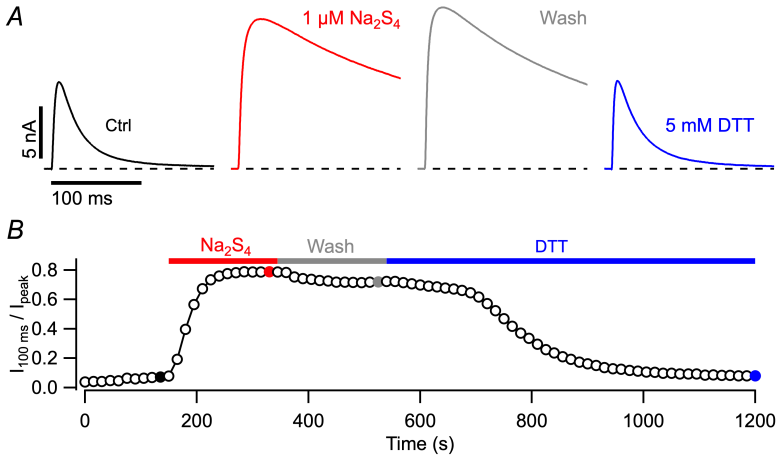

Figure 23: Restoration of Kv3.4 inactivation by DTT

As described in Figure 17, with application of 1 μM Na_2S_4, wash and followed by 5 mM DTT for Kv3.4.

Moreover, comparing to only one cysteine (C13) in the N terminus of Kv1.4, there are two in that of Kv3.4. Hence, mutants of Kv3.4 with single and double cysteine substituted to serine (C6S, C24S and C6S:C24S) were generated and treated with 1 mM NaHS or 1 μM Na_2S_4. After 300 s NaHS application, the inactivation in C24S was considerably slowed to inactivation index of 0.76 ± 0.03 (n = 5) similar as Kv3.4 (WT), while the

inactivation of C6S was only slowed down to a moderate degree with inactivation index of 0.44 ± 0.05 (n = 7). The responsiveness of Kv3.4 to NaHS cannot be abolished unless both cysteine residues were removed (C6S:C24S) (Figure 22B, top). The experiment of 1 μM Na_2S_4 was conducted in the same manner. The inactivation of Kv3.4 C6S and C24S mutants was remarkably but not entirely removed by Na_2S_4; for C6S:C24S, the sensitivity of its inactivation to Na_2S_4 was absent (Figure 22, second row).

Because RSS had almost no effect on the inactivation of the Kv3.4 C6S:C24S mutant, this mutant was also used to study whether other functional aspects of Kv3.4 channels can be modified by RSS. As shown in Figure 24, the voltage dependence of activation of Kv3.4 C6S:C24S was not shifted obviously after application of 1 μM Na_2S_4 for 7.5 min.

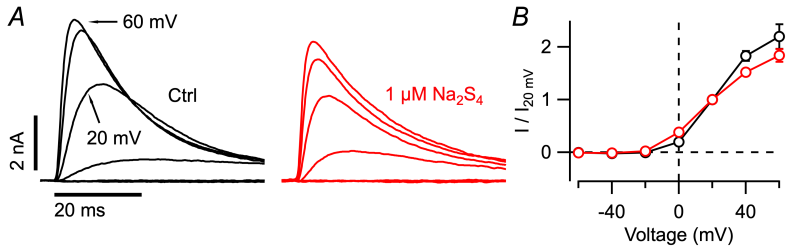

Figure 24: Impact of Na_2S_4 on the current-voltage relationship of Kv3.4-C6S:C24S
For Kv3.4 mutant C6S:C24S (n = 5) as described in Figure 20.

3.1.7 Effects of cysteine-specific modifiers on Kv3.4 N-type inactivation

It has been shown above (Figure 21) and before (Ruppersberg et al., 1991b; Stephens et al., 1996a; Hsieh, 2008) that specific cysteine-modifying reagents (e.g., diamide and DTNP) modulate Kv1.4 inactivation. However, effects of these reagents on Kv3.4 inactivation have not been investigated yet. As shown in Figure 22 (third and bottom rows), the inactivation in Kv3.4 was removed and the peak amplitude was increased by 300 s application of 10 μM diamide or 2 μM DTNP. Consistent with the results for NaHS and Na_2S_4, the mutants decreased the sensitivity of Kv3.4 inactivation to diamide and DTNP to different degrees: C6 seemed to play a major role, with the minor role of C24, but only mutation of C6 combined with C24 (C6S:C24S) fully diminished the sensitivity of inactivation to these reagents.

3.1.8 Polysulfide and cysteine-specific modifier signalings in intact cells

To study the effects of above stress mediators (e.g., Na_2S_4 and diamide) on Kv3.4 channels with a physiological intracellular milieu, recordings were performed in the cell-attached patch-clamp mode. Under control conditions, i.e., no pre-incubation of HEK293T cells expressing Kv3.4 with Na_2S_4 or diamide, Kv3.4 cell-attached current at 50 mV was recorded (Figure 25A, black) and the inactivation index ($I_{25\ ms}/I_{peak}$) was 0.17 ± 0.03 (n = 17) (Figure 25B, gray circles). After pre-incubation of HEK293T cells with 10 μM Na_2S_4 for 16 min or 100 μM diamide for 10 min, inactivation was slowed down notably (Figure 25A, red and blue). There was a clear trend that longer pre-incubation slows down inactivation more efficiently (Figure 25B).

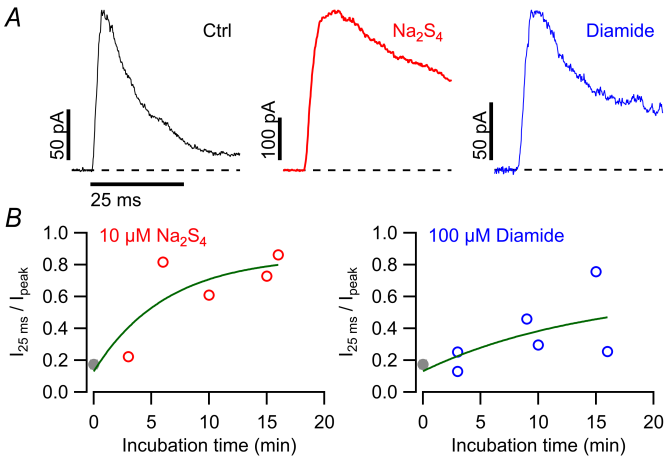

Figure 25: Modulation of Kv3.4 inactivation in intact HEK293T cells by Na_2S_4 and diamide

A. Cell-attached current traces of Kv3.4 channels in normal bath solution (black), 16-min pre-incubation of 10 μM Na_2S_4 (red) and 10-min pre-incubation of 100 μM diamide (blue). ***B***. Inactivation indices ($I_{25\ ms}/I_{peak}$) of Kv3.4 as a function of pre-incubation time with Na_2S_4 (left) and diamide (right). The gray data points with $I_{25\ ms}/I_{peak}$ of 0.17 ± 0.03 (n = 17), indicating experiments under normal bath solution condition. The fit with the continuous curve shows the potency of Na_2S_4 or diamide on Kv3.4 inactivation increased with pre-incubation durations.

To investigate whether Na_2S_4 and diamide changed the intracellular redox status, the redox-sensitive green fluorescent protein 2 (roGFP2) (Dooley et al., 2004) was used as an optical readout system. After treating HEK293T cells transiently expressing roGFP2 with Na_2S_4 (1 μM, 10 μM) and diamide (10 μM, 100 μM) at the concentration range used in this study, fluorescence ratios (F400/F470) of roGFP2 were increased (Figure 26), indicating cytosolic cysteine residues were oxidized. Thus, Na_2S_4 and diamide signaling occurred in intact cells. Fluorescence measurements were performed by Johanna M. Langner from Friedrich Schiller University Jena.

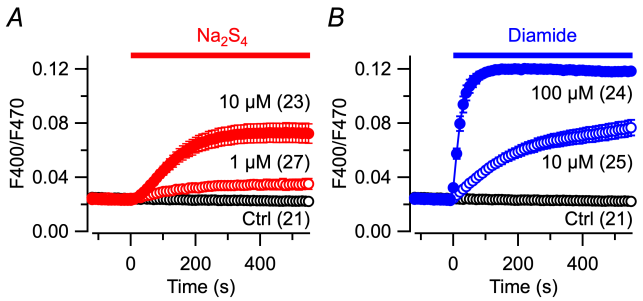

Figure 26: Optical sensing of Na_2S_4 and diamide

A. Time courses of fluorescence ratios (F400/F470) with excitation at 400 nm and 470 nm for HEK293T cells transiently expressing roGFP2. The bar indicates application of Na_2S_4 (1 μM, 10 μM), or normal bath solution (Ctrl) from time zero to 555 s. ***B***. For diamide (10 μM, 100 μM) as in ***A***.

3.1.9 Impact of ROS and RSS on Kv3.4 N-type inactivation

It has been described before that *tert*-butyl hydroperoxide, a generator of reactive oxygen species (ROS), removed the inactivation of Kv3.4 channels (Duprat et al., 1995). In this work the inactivation of Kv3.4 was susceptible to RSS, and many reports have described interactions of ROS and RSS signaling pathways (Kimura and Kimura, 2004; Lu et al., 2008; Sun et al., 2012; Suo et al., 2013; Zhang et al., 2013; Kabil et al., 2014; Hancock and Whiteman, 2016; Spassov et al., 2017). For instance, H_2S protects neurons from oxidative glutamate toxicity by enhancing antioxidant glutathione production (Kimura and Kimura, 2004). Therefore, the interaction of ROS and RSS on Kv3.4 inactivation was investigated. Hydrogen peroxide (H_2O_2) was utilized as the ROS generator and experiments were performed at pH 6.9.

As shown in Figure 27, after applying 200 μM H_2O_2, 100 μM NaHS, or the mixture of 100 μM H_2O_2 and 50 μM NaHS ("Mixed") for 300 s, the inactivation indices ($I_{100\ ms}/I_{peak}$) of Kv3.4 channels were slightly increased, as well as τ_{inact}. Because $I_{100\ ms}/I_{peak}$ were increased to 0.19 ± 0.02 (n = 6) by the "Mixed", and to 0.13 ± 0.02 (n = 6) by 100 μM NaHS, with P = 0.08; and peak currents were increased more by "Mixed" than 200 μM H_2O_2 and 100 μM NaHS, with $P < 0.01$, according to two-sided Student's t-test, thus, the "Mixed" affected the inactivation more potently than only 200 μM H_2O_2 or 100 μM NaHS application. It is likely that the hydrosulfide ion (HS^-) reacted with H_2O_2 to form hydrogen thioperoxide (HSOH), then HSOH reacted with HS^- to form polysulfides (Hoffmann, 1977), which were more potent in regulating the inactivation. The data indicate that RSS do not work in isolation in signaling, and that their potencies of modifying proteins strongly depend on the ROS level.

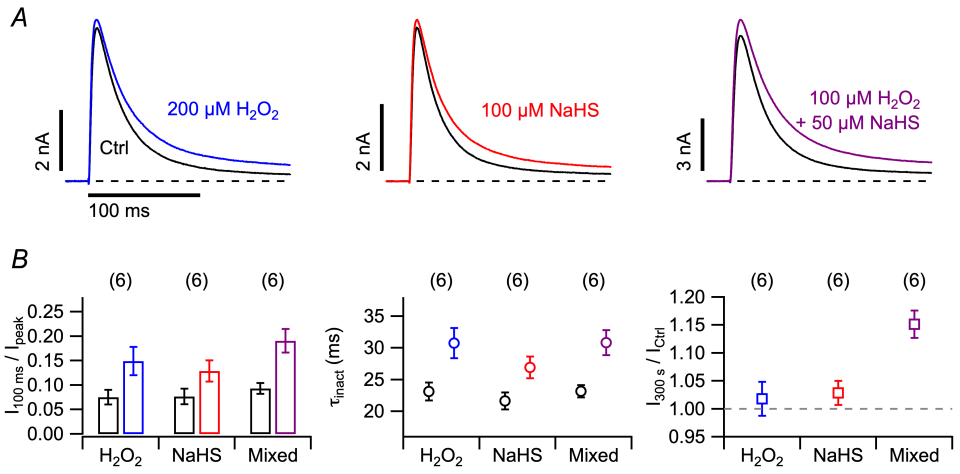

Figure 27: Effects of H_2O_2 and NaHS on Kv3.4 inactivation

A. Whole-cell current traces of Kv3.4 channels before (black) and 300 s after application of 200 μM H_2O_2 (left, blue), 100 μM NaHS (middle, red), or mixture of 100 μM H_2O_2 and 50 μM NaHS ("Mixed"; right, purple). ***B***. Effects of H_2O_2, NaHS, and "Mixed" at the concentrations as in ***A*** on inactivation indices ($I_{100\ ms}/I_{peak}$, left), τ_{inact} (middle) and peak current change ($I_{300\ s}/I_{Ctrl}$, right). Experiments were performed at pH 6.9. $I_{100\ ms}/I_{peak}$ and τ_{inact} means of H_2O_2, NaHS and "Mixed" are different from their own Ctrl groups with P values < 0.01 according to paired two-sided Student's t-tests. Two-sided Student's t-tests were performed between "Mixed", and H_2O_2 and NaHS groups: $P = 0.08$ for "Mixed" vs NaHS ($I_{100\ ms}/I_{peak}$), $P < 0.01$ for "Mixed" vs H_2O_2 and "Mixed" vs NaHS ($I_{300\ s}/I_{Ctrl}$). But there were no statistical differences for "Mixed" vs H_2O_2 ($I_{100\ ms}/I_{peak}$), "Mixed" vs H_2O_2 (τ_{inact}) or "Mixed" vs NaHS (τ_{inact}).

3.2 Modulation of Kvβ subunits induced N-type inactivation by stress mediators

3.2.1 Regulation of Kvβ1.1-induced N-type inactivation of Kv1.1 and Kv1.5 by stress mediators

Among the large family of α subunit Kv channels, only a limited number of them have the ability to induce N-type inactivation, such as Kv1.4 and Kv3.4. However, some auxiliary cytoplasmic Kvβ subunits (e.g., Kvβ1.1) with N-terminal inactivation ball domains can transform the non-inactivating or delayed rectifier type α subunit Kv channels (e.g., Kv1.1 and Kv1.5) to N-type inactivating channels (Rettig et al., 1994; Heinemann et al., 1996). Therefore, experiments were designed to test whether the examined stress mediators (i.e., H_2S, polysulfide, diamide and DTNP) would regulate N-type inactivation induced by Kvβ subunits.

When expressed alone in HEK293T cells, Kv1.1 (Figure 28A, left, black) and Kv1.5 (Figure 28B, left, black) produced non-inactivating K^+ current as previously reported (Heinemann et al., 1996), while coexpression with Kvβ1.1 resulted in rapidly inactivating

current after channels were activated by depolarizing the membrane to 50 mV (Figure 28A and B, middle and right, black). Extracellular application of 1 mM NaHS on Kv1.1 and Kv1.5 channels for 300 s did not alter their inactivation (Figure 28A and B, left, blue), while NaHS potently slowed down the inactivation of Kv1.1/Kvβ1.1 and Kv1.5/Kvβ1.1 complexes (Figure 28A and B, middle, blue). The inactivation index of Kv1.1/Kvβ1.1 was increased from 0.54 ± 0.05 to 0.92 ± 0.02 (n = 8) (Figure 28C, left), and from 0.26 ± 0.05 to 0.63 ± 0.04 (n = 9) for Kv1.5/Kvβ1.1 (Figure 28D, left). The loss of K^+ current inactivation was associated with a peak outward current increase, for Kv1.1/Kvβ1.1 about twofold (Figure 28C, right), for Kv1.5/Kvβ1.1 by 31 ± 9.1% (Figure 28D, right). Similar experiments with 1 μM Na_2S_4 were conducted. Consistent with the responses of Kv1.4 and Kv3.4 to Na_2S_4 application (Figure 15 and 22), the potency of this polysulfide was about 1000 times higher than NaHS in removing the inactivation of Kv1.1/Kvβ1.1 and Kv1.5/Kvβ1.1 with an increase of current amplitude about twofold for both combinations (Figure 28C and D, right).

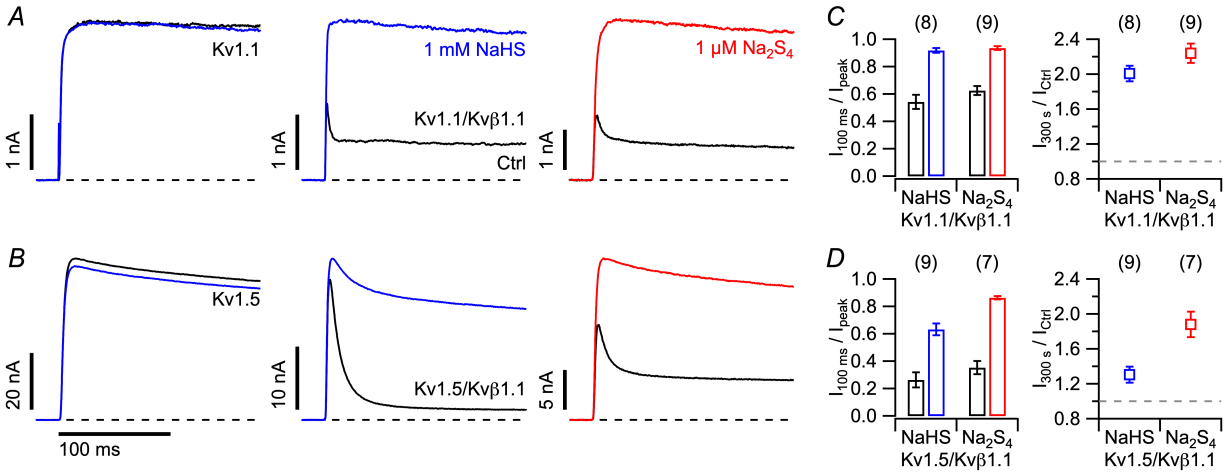

Figure 28: Kvβ1.1 confers NaHS and Na_2S_4 sensitivities to Kv1.1 and Kv1.5

Whole-cell current traces of Kv1.1 (***A***) and Kv1.5 channels (***B***) expressed alone and with Kvβ1.1 before (black) and 300 s after 1 mM NaHS (blue) or 1 μM Na_2S_4 (red) application. Inactivation indices (left) and peak current change (right) for Kv1.1/Kvβ1.1 (***C***) and Kv1.5/Kvβ1.1 (***D***).

Cysteine-specific modifiers diamide and DTNP were shown to modulate the inactivation of Kv1.4 and Kv3.4 (Figure 21 and 22, and see also Stephens et al. (1996a); Hsieh (2008)), so the impacts of these reagents on Kvβ1.1-induced N-type inactivation were studied. Upon application of 10 μM diamide or 20 μM DTNP (Figure 29), the inactivation indices of both Kv1.1/Kvβ1.1 and Kv1.5/Kvβ1.1 were dramatically increased, as well as τ_{inact} and peak current amplitudes.

Thus, the investigated reagents — NaHS, polysulfides, diamide and DTNP — not only impaired α subunit Kv1.4 and Kv3.4 channels N-type inactivation, but also the Kvβ1.1-induced inactivation of non-inactivating Kv1.1 and Kv1.5 channels.

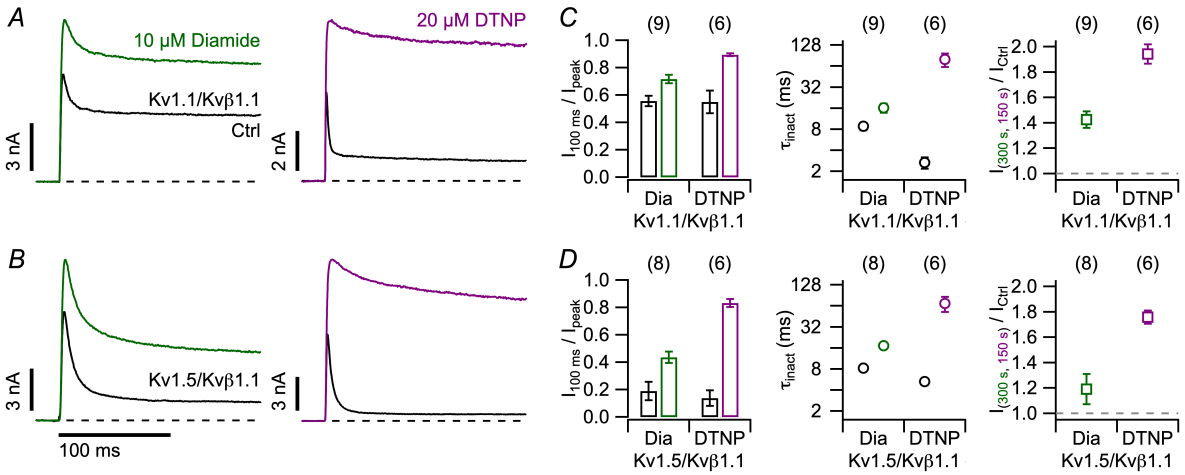

Figure 29: Effects of diamide and DTNP on Kvβ1.1-induced inactivation

Whole-cell current traces of Kv1.1/Kvβ1.1 (***A***) and Kv1.5/Kvβ1.1 (***B***) before (black) and after application of 10 μM diamide (300 s, green) or 20 μM DTNP (150 s, purple). Effects of diamide (Dia) and DTNP on inactivation indices (left), τ_{inact} (middle) and peak current (right) for Kv1.1/Kvβ1.1 (***C***) and Kv1.5/Kvβ1.1 (***D***).

3.2.2 Association of Kv1α subunits and Kvβ1.1 determines sensitivity of Kv1α/Kvβ1.1 inactivation to RSS

Comparison of the investigated reagents' (i.e., NaHS, Na_2S_4, diamide and DTNP) effects on Kv1.4 and Kv3.4 channels suggests that cysteine residue (C7) in the N-terminal ball domain of Kvβ1.1 would be responsible for the removal of inactivation. Therefore, cysteine mutant C7S of Kvβ1.1 (Kvβ1.1-C7S) was generated and expressed together with Kv1.1 and Kv1.5 in HEK293T cells to probe the underlying mechanisms.

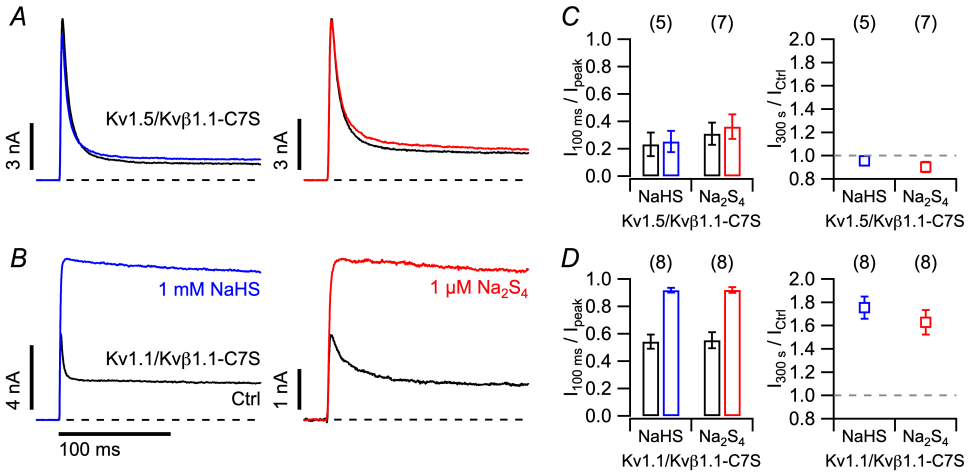

Figure 30: Sensitivity of Kvβ1.1-C7S induced inactivation to NaHS and Na_2S_4 depends on Kvα

As described in Figure 28, for Kv1.5/Kvβ1.1-C7S and Kv1.1/Kvβ1.1-C7S.

As expected, the inactivation of Kv1.5/Kvβ1.1-C7S remained stable after 300 s appli-

cation of 1 mM NaHS and 1 μM Na_2S_4 (Figure 30A) with almost unchanged inactivation index and fractional peak current (Figure 30C). However, the inactivation of Kv1.1/Kvβ1.1-C7S was removed by both NaHS and Na_2S_4 (Figure 30B): the inactivation index was increased from 0.55 ± 0.04 to 0.91 ± 0.02 (n = 8) by NaHS and so did Na_2S_4 (Figure 30D, left); NaHS increased the peak currents by 75 ± 9.6% (n = 8) and similar effect was observed by Na_2S_4 (Figure 30D, right). In addition, the removal effect of NaHS on the inactivation of Kv1.1/Kvβ1.1-C7S was not restored by the washout of NaHS and subsequent application of DTT (Figure 31), excluding the possibility that other cysteine residues of Kvβ1.1-C7S were sulfhydrated by NaHS. The results showed that sulfide species (H_2S and polysulfide) regulate Kvβ1.1-induced N-type inactivation in an α subunit Kv channel dependent manner.

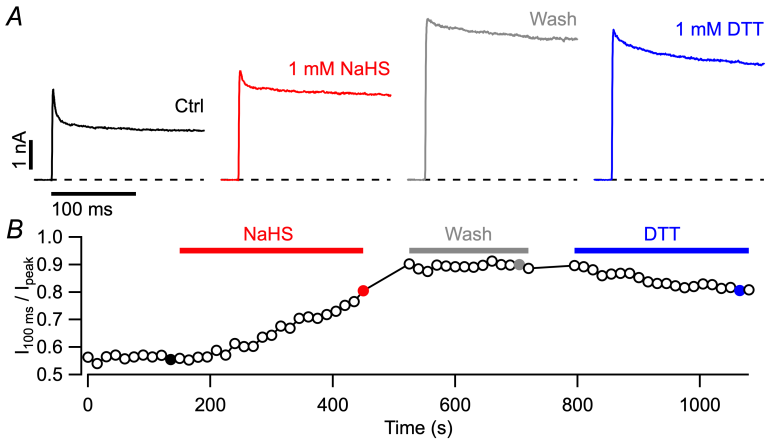

Figure 31: The removal of Kv1.1/Kvβ1.1-C7S inactivation by NaHS cannot be restored by DTT

As described in Figure 17, with application of 1 mM NaHS, washout of NaHS ("Wash") and followed by 1 mM DTT application. Because 75-s current-voltage relationship measurements were performed after NaHS application and "Wash", there are two gaps between the bars of NaHS, "Wash" and DTT application in ***B***.

Similar experiments with the application of the cysteine regulators diamide and DTNP were performed, but inactivation of both Kv1.1/Kvβ1.1-C7S and Kv1.5/Kvβ1.1-C7S remained consistent (Figure 32). The results obtained thus far showed that Kvβ1.1-induced inactivation of Kv1.1 and Kv1.5 can be removed by sulfide species — H_2S and polysulfide (Figure 28) and cysteine modifiers — diamide and DTNP (Figure 29), while the inactivation of Kv1.1 in combination with Kvβ1.1 cysteine mutant (C7S) behaved differently when treated with these two groups of chemicals (Figure 30 and 32).

Whether the removal effect on the inactivation of Kv1.1/Kvβ1.1-C7S by sulfide species was dependent on the core domain of Kvβ1.1 was also tested. Since Kvβ2.1 lacks an N-terminal inactivating ball domain, it does not introduce N-type inactivation to Kv1.1 and Kv1.5 (Heinemann et al., 1996). However, once the N-terminal inactivating ball domain of Kvβ1.1 was spliced to the N terminus of Kvβ2, the chimeric Kvβ sub-

unit N(Kvβ1.1) · C(Kvβ2) induced N-type inactivation of Kv1.1 and Kv1.5 (Heinemann et al., 1996). Therefore, the chimera N(Kvβ1.1) · C(Kvβ2) and its mutant N(Kvβ1.1-C7S) · C(Kvβ2) were generated and coexpressed with Kv1.1 in HEK293T cells and subjected to 1 μM Na_2S_4. After 300 s application of Na_2S_4, their inactivation was substantially modified (Figure 33). Thus, the sensitivity of Kv1.1/Kvβ1.1-C7S inactivation to sulfide species does not rely on the core domain of Kvβ1.1.

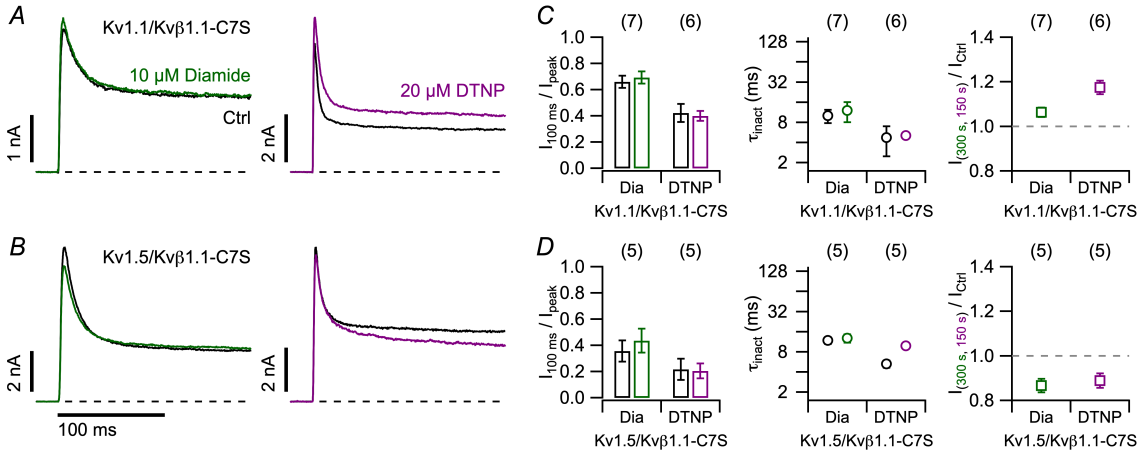

Figure 32: Sensitivity of Kvβ1.1-induced inactivation to diamide and DTNP was eliminated by C7S mutant

As described in Figure 29, for Kv1.1/Kvβ1.1-C7S and Kv1.5/Kvβ1.1-C7S.

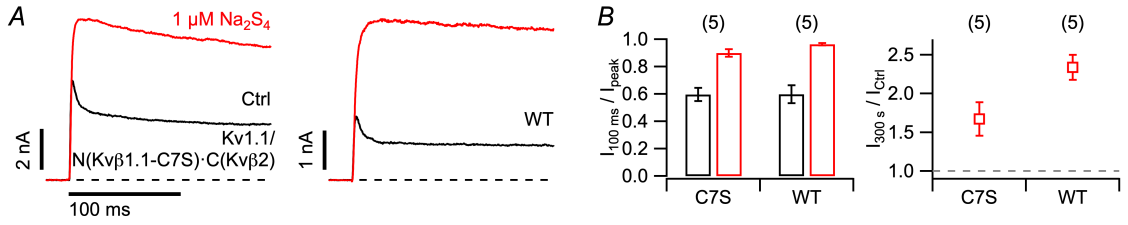

Figure 33: Modulation of Kv1.1/N(Kvβ1.1) · C(Kvβ2) inactivation by Na_2S_4

A. Whole-cell current traces of Kv1.1 channels coexpressed with N(Kvβ1.1-C7S) · C(Kvβ2) (C7S) and N(Kvβ1.1) · C(Kvβ2) (WT) before (black) and after application of 1 μM Na_2S_4 for 300 s (red). ***B***. Change of inactivation indices (left) and peak current (right) upon Na_2S_4 application.

It has been reported that Kvβ1.1-induced N-type inactivation is controlled by the enzymatic activity of the subunit's core domain using NADPH (reduced nicotinamide adenine dinucleotide phosphate) as a cofactor (Pan et al., 2008a). Once Kvβ1.1-bound NADPH was modified by the substrate 4-cyanobenzaldehyde (4-CY), the N-terminal ball domain was restrained resulting in a loss of inactivation (Pan et al., 2011). Two arginine residues R37 and R48 in the N terminus and two glutamic acid residues E265 and E349 in the core domain of Kvβ1.1 are important in this process (Pan et al., 2011). The inactivation of Kv1.1/Kvβ1.1-C7S:E349K did not show a notable response to 4-CY (Pan et al., 2011; Swain et al., 2015). This mutant was used to explore the impact of Na_2S_4 on the enzymatic activity of Kvβ1.1's core domain.

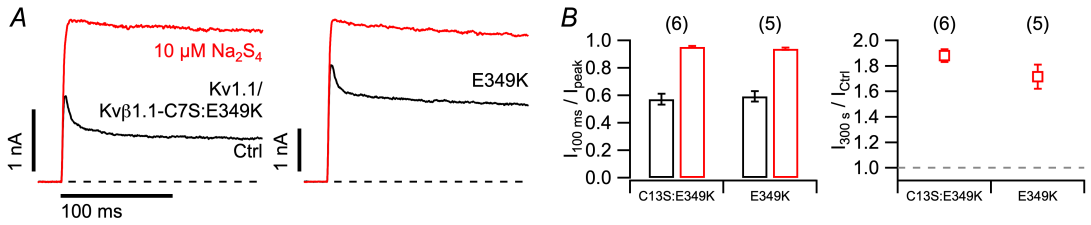

Figure 34: Na_2S_4 sensitivity of Kvβ1.1 is functionally independent of its enzymatic activity

A. Whole-cell current traces of Kv1.1 channels coexpressed with Kvβ1.1 mutants C7S:E349K and E349K before (black) and after application of 10 μM Na_2S_4 for 300 s (red). ***B***. Change of inactivation indices (left) and peak current (right) upon Na_2S_4 application.

As shown in Figure 34, application of 10 μM Na_2S_4 to Kv1.1/Kvβ1.1-C7S:E349K removed inactivation efficiently, with similar effect on Kv1.1/Kvβ1.1-E349K. So the sensitivity of Kvβ1.1 induced inactivation of Kv1.1 to Na_2S_4 is functionally independent of its enzymatic activity.

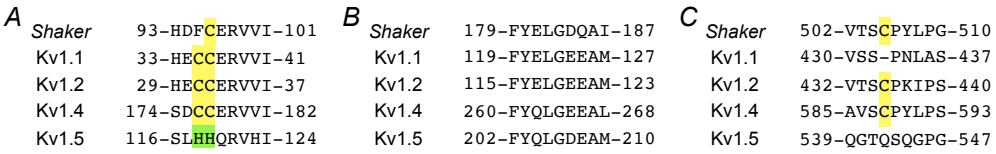

Figure 35: Alignment of *Shaker*, Kv1.1, Kv1.2, Kv1.4 and Kv1.5

Alignment of partial amino acid sequences of *Drosophila Shaker*, rat Kv1.1, human Kv1.2, rat Kv1.4 and human Kv1.5 amino acid sequences of distal N termini (***A***), Kvα/Kvβ1.1 interaction sites (***B***) and C termini (***C***) with cysteine and histidine residues highlighted.

Because the inactivation of Kv1.1 and Kv1.5 conferred by Kvβ1.1-C7S had diverse sensitivities to sulfide species (Figure 30), further research was focused on the difference between Kv1.1 and Kv1.5. As *Shaker*-related subfamily (Kv1, Kcna) members, Kv1.1 and Kv1.5 have conserved sequence motifs for Kvβ1.1 binding (Figure 35B) (Sewing et al., 1996). In the distal N terminus, two cysteine residues are located at position 35 and 36 (C35 and C36) in Kv1.1, C31 and C32 in Kv1.2, and C176 and C177 in Kv1.4, while Kv1.5 harbors two histidine residues (H118 and H119) at equivalent positions (Figure 35A). These cysteine residues may mediate the eliminating effect of NaHS and Na_2S_4 on inactivation even when C7 in Kvβ1.1 was mutated (Kv1.1/Kvβ1.1-C7S).

To explore the roles of C35 and C36 in Kv1.1, individual cysteine mutants C35A and C36A, and double cysteine mutant C35A:C36A of Kv1.1 were generated. After coexpressing with Kvβ1.1-C7S in HEK293T cells, Kv1.1-mutants/Kvβ1.1-C7S channel complexes functioned well with rapid N-type inactivation at 50 mV (Figure 36A, black). Upon extracellular application of 1 mM NaHS for 300 s, however, NaHS was ineffective in removing the inactivation of all assessed Kv1.1 mutants when coexpressed with Kvβ1.1-C7S (Figure 36A), with only little effect on inactivation indices and peak current amplitudes (Figure

36C). Additionally, experiments of Kv1.1 cysteine mutants in combination with Kvβ1.1 were carried out. After exposing to 1 mM NaHS for 300 s, the inactivation of all combinations was removed or slowed down considerably (Figure 36B and D). This finding suggests that sulfide species (H_2S and polysulfide) not only sulfhydrate cysteine residue (C7) of Kvβ1.1 subunit, but they also modulate cysteine residues of Kv1.1 channel α subunits.

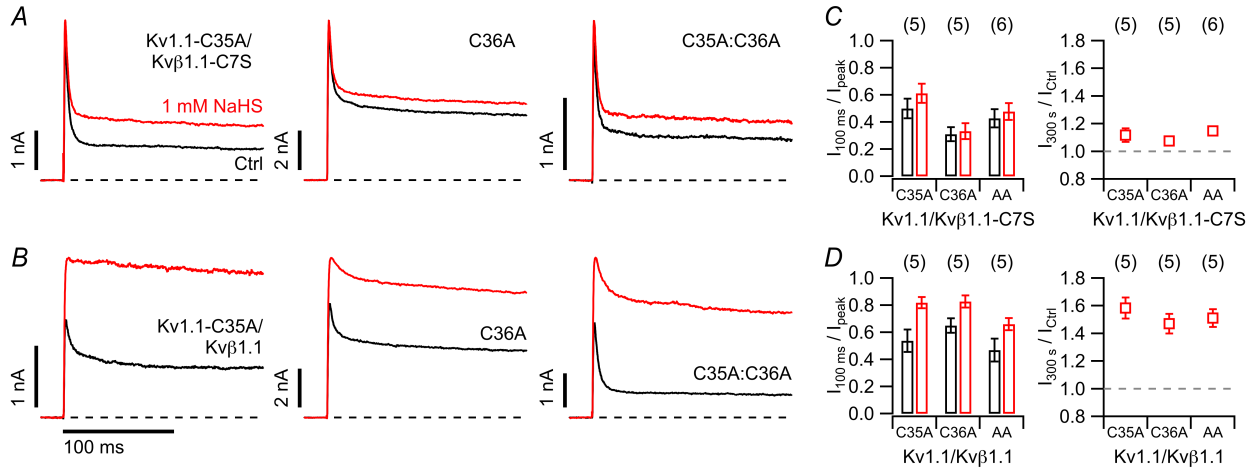

Figure 36: Effect of NaHS on Kv1.1 mutants coexpressed with Kvβ1.1

Whole-cell current traces of Kv1.1 cysteine mutants C35A, C36A and C35A:C36A (AA) coexpressed with Kvβ1.1-C7S (***A***) or Kvβ1.1 (***B***) before (black) and 300 s after application of 1 mM NaHS (red). ***C***. and ***D***. Change of inactivation indices (left) and peak current (right) upon NaHS application.

3.2.3 Regulation of Kv1.2/Kvβ1.1 inactivation by NaHS

Consistent with a previous report (Heinemann et al., 1996), the non-inactivating Kv1.2 channel gained N-type inactivation upon coexpression with Kvβ1.1 (Figure 37A, black). After application of 1 mM NaHS for 300 s, the inactivation of Kv1.2 was not altered (Figure 37A, left), but the inactivation of Kv1.2/Kvβ1.1 was largely impaired (Figure 37A, middle) with the increase of inactivation index from 0.44 ± 0.07 to 0.95 ± 0.02 (n = 7) and peak current was increased about twofold (1.93 ± 0.25, n = 7) (Figure 37B). When the C7S mutant of Kvβ1.1 was coexpressed with Kv1.2, NaHS slowed down the inactivation moderately (Figure 37A, right): the inactivation index was increased from 0.46 ± 0.05 to 0.60 ± 0.05 (n = 12) and current amplitude was increased by 27 ± 4% (n = 12) (Figure 37B). Similar effects were observed after 300 s application of 10 μM Na_2S_4 on Kv1.2/Kvβ1.1-C7S (Figure 38). Thus, C7 in Kvβ1.1 mainly mediated the effects of sulfide species on the inactivation of Kv1.2/Kvβ1.1.

In *Shaker* K^+ channels, intrasubunit disulfide bridges are formed between cysteine residues in the N terminus (C96) and C terminus (C505) under oxidizing conditions (Schul-

teis et al., 1996). Interestingly, in the C-terminal sequence alignment of *Shaker*, Kv1.1, Kv1.2, Kv1.4 and Kv1.5 channels (Figure 35C), there is one cysteine (C435) located at the equivalent position of Kv1.2 as *Shaker* (C505). An intrasubunit disulfide bridge could also be formed in Kv1.2 between C31 or C32 and C435 upon sulfide species application as disulfide bridge formation between C96 and C505 in *Shaker* K^+ channels upon oxidation (Schulteis et al., 1996), and then affect the inactivation of Kv1.2/Kvβ1.1 channel complex. Therefore, Kv1.2-C435S mutant was generated and coexpressed with Kvβ1.1 and Kvβ1.1-C7S, subsequently the combinations were exposed to 10 μM Na_2S_4. However, similar results were obtained of Kv1.2-C435S/Kvβ1.1 (Figure 39) as that of Kv1.2/Kvβ1.1 (Figure 37 and 38). Thus, effects of sulfide species on inactivation of Kv1.2/Kvβ1.1 are not related to N- and C-terminal disulfide bridge formation.

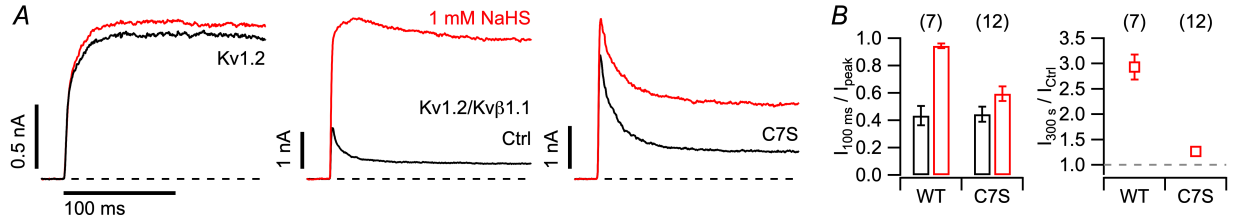

Figure 37: Kvβ1.1 confers NaHS sensitivity to non-inactivating Kv1.2

A. Whole-cell current traces of Kv1.2 channels expressed alone (left), coexpressed with Kvβ1.1 (middle) and its mutant C7S (right) before (black) and 300 s after application of 1 mM NaHS (red). ***B***. Change of inactivation indices (left) and peak current (right) upon NaHS application.

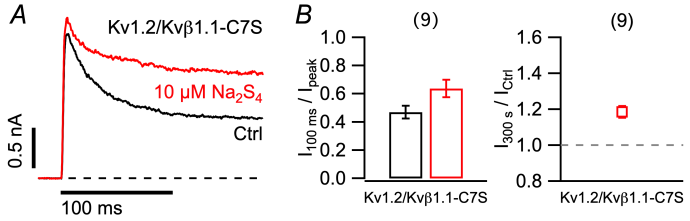

Figure 38: Effect of Na_2S_4 on Kv1.2/Kvβ1.1-C7S

As in Figure 37, for 10 μM Na_2S_4 on Kv1.2/Kvβ1.1-C7S.

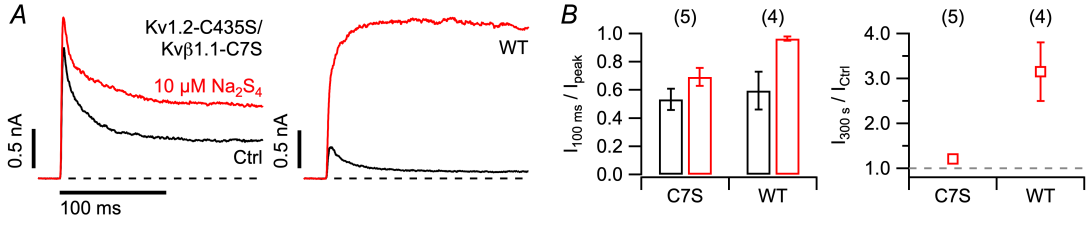

Figure 39: Effect of Na_2S_4 on Kv1.2 C-terminal cysteine mutant

As described in Figure 37, for Kv1.2-C435S mutant.

3.2.4 Effect of NaHS on the inactivation of Kv1.4 coexpressed with Kvβ1.1

So far, the impacts of various stress mediators (NaHS, polysulfides, diamide and DTNP) on the N-type inactivation of Kv1.4 and induced by Kvβ subunits have been examined. However, Kv1.4 often coassembles with Kvβ subunits under physiological condition, such as Kvβ1.1 (Rettig et al., 1994; McCormack et al., 1995; Leicher et al., 1996; McIntosh et al., 1997; Rhodes et al., 1997; Swain et al., 2015), and the Kv1.4/Kvβ1.1 complex harbors eight N-terminal inactivating ball domains. Consequently, coexpression of Kv1.4 and Kvβ1.1 resulted in outward K^+ currents (Figure 40A) which inactivated more rapidly (τ_{inact} = 4.3 ± 0.5 ms, n = 6; Figure 40C) than those mediated by Kv1.4 alone (τ_{inact} = 83.3 ± 1.9 ms, n = 10; Figure 13) at pH 7.4.

After exposing Kv1.4/Kvβ1.1 to 1 mM NaHS for 10 min, its inactivation was substantially slowed down (Figure 40A) with increased inactivation index from 0.22 ± 0.07 to 0.55 ± 0.05, n = 6 (Figure 40B) and slowed τ_{inact} to 109.9 ± 21.5 ms, n = 6 (Figure 40C), corresponding to slow C-type inactivation of Kv1.4. The underlying mechanisms were firstly explored with Kv1.4 mutant C13S coexpressed with Kvβ1.1 (Kv1.4-C13S/Kvβ1.1). Inactivation of the channel complex was slowed by NaHS to a degree similar as N-type inactivation of Kv1.4 (Figure 40A). While regardless of Kv1.4 or Kv1.4-C13S, after coexpression with Kvβ1.1-C7S, the inactivation of these two combinations (Kv1.4/Kvβ1.1-C7S and Kv1.4-C13S/Kvβ1.1-C7S) were not altered by NaHS. These results suggest that Kv1.4 and Kvβ1.1 cooperatively introduce inactivation and the effect of NaHS on the inactivation of Kv1.4/Kvβ1.1 is determined by the Kvβ1.1 N-terminal cysteine residue (C7).

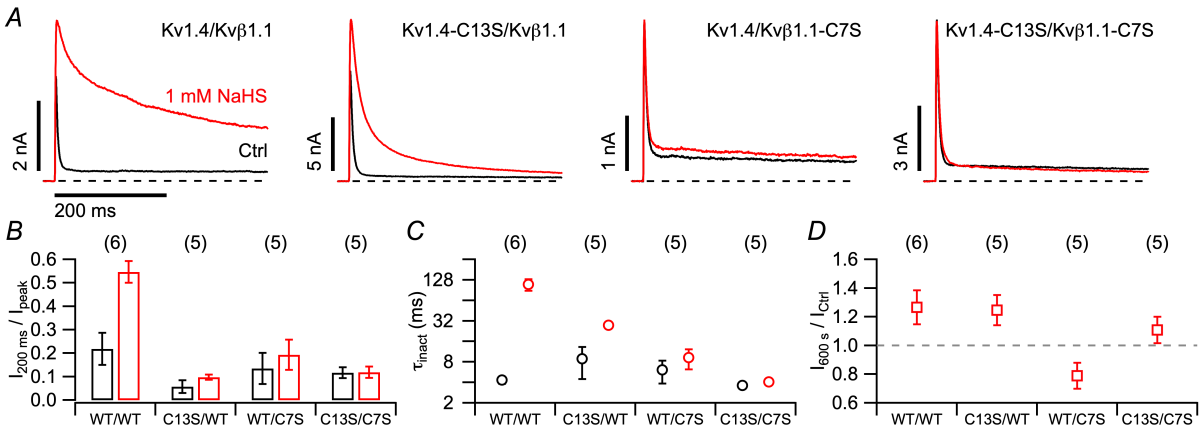

Figure 40: Effect of NaHS on Kv1.4/Kvβ1.1 complex

A. Whole-cell current traces of Kv1.4 channels (WT or C13S) coexpressed with Kvβ1.1 (WT or C7S) before (black) and 600 s after application of 1 mM NaHS (red). ***B***. Change of inactivation indices (left), τ_{inact} (middle) and peak current (right) upon NaHS application.

3.2.5 Effects of stress mediators on other Kvβ subunits induced inactivation

As a splice variant of Kvβ1, Kvβ1.2 is known to induce N-type inactivation of non-inactivating Kv1 channels (De Biasi et al., 1997; Rasmusson et al., 1997; Pérez-García et al., 1999). In contrast to only one cysteine (C7) in the N terminus of Kvβ1.1, Kvβ1.2 harbors two cysteine residues (C8 and C28). Accordingly, the effect of NaHS was also evaluated on Kvβ1.2-induced inactivation of Kv1.1 and Kv1.5.

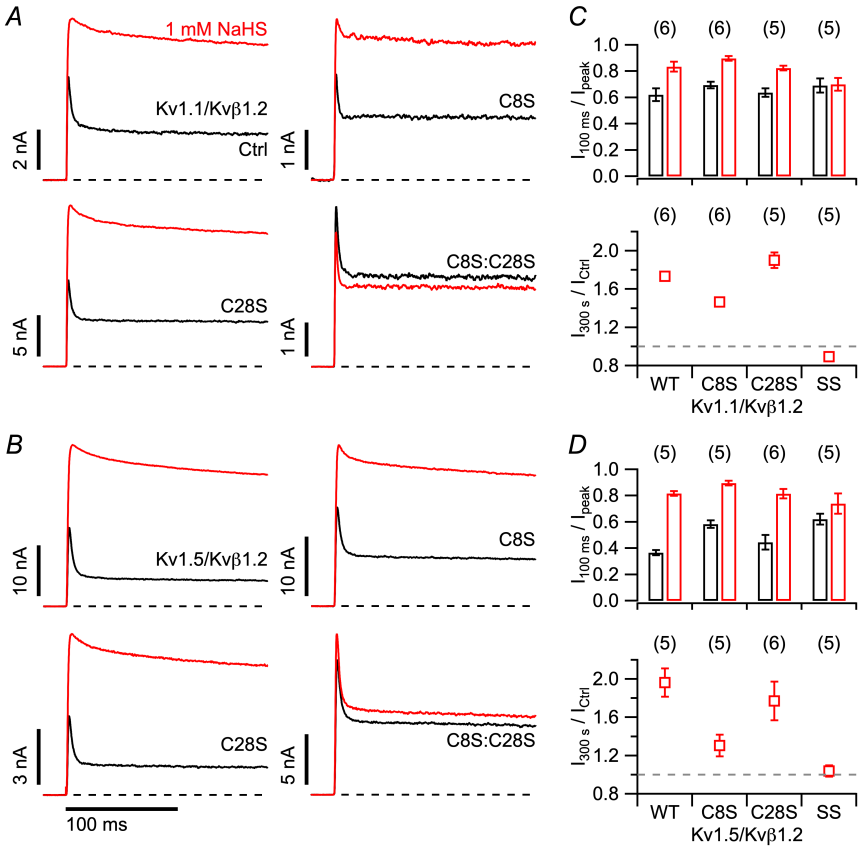

Figure 41: Effect of NaHS on Kvβ1.2-induced inactivation of Kv1.1 and Kv1.5

Whole-cell current traces of Kv1.1 (***A***) and Kv1.5 (***B***) coexpressed with Kvβ1.2 and its cysteine mutants C8S, C28S and C8S:C28S (SS) before (black) and 300 s after application of 1 mM NaHS (red). Change of inactivation indices (top) and peak current (bottom) upon NaHS application for Kv1.1/Kvβ1.2 (***C***) and Kv1.5/Kvβ1.2 (***D***).

N-type inactivation was introduced upon coexpression of Kv1.1 and Kv1.5 with Kvβ1.2 (Figure 41A, B). The inactivation of both Kv1.1/Kvβ1.2 and Kv1.5/Kvβ1.2 was slowed down markedly by 1 mM NaHS. To elucidate if cysteine residues are required in the removal of Kvβ1.2-induced inactivation, mutants C8S, C28S and C8S:C28S of Kvβ1.2 were generated. All the mutated constructs induced N-type inactivating K^+ current of Kv1.1 and Kv1.5 when coexpressed in HEK293T cells (Figure 41A, B). Application of NaHS slowed down the inactivation of Kvβ1.2 single cysteine mutants C8S and C28S coexpressed

with Kv1.1 and Kv1.5, while the sensitivity of inactivation to NaHS was largely reduced by Kvβ1.2-C8S:C28S. Hence, cysteine residues C8 and C28 in the Kvβ1.2 N terminus mediate the impairing effect on inactivation of Kv1.1/Kvβ1.2 and Kv1.5/Kvβ1.2 by NaHS.

The distal N termini of all three members of Kvβ1 differ in the number of cysteine residues: Kvβ1.1 harbors a cysteine at position 7 (C7), Kvβ1.2 harbors two cysteine at position 8 and 28 (C8, C28), while Kvβ1.3 has no cysteine residue. Therefore, N-type inactivation of Kv1 channels mediated by Kvβ1 isoforms are diversified with respect to the modulation by different stress mediators. For example, inactivation of Kv1.5/Kvβ1.3 is insensitive to the membrane permeable oxidizing agent *tert*-butyl hydroperoxide; yet Kvβ1.3 gained oxidation sensitivity by replacing N-terminal arginine (R5) or threonine (T6) with cysteine (Decher et al., 2008). So, experiments were conducted to explore the effects of NaHS and DTNP, as modulators of Kvβ1.1- and Kvβ1.2-induced inactivation of Kv1.5 (Figure 28, 29 and 41), on the inactivation of Kv1.5/Kvβ1.3.

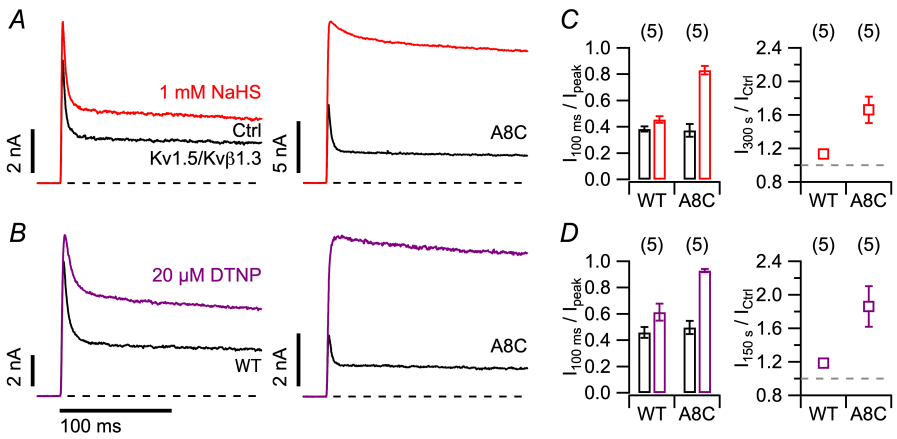

Figure 42: Effects of NaHS and DTNP on Kv1.5/Kvβ1.3

Whole-cell current traces of Kv1.5/Kvβ1.3 and mutant Kv1.5/Kvβ1.3-A8C before (black) and after application of 1 mM NaHS for 300 s (red, in ***A***) or 20 μM DTNP for 150 s (purple, in ***B***). Change of inactivation indices (left) and peak current (right) for Kv1.5/Kvβ1.3 and Kv1.5/Kvβ1.3-A8C upon NaHS (***C***) or DTNP (***D***) application.

As shown in Figure 42, when Kv1.5 was coexpressed with Kvβ1.3 in HEK293T cells, rapid and stable N-type inactivation was introduced. After 300 s application of 1 mM NaHS or 150 s application of 20 μM DTNP, the inactivation of Kv1.5/Kvβ1.3 was slightly showed down. Then a Kvβ1.3-A8C mutant was generated by introducing cysteine instead of alanine at position 8 (A8) and coexpressed with Kv1.5. Inactivation of Kv1.5/Kvβ1.3-A8C was largely disrupted by both NaHS and DTNP. This result suggests that inactivation of Kv1.5 can be induced by Kvβ1.3 without cysteine residue in its N-terminal inactivating ball domain, and the sensitivity of Kv1.5/Kvβ1.3 inactivation to NaHS and DTNP was enhanced in the cysteine insertion mutant.

Kvβ3.1, the third subfamily member of Kvβ family, has only 68% amino acid sequence homology to Kvβ1.1 (Heinemann et al., 1995). This subunit possesses a long N-terminal structure and it can induce N-type inactivation on N-terminal deleted Kv1.4 (Kv1.4Δ1-110) which inactivates slowly (Heinemann et al., 1995). The inactivation of Kv1.5 was also enhanced once coexpressed with Kvβ3.1 (England et al., 1995; Leicher et al., 1998). In this work, the function of Kv1.1/Kvβ3.1 assembly and its response to NaHS were studied.

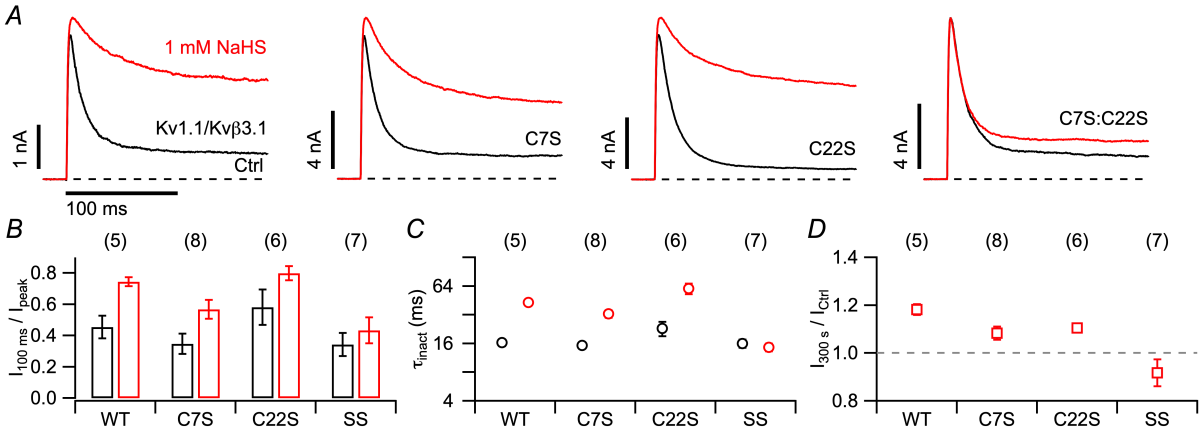

Figure 43: Effect of NaHS on Kvβ3.1-induced inactivation

A. Whole-cell current traces of Kv1.1 channels coexpressed with Kvβ3.1 and its mutants C7S, C22S, and C7S:C22S (SS) before (black) and 300 s after application of 1 mM NaHS (red). Change of inactivation indices (***B***), τ_{inact} (***C***) and peak current (***D***) upon NaHS application.

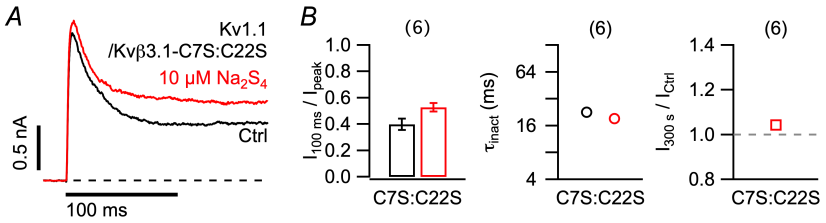

Figure 44: Effect of polysulfide on inactivation of Kv1.1/Kvβ3.1-C7S:C22S

As described in Figure 43, for Kv1.1/Kvβ3.1-C7S:C22S with 10 μM Na_2S_4 application.

As shown in Figure 43, N-type inactivation of Kv1.1 was introduced by Kvβ3.1. After 300 s application of 1 mM NaHS, the inactivation of Kv1.1/Kvβ3.1 was greatly impaired. Because the N-terminal structure of Kvβ3.1 contains two cysteine residues C7 and C22, cysteine mutants C7S, C22S and C7S:C22S were generated to investigate how inactivation of Kv1.1/Kvβ3.1 was regulated by NaHS. For both single cysteine mutations C7S and C22S of Kvβ3.1 coexpressed with Kv1.1, the slow-down effect on their inactivation by NaHS was similar to that of Kvβ3.1, while the double cysteine mutation C7S:C22S abolished the impact of NaHS. The inactivation of Kv1.1/Kvβ3.1-C7S:C22S was also resistant to the effect of the much more potent polysulfide Na_2S_4 at 10 μM (Figure 44). Thus, the sensitivity of Kv1.1/Kvβ3.1 inactivation to sulfide species was mediated by cysteine residues C7 and C22 in the N terminus of Kvβ3.1.

3.3 Effect of hemin on N-type inactivating Kv channels

Heme (Fe^{2+}-protoporphyrin-IX) is not only a stable protein cofactor, but free intracellular heme also acts as an acute signaling molecule to impair N-type inactivation of Kv1.4 by binding to the $CXXHX_{18}H$ motif, involving cysteine (C13) and histidine (H16 and H35) residues, in the N terminus (Sahoo et al., 2013). In the same report, it is hypothesized that binding of heme to the $CXXHX_{18}H$ motif of Kv1.4 reduces the flexibility of the ball domain, which hinders the ball domain from reaching the channel's cavity to induce N-type inactivation (Sahoo et al., 2013). After aligning the N-terminal inactivating ball domains, Kv3.4 harbors C6 and C24, Kvβ1.1 harbors C7 and H10, Kvβ1.2 harbors H2, C8, C28 and H31, Kvβ3.1 harbors C7 and C22, while there is no cysteine or histidine residue in the ball domain of Kvβ1.3. In order to evaluate whether heme regulates other A-type Kv channels in a similar manner as that of Kv1.4, Kv3.4 and Kvβ1 subunits, i.e., those mediating N-type inactivation, were expressed in HEK293T cells and effects of hemin on the resulting channels were studied.

3.3.1 Regulation of Kv3.4 inactivation by hemin

Both Kv1.4 and Kv3.4 are A-type Kv channels, but compared to what is known for Kv1.4 (Sahoo et al., 2013), the effect of hemin on Kv3.4 is unknown. Because hemin is membrane impermeable, it was applied intracellularly in the inside-out recording mode when Kv1.4 channels were expressed in *Xenopus* oocytes (Sahoo et al., 2013). Though the *Xenopus* oocytes expression system is valuable to study the function of ion channels (Goldin, 1992; Goldin and Sumikawa, 1992; Shin et al., 1998), the most serious disadvantage is that the amphibian cells are not the mammalian cells in which Kv1.4 and Kv3.4 are normally expressed (Tapper and George, 2003; Goldin, 2006).

In addition, when Kv3.4 channels were transiently expressed in HEK293T cells and their currents were recorded in the whole-cell mode, tens of nanoamperes (nA) current amplitudes could be measured upon depolarizing to 50 mV from –100 mV with 140 mM K^+ in the bath solution; and hundreds of picoamperes (pA) or even several nA currents of Kv3.4 can be recorded in the inside-out or cell-attached mode. Thus, Kv3.4 were expressed in HEK293T cells and inside-out recordings were performed to study if and how hemin regulates inactivation of Kv3.4 in this work. Since the inactivation of Kv3.4 is known to

depend on the redox potential (Ruppersberg et al., 1991b), its inactivation is fast in the cell-attached mode with reducing cytosol when the cell remains intact, but the inactivation gets increasingly slower in the inside-out mode when the cytosolic side of the excised membrane patch is exposed to the bath solution which is saturated with ambient oxygen. To exclude ROS effects on Kv3.4 inactivation, reduced glutathione (GSH) at 200 μM was included in the bath solution in all inside-out recordings for the study of hemin effects.

As depicted in Figure 45, rapidly inactivating Kv3.4 currents (Ctrl, in black) were recorded after the establishment of inside-out mode with averaged inactivation indices ($I_{50\ ms}/I_{peak}$) below 0.18, and this inactivation remained constant after 105 s (0 Hemin, in brown). Therefore, effects of various concentrations of hemin were studied in the time course of 105 s. After 40 nM hemin application, $I_{50\ ms}/I_{peak}$ of Kv3.4 was slightly increased to 0.26 ± 0.03 from 0.18 ± 0.04 (n = 10). When the hemin concentration was further increased, the impact on inactivation was larger and $I_{50\ ms}/I_{peak}$ of Kv3.4 was raised about four times to 0.37 ± 0.06 from 0.09 ± 0.02 (n = 11) in response to 200 nM hemin, and to 0.48 ± 0.10 from 0.13 ± 0.04 (n = 10) for 1 μM hemin. Besides the effects on inactivation, intracellular hemin affected the peak current amplitude to a small degree (Figure 45C).

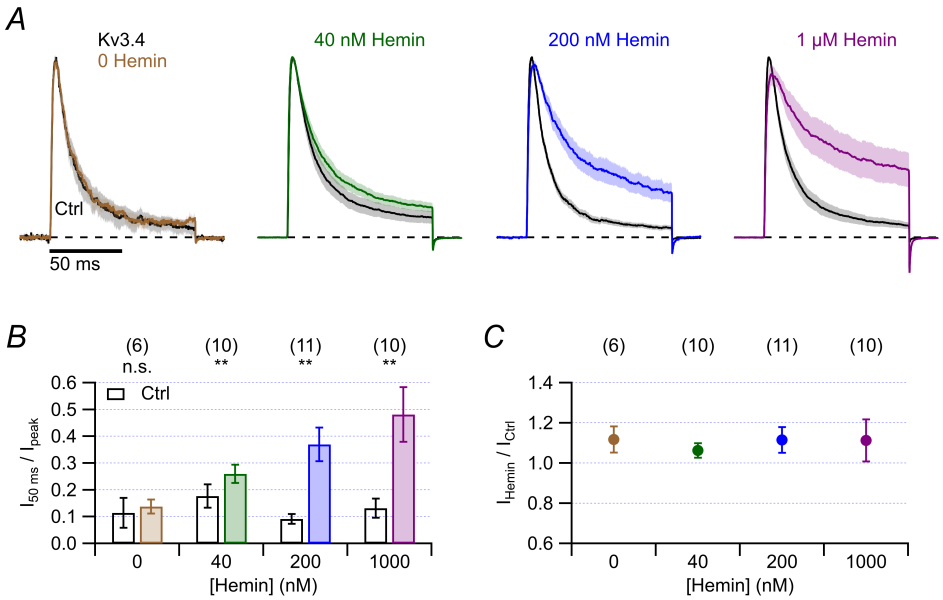

Figure 45: Effects of hemin on Kv3.4 inactivation

A. Inside-out current traces of Kv3.4 in solutions containing 200 μM reduced GSH before (black) and 105 s after application of solutions containing the indicated concentrations of hemin (color). Thick traces are mean values with SEM in shade. Currents were recorded every 15 s upon depolarizing to 50 mV from –100 mV, with pipette and bath solutions adjusted to pH 7.9. ***B***. Inactivation indices ($I_{50\ ms}/I_{peak}$) of Kv3.4 under different conditions as described in ***A***. ***C***. Fractional change of the peak current of Kv3.4 channels. Paired Student's t-tests were performed in ***B***: n.s., not significant; ** $P < 0.01$.

After Kv3.4 inactivation was slowed down by 200 nM hemin, the effect of hemin was partially reversed by washing with 200 μM reduced GSH containing solution (Figure 46),

indicating a stable physical interaction between hemin and the inactivating ball domain of Kv3.4 channel, as that of Kv1.4 channel (Sahoo et al., 2013).

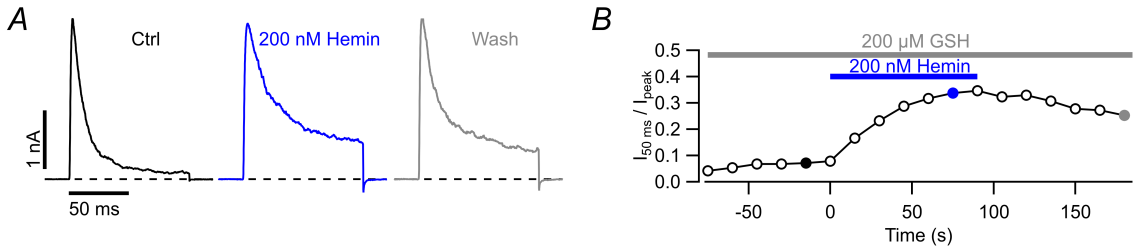

Figure 46: Impact of washing out hemin on Kv3.4 inactivation

A. Inside-out current traces of Kv3.4 under control condition with 200 μM reduced GSH (Ctrl, in black), and 75 s after application of 200 nM hemin (in blue), then followed by 90 s washing with hemin-free solutions (Wash, in grey). ***B***. Time course of inactivation indices ($I_{50\ ms}/I_{peak}$) for the indicated applications. The highlighted filled data points correspond to the current traces shown in ***A***.

Protoporphyrin IX (ppIX), as the ring structure of hemin without a central metal ion, was also applied to Kv3.4. The inactivation of Kv3.4 was not slowed down by ppIX even at 2 μM, and the effect of 200 nM hemin was also resistant to it (Figure 47).

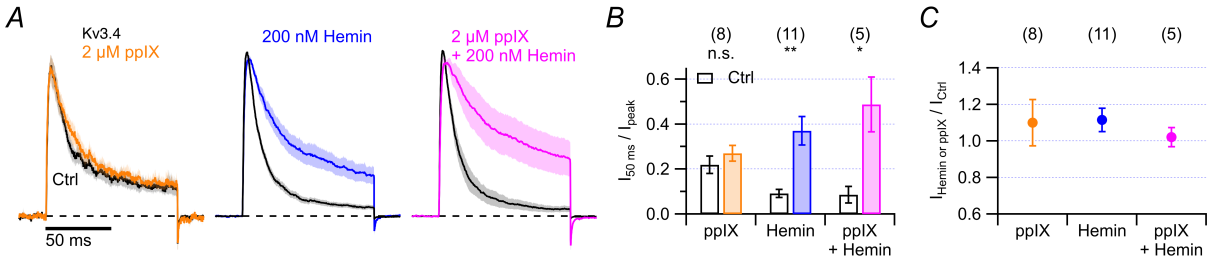

Figure 47: Effects of protoporphyrin IX (ppIX) on the inactivation of Kv3.4

As in Figure 45, for 2 μM protoporphyrin IX (ppIX) alone or in combination with 200 nM hemin application to Kv3.4. n.s., not significant; * $P < 0.05$; ** $P < 0.01$.

Because heme regulates Kv1.4 inactivation by targeting cysteine/histidine residues, similar experiments as for Kv3.4 were performed with its cysteine mutants C6S, C24S and C6S:C24S to explore the underlying mechanism of hemin effects on Kv3.4. After applying 200 nM hemin, the $I_{50\ ms}/I_{peak}$ was increased to 0.18 ± 0.05 from 0.10 ± 0.01 (n = 5) for single cysteine mutants C6S, and to 0.25 ± 0.05 from 0.15 ± 0.03 (n = 8) for C24S, but the inactivation of the double cysteine mutant C6S:C24S of Kv3.4 remained relatively stable: the $I_{50\ ms}/I_{peak}$ was only changed from 0.12 ± 0.02 to 0.11 ± 0.02 (n = 5) after hemin application (Figure 48).

Thus, not only Kv1.4 inactivation is susceptible to hemin, the inactivation of Kv3.4 can be also regulated by hemin. The effects of hemin Kv3.4 inactivation rely on the presence of cysteine residues in its N-terminal ball domain.

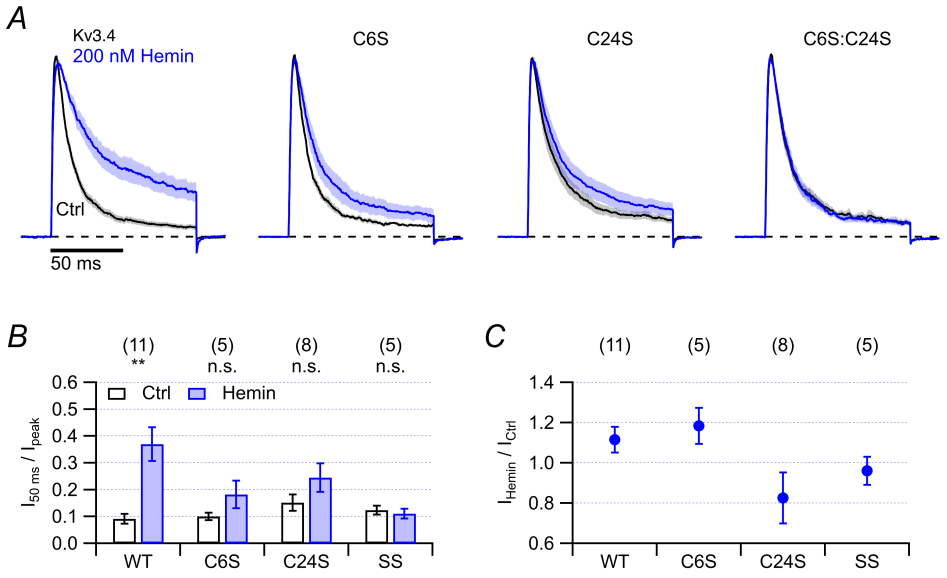

Figure 48: Effects of 200 nM hemin on the inactivation of Kv3.4 mutants

As in Figure 45, for 200 nM hemin application to Kv3.4 mutants. The Kv3.4 (WT) data was the same as in Figure 45.

3.3.2 Impact of hemin on Kvβ1-induced inactivation of Kv1.4

Hemin is usually dissolved in basic buffer, such as 1 mM hemin in 30 mM NaOH (Sahoo et al., 2013). But the inactivation of Kv1.4 depends on intracellular pH values; its inactivation is progressively slowed from pH 6.0 to pH 8.0 in the physiologically relevant range (Padanilam et al., 2002). When currents of Kv1.4 channels were recorded in the whole-cell mode with both bath and pipette solutions adjusted to pH 7.9, only showed slow C-type inactivating K^+ currents with inactivation index ($I_{50\ ms}/I_{peak}$) of 0.80 ± 0.02 and τ_{inact} of 161.3 ± 11.6 ms (n = 12) was observed (Figure 49). However, under the same condition, Kvβ1.1 can introduce stable N-type inactivation to Kv1.4 with $I_{50\ ms}/I_{peak}$ of 0.04 ± 0.01 and τ_{inact} of 4.9 ± 0.5 ms (n = 5). In addition, the currents of the Kv1.4/Kvβ1.1 complex were large and made it possible to perform inside-out recordings. Therefore, Kv1.4/Kvβ1.1 was used to study the effects of hemin on Kvβ1-induced inactivation.

When Kv1.4 was expressed alone and inside-out recordings were performed at pH 7.9, slow C-type inactivation was observed with $I_{50\ ms}/I_{peak}$ of 0.60 ± 0.03 (n = 4) and 0.58 ± 0.06 (n = 6), and the inactivation was not altered after application of 200 nM and 500 nM hemin for 120 s (Figure 50A, C). This agrees with the previous report that C-type inactivation in Kv1.4Δ2-110, i.e., a N-terminal deletion mutant of Kv1.4 which only exhibits residual C-type inactivation (Heinemann et al., 1996), was not affected by hemin (Sahoo et al., 2013).

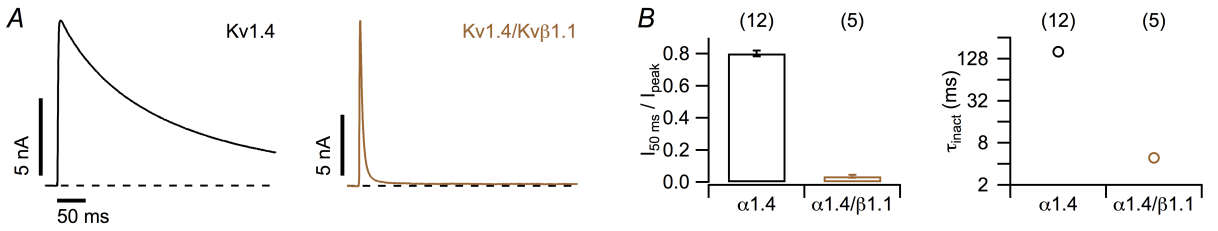

Figure 49: Kvβ1.1 induces N-type inactivation of Kv1.4 at pH 7.9

A. Representative whole-cell current traces of Kv1.4 channels expressed alone (left) and coexpressed with Kvβ1.1 (right) with depolarization to 50 mV from a holding potential of –100 mV. Both pipette and bath solutions were adjusted to pH 7.9. ***B***. Inactivation indices ($I_{50\ ms}/I_{peak}$) and τ_{inact} of indicated channel types.

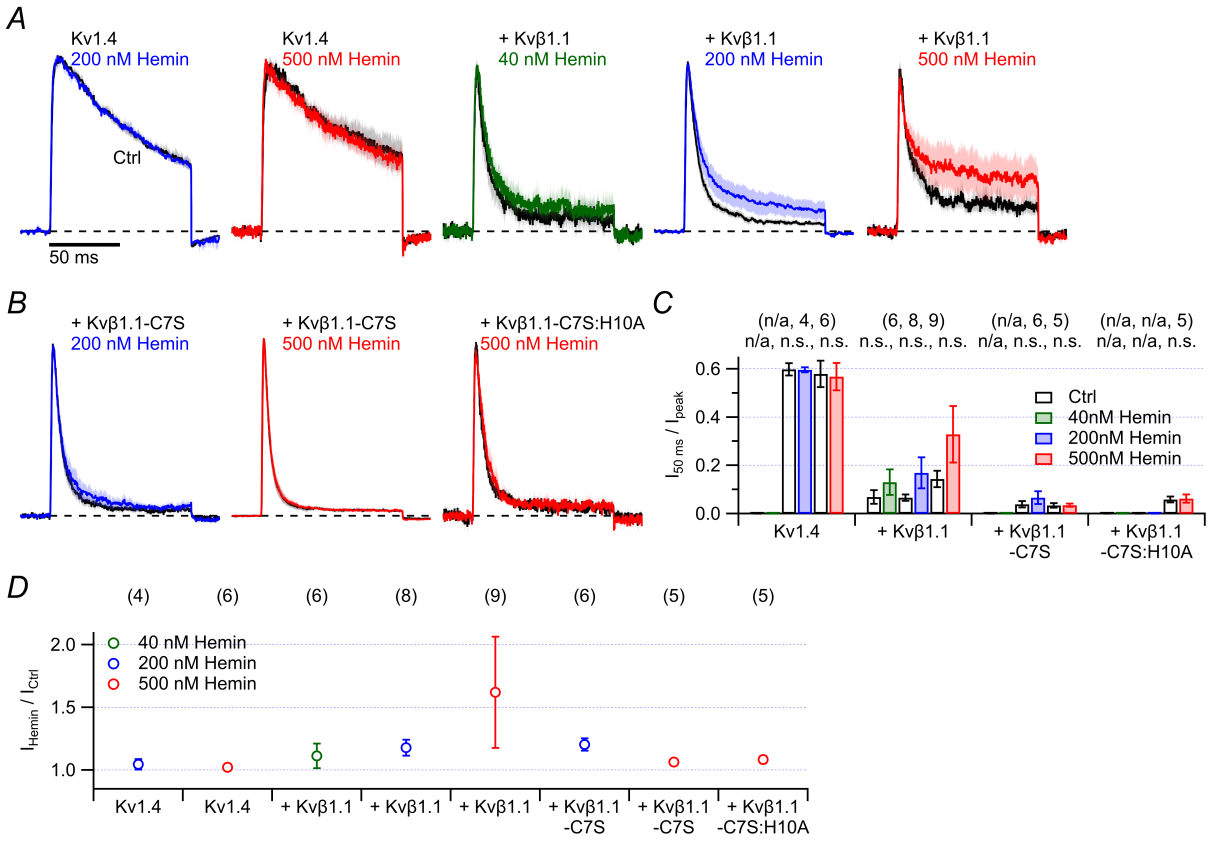

Figure 50: Effects of hemin on inactivation of Kv1.4 and Kv1.4/Kvβ1.1

As in Figure 45, except currents were recorded every 60 s, for Kv1.4, Kv1.4/Kvβ1.1 and Kv1.4/Kvβ1.1-C7S:H10A. n/a, not available.

Rapid N-type inactivation of Kv1.4 was introduced by Kvβ1.1, and $I_{50\ ms}/I_{peak}$ was slightly increased to 0.13 ± 0.05 from 0.07 ± 0.03 (n = 6) upon 40 nM hemin application for 120 s, and to 0.17 ± 0.06 from 0.07 ± 0.01 (n = 8) by 200 nM hemin. A larger effect was noticed when 500 nM hemin was applied, $I_{50\ ms}/I_{peak}$ was increased to 0.33 ± 0.12 from 0.14 ± 0.03 (n = 9) (Figure 50A, C). There was also a larger increase of peak current after applying 500 nM hemin (Figure 50D). Because C13 and H16 in the N terminus of Kv1.4 are part of a heme-binding motif (CXXH) mediating the sensitivity of the channel to hemin (Sahoo et al., 2013), C7 and H10 in the homologous region of Kvβ1.1 may also

be targeted by hemin. Therefore, Kvβ1.1-C7S and Kvβ1.1-C7S:H10A were generated, co-expressed with Kv1.4, and subjected to hemin to explore the mechanism. The inactivation of both Kv1.4/Kvβ1.1-C7S and Kv1.4/Kvβ1.1-C7S:H10A was insensitive to 500 nM hemin (Figure 50B, C).

The Kvβ1.1 protein is encoded by Kcnab1 gene, and Kvβ1.2 and Kvβ1.3 are encoded by two other splice variants of this gene. Kvβ1.1-1.3 have conserved C-terminal regions but different N-terminal sequences (Pongs and Schwarz, 2010). A CXXH motif is also located in the ball domain of Kvβ1.2, but this motif is absent in Kvβ1.3. It has been reported that Kvβ1.2 enhances N-type inactivation and increases the rate of C-type inactivation in Kv1.4 (Accili et al., 1998). Consequently, after expressing Kvβ1.2 with Kv1.4, Kv1.4/Kvβ1.2 showed N-type and C-type inactivation (Figure 51A, left black). The inactivation of Kv1.4/Kvβ1.3 (Figure 51A, middle black) was similar to that of Kv1.4/Kvβ1.2, probably Kvβ1.3 had a similar effect on N-type and C-type inactivation of Kv1.4. While 500 nM hemin slowed the inactivation of Kv1.4/Kvβ1.2 by increasing the $I_{50\ ms}/I_{peak}$ from 0.40 ± 0.04 to 0.58 ± 0.08 (n = 10), and increase the peak current about 50% (Figure 51A, B, C, left). this treatment did not slow down the inactivation of Kv1.4/Kvβ1.3 (Figure 51A, B, middle). But after the cysteine was introduced in the N-terminal ball domain (A8C) of Kvβ1.3, the sensitivity of Kv1.4/Kvβ1.3 to hemin was gained: the $I_{50\ ms}/I_{peak}$ was increased from 0.26 ± 0.03 to 0.47 ± 0.09 (n = 6) for Kv1.4/Kvβ1.3-A8C (Figure 51, right).

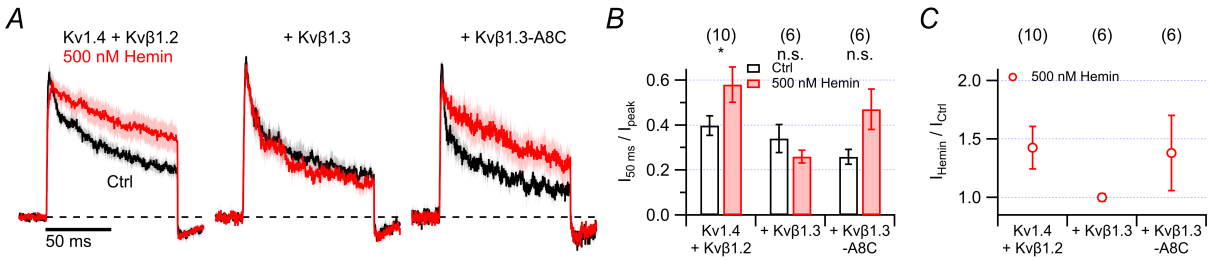

Figure 51: Effects of 500 nM hemin on inactivation of Kv1.4/Kvβ1.2 and Kv1.4/Kvβ1.3
As in Figure 50, for Kv1.4/Kvβ1.2, Kv1.4/Kvβ1.3 and Kv1.4/Kvβ1.3-A8C.

Thus, hemin regulates Kvβ1-induced inactivation by targeting cysteine/histidine residues.

4 Discussion

4.1 RSS potently modulate A-type Kv channels

Reactive sulfur species (RSS) are a family of sulfur-containing compounds, including H_2S, hydropersulfide, polysulfide, elemental sulfur, thiosulfate and sulfate (Mishanina et al., 2015; Lau and Pluth, 2019). They are found in biological systems and are crucial in various fundamental biological processes due to their unique properties and wide range of accessible oxidation states, from –2 as in H_2S to +6 as in SO_4^{2-} (Figure 52) (Giles et al., 2001; Giles and Jacob, 2002; Li et al., 2011; Peers et al., 2012; Wang, 2012; Gruhlke and Slusarenko, 2012; Paulsen and Carroll, 2013; Yang et al., 2017; Liu et al., 2018). In RSS, the critical gaseous cell-signaling molecule H_2S has been intensively studied and recognized as the third member of gasotransmitters after NO and CO (Wang, 2002, 2003, 2014).

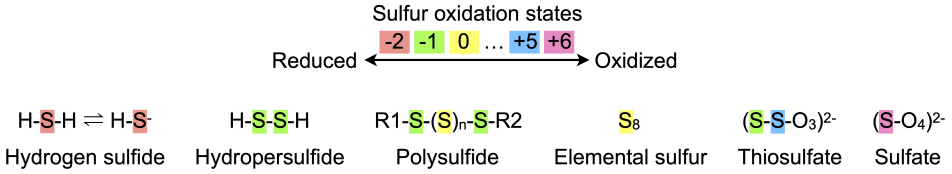

Figure 52: Sulfur oxidation states of some biologically relevant RSS

The red (–2), green (–1), yellow (0), blue (+5) and purple (+6) rectangles represent the valence states of specified sulfur. Modified after Mishanina et al. (2015).

Many biological effects of RSS are mediated through ion channels. For example, H_2S acts as an endothelium-derived relaxing factor by directly opening vascular smooth muscle K_{ATP} channels, which leads to hyperpolarization of vascular smooth muscle cells, reduction of voltage-gated Ca^{2+} influx, and vasodilation of blood vessels (Zhao et al., 2001; Li et al., 2011; Peers et al., 2012). Deficiency of endogenous H_2S, through genetic deletion of the H_2S biosynthesis enzyme CSE, contributes to the development of hypertension (Yang et al., 2008; Mustafa et al., 2009, 2011). H_2S and polysulfides facilitate the induction of hippocampal long-term potentiation (LTP) by activating TRPA1 channels, which enhances the activity of N-methyl-D-aspartate receptors (Abe and Kimura, 1996; Kimura et al., 2013; Kimura, 2015).

In this work, one additional class of ion channels — A-type Kv channels — was identified to be modulated by RSS. A-type Kv channels, such as Kv1.4 and Kv1.1/Kvβ1.1 channels, are rapidly inactivating K^+ channels. They are essential for fine-tuning of neuronal excitability (Connor and Stevens, 1971; Rudy, 1988; Amberg et al., 2003; Cai et al., 2007; Zemel et al., 2018). The rapid inactivation of native A-type Kv channels (e.g., Kv1.4 and Kv3.4) in DRG neurons can be slowed down by polysulfide Na_2S_4 (Figure 12). For a systematic study of RSS effects on A-type Kv channels, RSS were applied with the H_2S donor NaHS and polysulfide donors Na_2S_n, and A-type Kv channels of Kvα subunits Kv1.4 and Kv3.4 were heterologously expressed in mammalian HEK293T cells. The N(β)-inactivation of non-inactivating delayed rectifier Kv1 channels induced by the brain-derived Kvβ subunits was also investigated.

The major findings of this study are: RSS impair N-type inactivating K^+ currents of Kv1.4, Kv3.4 and Kv1/Kvβ (except Kv1.5/Kvβ1.3) channels; RSS target cysteine residues in the N termini of A-type Kv channels; RSS sulfhydrate cysteine residue of a recombinant peptide corresponding to the inactivation ball domain of Kv1.4 N terminus; RSS affect the inactivation of Kv1.1/Kvβ1.1 and Kv1.5/Kvβ1.1 differently.

4.2 Mechanisms for modulation of A-type Kv channels by RSS

4.2.1 Effects of H_2S on A-type Kv channels are mediated by polysulfides

The signaling mechanism of H_2S has been proposed to involve sulfhydrating reactive cysteine residues in target proteins (Mustafa et al., 2009; Krishnan et al., 2011; Paul and Snyder, 2012), with the addition of H_2S-derived sulfur to the thiol group of the reactive cysteine (Cys-SH) to yield Cys-S-SH. Sulfhydration is similar to NO nitrosylation, the formation of Cys-S-NO by attaching NO to Cys-SH (Hess et al., 2005). Both sulfhydration and nitrosylation influence the localization, stability and activity of the target protein (Hess et al., 2005; Paul and Snyder, 2012). For instance, H_2S activates K_{ATP} channels by sulfhydrating C43 in the Kir6.1 subunit of the channel (Mustafa et al., 2011). However, H_2S and HS^-, with sulfur in its most reduced state (–2) (Figure 52), can only act as reductants (Toohey, 2011; Greiner et al., 2013). In agreement with this, H_2S was reported to only break the disulfide bond located between C1024 and C1045 in the type 2 recep-

tor of vascular endothelial growth factor (VEGFR2) (Tao et al., 2013; Kimura, 2015). In contrast, polysulfides, with more oxidized sulfur (oxidation states of –1 and 0 as shown in Figure 52), readily receive electrons from cysteine and transfer sulfur atoms to cysteine (Kimura, 2015; Mishanina et al., 2015; Filipovic et al., 2018). Therefore, much of what is known as H_2S signaling, such as sulfhydration, may actually have been mediated by polysulfides (Greiner et al., 2013; Filipovic et al., 2018; Liu et al., 2018).

When investigating the effects of different concentrations of NaHS on Kv1.4 inactivation, various responses of the inactivation to 200 μM NaHS were observed (Figure 14), from nearly no effect to significant slowing of the inactivation. Compared with freshly prepared NaHS solutions within 1 h, the "aged" NaHS solutions after overnight preparation (e.g., 20 h) had a greater effect on slowing Kv1.4 inactivation. Because polysulfides were identified after dissolving H_2S gas and various H_2S donors or releasing agents, including sulfide salts NaHS and Na_2S (sodium sulfide), and H_2S slow-releasing compound morpholin-4-ium 4-methoxyphenyl(morpholino) phosphinodithioate (GYY4137) in respective solutions (Greiner et al., 2013), and many studies have implied that polysulfides might act as the real signaling transmitter instead of H_2S (Greiner et al., 2013; Ono et al., 2014), it was hypothesized that the inactivation of Kv1.4, as well as other A-type Kv channels (Kv3.4 and Kv1/Kvβ, except Kv1.5/Kvβ1.3), is regulated by polysulfides formed in NaHS solutions.

Experiments with direct application of polysulfides at 1 μM (e.g., Figure 15, 22 and 28), even at 100 nM (Figure 16), effectively modified inactivation, with the greater number of sulfur atoms increasing the potency. These observations confirmed the hypothesis that polysulfides are the actual active molecules that regulate inactivation of A-type Kv channels in the concentrations range existing in native biological systems (average value of 60-70 nM in HeLa cells) (Yang et al., 2018). This agrees with the previous reports that Na_2S_3 activated the TRPA1 channel much more potently (approximately 1000 times) than NaHS (Streng et al., 2008; Ogawa et al., 2012; Kimura et al., 2013). We therefore conclude that polysulfides Na_2S_n with a varying number of sulfur atoms, generated in NaHS solutions, actually regulate the inactivation of A-type Kv channels.

Except the generation of polysulfides in H_2S gas and various H_2S donors or releasing agents (Greiner et al., 2013), many studies have reported the biosynthesis of polysulfides in mammalian cells (Kimura et al., 2015; Akaike et al., 2017; Kimura et al., 2017; Kimura, 2019). As demonstrated in Figure 53, polysulfides were suggested to be generated from 3-mercaptopyruvate (3MP) by 3-mercaptopyruvate sulfurtransferase (3MST) and from oxidation of H_2S involving 3MST and rhodanese (Rho) (Kimura et al., 2015), and from L-cysteine by cysteinyl-tRNA synthetases (CARS) (Akaike et al., 2017). In addition to the

biosynthesis, polysulfides can be generated by the chemical interaction between H_2S and NO (Eberhardt et al., 2014; Cortese-Krott et al., 2015; Miyamoto et al., 2017), and from the catalysis of H_2S by copper/zinc superoxide dismutase (SOD) (Olson et al., 2018). In comparison with the biosynthesis of H_2S (Figure 7), the generations of both polysulfides and H_2S are closely associated and they coexist, though the exact physiological functional roles of H_2S and polysulfides are controversial (Paul and Snyder, 2012; Greiner et al., 2013; Kimura, 2015; Filipovic et al., 2018). Recently, fluorescent probes have been developed to detect levels of H_2S (Lippert et al., 2011; Liu et al., 2011; Peng et al., 2011; Xuan et al., 2012c; Hammers et al., 2015) and polysulfides (Liu et al., 2014; Chen et al., 2015a,b; Lin et al., 2015; Kawagoe et al., 2017; Yang et al., 2018; Chen et al., 2019) in living systems. The quantitative information about endogenous H_2S and polysulfides levels in cells and *in vivo* may help to understand the intricate physiological functions of them.

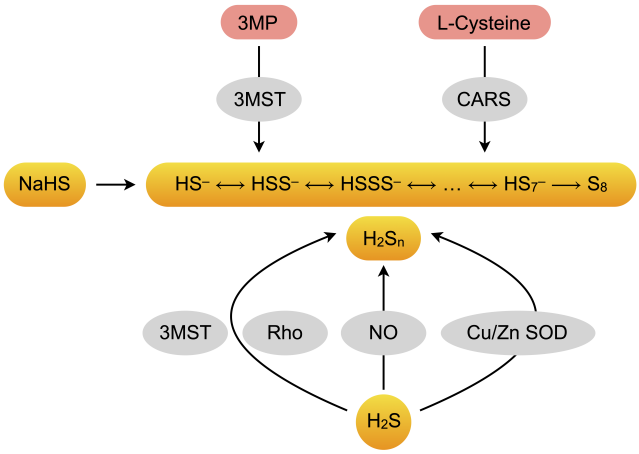

Figure 53: Generation of polysulfides

Polysulfides (mixture of H_2S_n) can be generated by auto-oxidation in NaHS solutions (Greiner et al., 2013; Kimura, 2015), chemical interaction between H_2S and NO (Eberhardt et al., 2014; Cortese-Krott et al., 2015; Miyamoto et al., 2017), and catalysis of H_2S by copper/zinc superoxide dismutase (SOD) (Olson et al., 2018). They can also be biosynthesized from 3-mercaptopyruvate (3MP) by 3-mercaptopyruvate sulfurtransferase (3MST) and from oxidation of H_2S involving 3MST and rhodanese (Rho) (Kimura et al., 2015), and from L-cysteine by cysteinyl-tRNA synthetases (CARS) (Akaike et al., 2017).

4.2.2 Modification of cysteine residues by RSS

Although N-terminal inactivating ball domains of Kvα and Kvβ subunits share little sequence similarity as indicated in the sequence alignment in Figure 4 and Figure 6, with the exception of Kvβ1.3, they contain at least one cysteine residue. Cysteines enable the inactivation of these channels to be susceptible to redox changes (Ruppersberg et al., 1991b; Rettig et al., 1994; Stephens and Robertson, 1995; Decher et al., 2008), and the oxidant signal is transformed to a biological response: modulation of neuronal excitability by regulation of K^+ channels. When mutations of cysteine residues in the N termini of A-type Kv

channels (except Kv1.1/Kvβ1.1) were generated, the sensitivity of their N-type inactivation to RSS was largely reduced, suggesting direct actions of RSS on these residues. It has been proposed that oxidation of cysteines induces formation of disulfide bridges with another protein or glutathione, or forming sulfenic acid, sulfinic acid and sulfonic acid (Reddie and Carroll, 2008; Marino and Gladyshev, 2011; Paulsen and Carroll, 2013; Sahoo et al., 2014) (Figure 54A). The exact molecular mechanism of modifying these cysteines by RSS, however, has remained elusive since it is not clear if cysteine forms a disulfide bridge with another protein or glutathione, or another type of post-translational modification of this residue has happened.

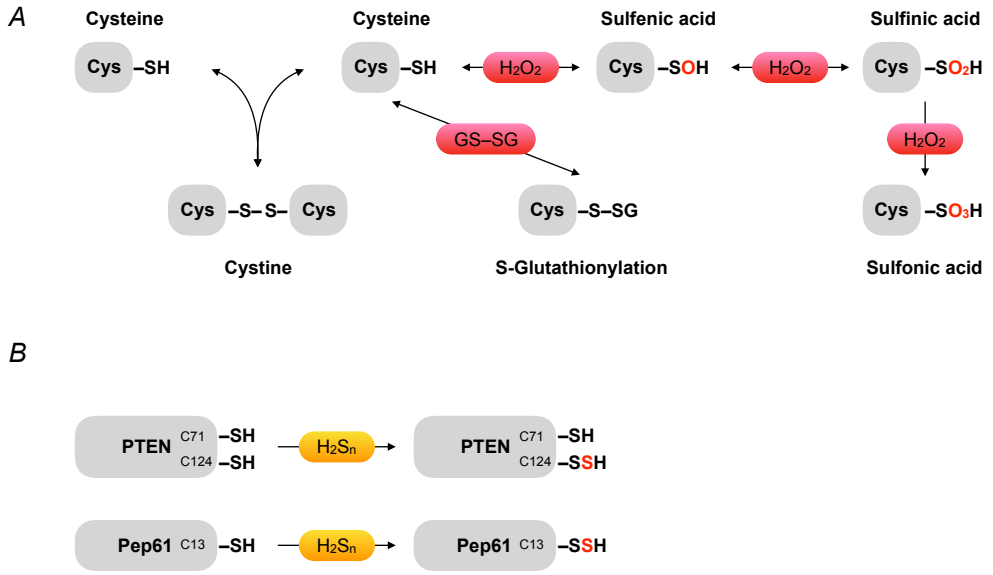

Figure 54: Modulation of reactive cysteine residues

Modification of cysteine upon oxidative stress (***A***), and sulfhydration of cysteines in the lipid phosphatase and tensin homolog (PTEN) and recombinant protein encompassing the inactivating ball domain of Kv1.4 (Pep61) by polysulfides (***B***). GSSG, oxidized glutathione. Modified after Sahoo et al. (2014); Kimura (2019).

As a model protein and a tumor suppressor (Lee et al., 2002), the lipid phosphatase and tensin homolog (PTEN) has been used by Greiner and colleagues to study polysulfide functions (Greiner et al., 2013). PTEN harbors two cysteine residues C71 and C124, and oxidation of this protein results in a disulfide bridge formation between these two cysteines (Lee et al., 2002). Greiner et al. demonstrated that polysulfides formed in H_2S donors, as the oxidizing species, lead to very rapid oxidation of PTEN through sulfhydration of C124 (Greiner et al., 2013) (Figure 54B). To test whether N-terminal cysteine residues in A-type Kv channels were sulfhydrated by RSS, we performed mass spectrometry analysis of the recombinant protein (Pep61) encompassing the inactivating ball domain of Kv1.4. After exposing Pep61 to RSS, a mass corresponding to one sulfur atom was added, while C13S mutation of Pep61 eliminated the sulfur addition effect (Figure 18). Thus, the underlying mechanism of RSS regulating Kv1.4 N-type inactivation is through sulfhydration of cysteine residue in its inactivation ball domain.

In Kv3.4, C6 and C24 are spatially close to each other and located in the stable four-leaf clover-like conformation of the ball domain (Antz et al., 1997, 1999), such that these two cystein residues can form an intra-subunit disulfide bridge in the oxidized state (Antz et al., 1997). As shown in Figure 22, single cysteine mutants C6S and C24S have different sensitivities to RSS, and C6 is more important in sensing RSS effects than C24. Insensitivity of Kv3.4 to RSS was achieved only when both cysteines were mutated (C6S:C24S), indicating that RSS regulate Kv3.4 inactivation through post-translational modification other than forming a disulfide bridge between C6 and C24. The other A-type Kv channel in the Kv3 subfamily, Kv3.3 (Kcnc3), harbors only one cysteine (C6) in the N-terminal inactivating ball domain. It is conceivable that inactivation of this channel is also susceptible to RSS modification.

4.2.3 Effect of RSS on Kv1.1/Kvβ1.1 inactivation is independent of Kvβ1.1 enzymatic activity

The Kvβ1.1 subunit confers rapid N-type inactivation to non-inactivating delayed rectifier Kv1.1 and Kv1.5 channels (Rettig et al., 1994; Heinemann et al., 1996), and the inactivation of Kv1.1/Kvβ1.1 and Kv1.5/Kvβ1.1 was sensitive to both RSS (Figure 28) and cysteine-specific modifiers (DTNP and diamide) (Figure 29). Because Kvβ1.1 harbors a ROS-sensitive cysteine residue (C7) in its N-terminal ball domain (Rettig et al., 1994), this cysteine residue was mutated to serine (C7S) to explore the underlying mechanisms of RSS and DTNP/diamide effects. Almost no effects of DTNP/diamide on Kv1.1/Kvβ1.1-C7S and Kv1.5/Kvβ1.1-C7S inactivation were observed (Figure 32), there were also no effects of RSS on the inactivation of Kv1.5/Kvβ1.1-C7S (Figure 30). However, the inactivation of Kv1.1/Kvβ1.1-C7S was still sensitive to RSS (Figure 30), similar to that of Kv1.1/Kvβ1.1 (Figure 28). These results suggest RSS specially modulate inactivation of Kv1.1/Kvβ1.1 without involving the critical cysteine residue C7 in Kvβ1.1.

Kvβ1.1 is not only able to induce N-type inactivation of Kv1.1, but its conserved core region also functionally and structurally belongs to aldo-keto reductases (AKR) protein superfamily using NADPH (reduced nicotinamide adenine dinucleotide phosphate) as a co-factor to catalyze a redox reaction (Weng et al., 2006). The core region of Kvβ1.1 consists of a triosephosphate isomerase barrel structure, conserved key catalytic residues and a bound NADPH cofactor (Gulbis et al., 1999). Once the bound NADPH in Kvβ1.1 core is converted to $NADP^+$ (nicotinamide adenine dinucleotide phosphate) in Kv1.1/Kvβ1.1, either enzymatically by a substrate such as 4-cyanobenzaldehyde (4-CY), or nonenzymatically

by an oxidant (e.g., H_2O_2) or by exchange with $NADP^+$, inhibits the inactivation (Weng et al., 2006; Pan et al., 2008a, 2011). Interestingly, the inactivation of Kv1.1/Kvβ1.1-C7S was also impaired after applying 4-CY (Pan et al., 2008a). This phenomenon was explained by restraining the N-terminal ball domain from blocking the channel, which was induced by oxidizing the core region bounded cofactor NADPH to $NADP^+$ (Pan et al., 2011). When E349 in the core region was mutated, the inactivation of Kv1.1/Kvβ1.1-C7S:E349K was resistant to 4-CY (Pan et al., 2011; Swain et al., 2015). It is conceivable to assume that RSS regulate the inactivation of Kv1.1/Kvβ1.1-C7S in this manner, but this assumption was disproved by the results that 10 μM Na_2S_4 removes the inactivation of Kv1.1/Kvβ1.1-C7S:E349K (Figure 34), indicating the effect of RSS on Kv1.1/Kvβ1.1 is not related to the enzymatic activity of Kvβ1.1 core region.

4.2.4 Association of Kv1 channels with Kvβ1.1

Kv1 channels are widely expressed throughout the nervous system and are important in controlling neuronal excitability (Wulff et al., 2009). For instance, Kv1.1 channels are predominantly found in the brain and located on axons and nerve terminals (Rhodes et al., 1997; Monaghan et al., 2001; Trimmer and Rhodes, 2004; Willis et al., 2018), and they play a key role in adjusting the electrical activity of neurons. Mutations in the Kcna1 gene are related to neurological diseases, such as Episodic Ataxia Type 1, which is an autosomal dominant neurological disorder characterized by motor discoordination, involuntary muscle contraction and seizures (Browne et al., 1994; Herson et al., 2003; Imbrici et al., 2006; van der Wijst et al., 2018). Kv1α subunits have been shown to form heteromultimers in the central nervous system (CNS) (Trimmer and Rhodes, 2004; Vacher et al., 2008; Wulff et al., 2009; Jan and Jan, 2012; Ovsepian et al., 2016). For example, using channel specific toxins and antibodies, Kv1.1/Kv1.2 heterotetramers were identified in human brain and contribute to native Kv1 channels (Willis et al., 2018). Kv1 channels are also found in peripheral tissues, such as Kv1.5 channels are highly expressed in the cardiac atrium and contribute to the ultrarapid delayed rectifier K^+ current (I_{Kur}) (Fedida et al., 1993; Wang et al., 1993), which is critical for the early phases of atrial AP repolarization (Wettwer et al., 2004). Atrial fibrillation and sudden cardiac death are associated with alterations in Kv1.5 channels (Wettwer et al., 2004; Olson et al., 2006; Nielsen et al., 2007).

Immunoblot and reciprocal co-immunoprecipitation analyses have indicated that all Kv1α subunits assemble with Kvβ subunits, and vice versa (Rhodes et al., 1996). Kv1α and Kvβ subunits are assembled in the endoplasmic reticulum and remain as stable complex (Nagaya and Papazian, 1997). The deletion of the Kvβ1.1 gene in mice results in a reduced

K^+ current inactivation in hippocampal CA1 pyramidal neurons, broadening of frequency-dependent spike and reduced slow afterhyperpolarization. The phenotype of these mice shows impairment of learning and memory in the Morris water maze test (Giese et al., 1998). This result suggests the importance of Kvβ subunits in conferring inactivation of Kv1 channels.

Kv1α and Kvβ subunits interact with each other through conserved sites in the N termini of Kv1 (Figure 35B) (Sewing et al., 1996), but after aligning the distal N termini of Kv1 channels, except double histidine residues (H118 and H119) existed in Kv1.5 next to the T1 domain, Kv1.1 (C35 and C36), Kv1.2 (C31 and C32), and Kv1.4 (C176 and C177) harbor double cysteine residues at equivalent positions (Figure 35A). In the case of Kv1.1/Kvβ1.1-C7S, the sensitivity of its inactivation to RSS was eliminated when either cysteine in the N terminus of Kv1.1 was mutated (C35A, C36A) (Figure 36), indicating vital roles of Kv1.1 N-terminal cysteine residues. However, the available crystal structures of Kv1/Kvβ are uninformative about the distal N terminus of the Kv channel: Kv1 T1 domain is tilted in a small degree with respect to the central four-fold axis of the Kv1/Kvβ channel complex (Long et al., 2005b), and Kv1 C terminus is shifted towards Kvβ subunit for closer contact (Sokolova et al., 2003). It is assumed that C35 and C36 of Kv1.1 are vital to maintain the N-type inactivation of Kv1.1/Kvβ1.1, RSS induced disufide bridge formation and lead to loss of inactivation, while the disulfide bridge cannot be formed when either C35 or C36 was mutated. Because of the existence of C31 and C32 in Kv2.1, RSS also regulated Kv1.2/Kvβ1.1-C7S inactivation (Figure 37 and 38), e.g., 10 μM Na_2S_4 moderately slowed down the inactivation by increasing the inactivation index from 0.47 ± 0.04 to 0.64 ± 0.06 ($n = 9$) (Figure 38). Both Kv1.4 and Kvβ1.1 possess inactivating ball domains, and the inactivation of Kv1.4 was accelerated by assembling with Kvβ1.1 (Rettig et al., 1994; McIntosh et al., 1997) (Figure 40 and 49), and it was supposed that inactivation can be induced by inactivating ball domains from either Kv1.4 or Kvβ1.1, thus, the sensitivity of Kv1.4/Kvβ1.1-C7S to RSS was different to that of Kv1.1/Kvβ1.1-C7S and Kv1.2/Kvβ1.1-C7S, even distal C176 and C177 of Kv1.4 were likely to be modified by RSS. Nevertheless, the involvement of N-terminal cysteines of Kv1α subunits in sensing RSS effects can not be excluded.

The interface of protein-protein interaction is usually large and extensive, so small-molecule compounds are very difficult to interfere with the interaction (Wells and McClendon, 2007). Conversely, the interface between Kv1 and Kvβ1.1 lacks extensive interaction (Gulbis et al., 2000; Long et al., 2005b) and forms a deep pocket suitable for small-molecule compounds (Pan et al., 2008b), suggesting the association of Kv1 and Kvβ1.1 is tunable. Structural and electrophysiological studies have demonstrated that cortisone, an

anti-inflammatory glucocorticoid, and its analogues promote dissociation of Kvβ1.1 from Kv1.1 through targeting the interface site of two adjacent Kvβ subunits (Pan et al., 2008b, 2012). The dynamic modulation of Kv1 channel activities by regulating association with Kvβ may be important for proper cellular responses to the different redox environments that mammals experience during development. After the removal of Kv1.1/Kvβ1.1-C7S inactivation by RSS, subsequently applied reducing agent DTT was not capable of restoring the inactivation (Figure 31). Although two cysteine residues in the distal N terminus of Kv1.1 were targeted (Figure 36), it may also affect the association of Kv1.1 and Kvβ1.1, thereby hamper the availability of the Kvβ1.1 ball domain and remove the inactivation (Figure 55B).

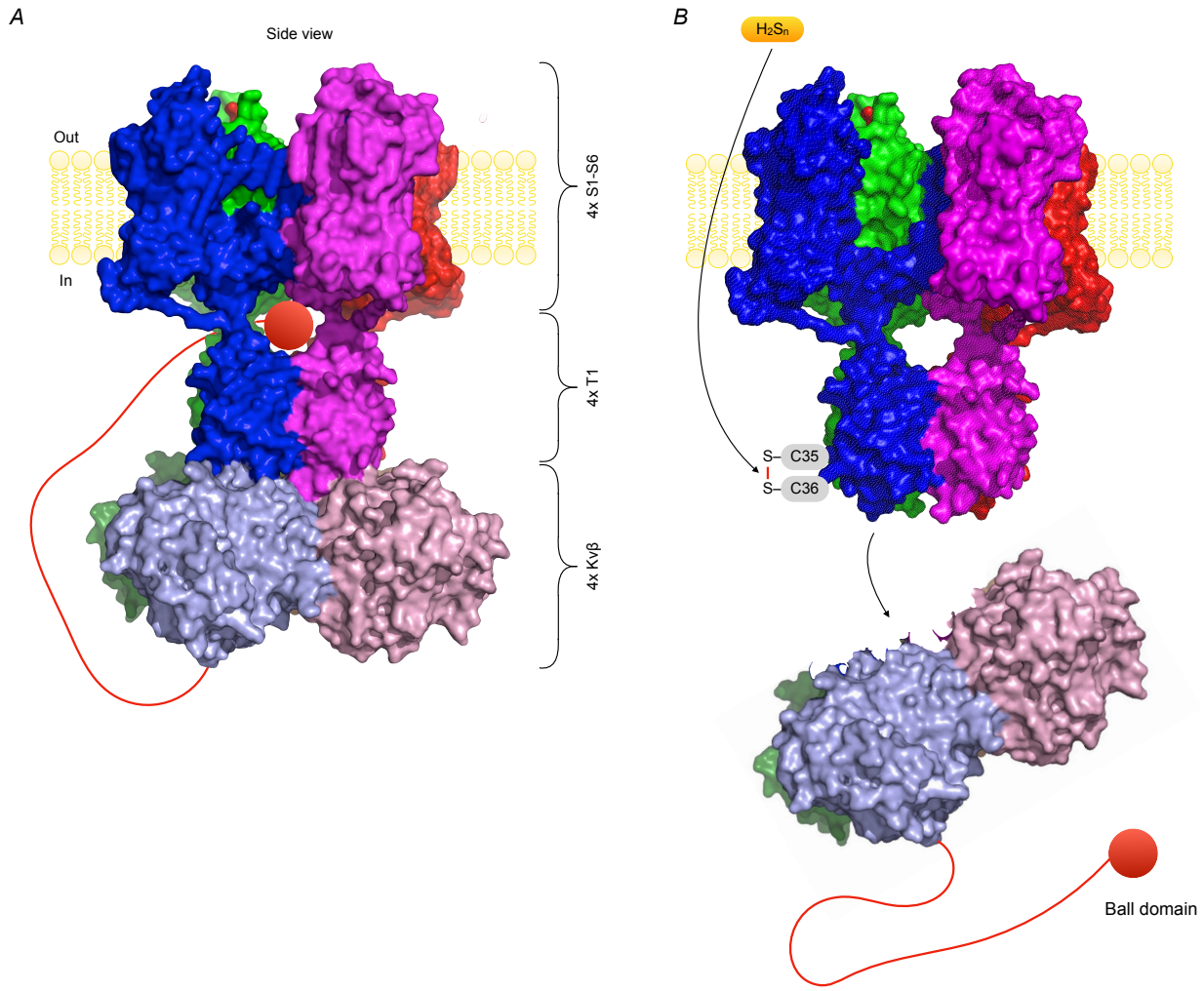

Figure 55: Modulation of Kv1 and Kvβ1.1 association

A. Structure of Kv1/Kvβ as described in Figure 5A, with an N-terminal inactivating Kvβ ball domain entering the pore through a lateral opening between S1 and T1 domain (Gulbis et al., 2000). ***B***. RSS can diffuse into the cell and induce disulfide bridge formation between C35 and C36 in Kv1.1. This may disrupt the association between the Kv1.1 α and Kvβ subunits and eliminates inactivation. Modified after Kohout and Isacoff (2008).

4.3 A model for modulation of A-type Kv channels by RSS and heme

Compromised mobility of the inactivating ball domain could be a general mechanism for modulating the inactivation of A-type Kv channels. For example, it has been reported that the inactivation of Kv1.4, Kv3.4 and Kv1.1/Kvβ1 was removed in the presence of phosphatidylinositol 4,5-bisphosphate (PIP_2) (Oliver et al., 2004), a phospholipid of the cytoplasmic leaflet of plasma membranes (Suh and Hille, 2008). The positively charged Kvα and Kvβ inactivating ball domains were immobilized to the inner leaflet of the membrane by the negatively charged headgroups of PIP_2, thereby the inactivating ball domains were prevented from accessing the channel pore (Oliver et al., 2004).

Several studies have reported that heme regulates ion channels, such as BK_{Ca}, Kv1.4 and K_{ATP} channels (Tang et al., 2003; Sahoo et al., 2013; Burton et al., 2016). Heme modulates the channel activity by interacting with a cytoplasmic domain, for the Kv1.4 channel, heme is suggested to bind to its N-terminal $CXXHX_{18}H$ motif, which stabilizes the flexible ball domain (Sahoo et al., 2013). Other A-type Kv channels, Kv3.4 and Kvβ1-induced, harbor no homologous N-terminal ball domains as that of Kv1.4 but cysteine and/or histidine residues, so heme might also bind to these ball domains and regulate their inactivation. It was observed that hemin removed the inactivation of Kv3.4 (Figure 45), Kv1.4/Kvβ1.1 (Figure 50) and Kv1.4/Kvβ1.2 (Figure 51), and mutations of C6:C24 in Kv3.4 (Figure 48) and C7:H10 in Kvβ1.1 (Figure 51) eliminated hemin effects. In addition, Kvβ1.3, the splice variant of Kvβ1.1, possesses no heme coordinating cysteine or histidine residues, and the inactivation of Kv1.4/Kvβ1.3 was not regulated by hemin (Figure 51), but its hemin sensitivity was gained after inserting a cysteine residue to the N terminus of Kvβ1.3 (A8C). It can be postulated that cysteine containing Kvβ3.1 can render hemin sensitivity to Kv1.4/Kvβ3.1. This leads to the assumption that heme regulates A-type Kv channels, following a common mechanism by binding to cysteine and/or histidine residues in the N-terminal ball domains from Kvα or Kvβ subunits.

The regulation of A-type Kv channels by RSS and heme may be proposed in the model as shown in Figure 56: after an A-type Kv channel has recovered from inactivation, its inactivating ball domain is exposed to RSS or heme. RSS can sulfhydrate cysteine and heme can bind to histidine and/or cysteine in the ball domain, both effects will induce a partial secondary structure of the ball-and-chain machinery and reduce the flexibility of this machinery, which makes it impossible for the ball peptide to reach its binding sites in channel's cavity to introduce inactivation.

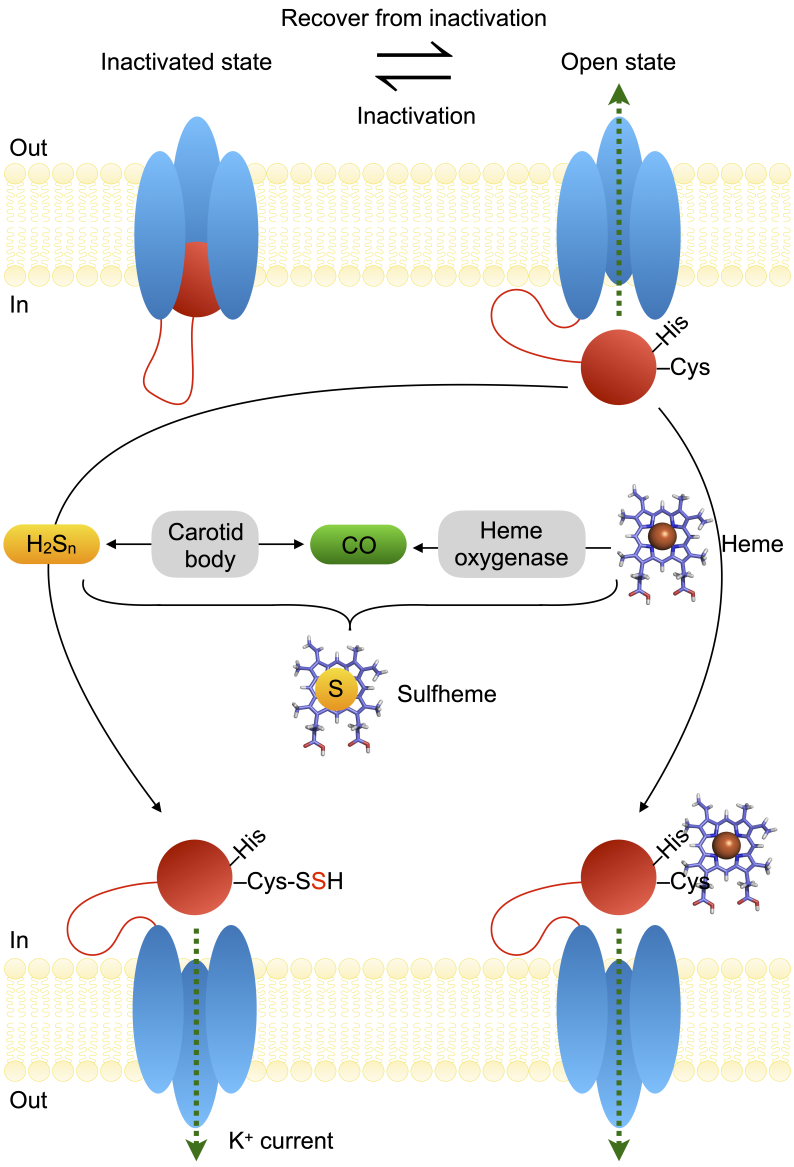

Figure 56: Proposed model for modulating A-type Kv channel by RSS and heme, and crosstalk between RSS and heme

Following the recovery of A-type Kv channels from the inactivated state, cysteine (Cys) and/or histidine (His) residues in the ball domain are exposed to RSS or heme. It is assumed that RSS sulfhydrate the Cys to Cys-SSH, and heme binds to Cys and/or His (Sahoo et al., 2013), both modifications hamper the ball domains from reaching the channel's cavity and impair the inactivation. Crosstalk between RSS and heme: H_2S can interact with heme to form sulfheme by incorporating H_2S to one of the pyrrole rings of heme (Pietri et al., 2011); RSS and CO, which is generated from heme by heme oxygenase, sense O_2 in carotid body under hypoxia.

4.4 Interactions of RSS and heme/CO

Almost all A-type Kv channels, including Kvα and Kvβ subunits induced, harbor cysteine and/or histidine residues in their inactivating ball domains, rendering their inactivation susceptible to both RSS and heme signalings (Sahoo et al., 2013, 2014) (Figure 56). It has been indicated that H_2S can bind to hemeproteins to induce different effects (Szabó, 2007;

Cooper and Brown, 2008). For instance, the activation of K_{ATP} channels by H_2S may be mediated by interactions of H_2S with cytochrome *c* oxidase, myoglobin and hemoglobin, which reduces oxygen (O_2) transport and ATP production in the mitochondria and activates K_{ATP} channels (Berzofsky et al., 1971a,b, 1972a,b; Chatfield and Mar, 1992). H_2S can be incorporated into one of the pyrrole rings of heme, yielding sulfheme, which influences H_2S reactivity with hemeproteins (Pietri et al., 2011).

As an increasingly recognized cell-signalling molecule, carbon monoxide (CO) is produced by catabolizing heme through heme oxygenase (HO) (Heinemann et al., 2014). Both H_2S and CO are important for O_2 sensing in the carotid body (Peng et al., 2010; Makarenko et al., 2012; Peng et al., 2014), the critical O_2-sensing organ to activate the brainstem respiratory during hypoxia (Lopez-Barneo et al., 2008). In hypoxia which results from reduced O_2 levels, HO activity is inhibited and CO generation is decreased. Because CO inhibits H_2S generation by its biosynthesis enzyme cystathionine γ-lyase (CSE) (Peng et al., 2010), decreased CO generation can increase H_2S generation, which stimulates the carotid body sensory nerve activity, and finally increases breathing (Yuan et al., 2015). In addition, it has been proposed that the modification of HO by H_2S could largely affect O_2 sensing (Matsui et al., 2018). Therefore, O_2, CO and H_2S are shown to work in concert to regulate breathing in the carotid body to maintain homeostasis.

Thus, under physiological conditions, RSS and heme are likely to interplay with each other to modulate A-type Kv channels and thereby neuronal excitability (Figure 56).

4.5 Physiological implications of modulating A-type Kv channels by RSS and heme

In several pain models, expression levels of A-type Kv channels are decreased (Everill and Kocsis, 1999; Stewart et al., 2003; Takeda et al., 2006; Xu et al., 2006; Zhang et al., 2007a; Cao et al., 2010; Duan et al., 2012; Zhu et al., 2012; Zhang et al., 2019). For instance, the mRNA levels and current densities of A-type Kv channels are significantly reduced in DRG neurons of a rat model of diabetic neuropathic pain, these reductions depend on brain-derived neurotrophic factor (BDNF), and pre-treatment of the neurons with anti-BDNF antibodies restores the reductions (Cao et al., 2010). Many experiments have shown that excitability changes in the DRG neurons can be reversed by using drugs to increase A-type K^+ currents (Sculptoreanu et al., 2004; Duan et al., 2012; Ritter et al., 2015a). Such as diclofenac, a nonsteroidal anti-inflammatory drug, enhances A-type K^+

currents in DRG neurons and attenuates the pain phenotype in a bone cancer model in a dose-dependent manner (Duan et al., 2012). In this work, RSS efficiently slowed the inactivation of natively expressed A-type Kv channels in DRG neurons, and both RSS and hemin slowed the inactivation of heterologously expressed Kv1.4 and Kv3.4 channels, subsequent enhanced K^+ current flow could contribute to membrane hyperpolarization and reduce neuronal hyperexcitability, thereby attenuate chronic pain.

Modulation of A-type Kv channels has also been implicated in mammalian learning and memory (Giese et al., 1998; Schreurs et al., 1998; Need et al., 2003). The Kvβ1.1 subunit is widely expressed in the brain (Rhodes et al., 1996; Butler et al., 1998), its deficiency in Kvβ1.1 knockout (Kvβ1.1$^{-/-}$) mice resulted in reduced K^+ current inactivation in hippocampal CA1 pyramidal neurons, and deficiency in learning and memory as tested in the learning of a water maze and in the social transmission of food preference task (Giese et al., 1998). The levels of H_2S are severely decreased in the brains of Alzheimer's disease (AD) patients (Eto et al., 2002), and treatment of H_2S donor NaHS improved the performance of learning and memory in various mouse and rat models of AD (Xuan et al., 2012b; Vandini et al., 2018). Thus, effects of RSS on Kvβ1.1, as well as other Kvβ subunits, induced inactivation in this study, could be used to better understanding the physiological functions of RSS, such as neuronal cytoprotection.

4.6 Outlook

Table 3: Investigated Kv channels after RSS and hemin application

Kvα	NaHS	Na_2S_n	Hemin
Kv1.1	✓	-	-
Kv1.2	✓	-	-
Kv1.4	✓	✓	✓
Kv1.5	✓	-	-
Kv3.4	✓	✓	✓

Kvα/Kvβ	NaHS	Na_2S_n	Hemin
Kv1.1/Kvβ1.1	✓	✓	-
Kv1.1/Kvβ1.2	✓	-	-
Kv1.1/Kvβ3.1	✓	✓	-
Kv1.2/Kvβ1.1	✓	✓	-
Kv1.4/Kvβ1.1	✓	-	✓
Kv1.4/Kvβ1.2	-	-	✓
Kv1.4/Kvβ1.3	-	-	✓
Kv1.5/Kvβ1.1	✓	✓	-
Kv1.5/Kvβ1.2	✓	-	-
Kv1.5/Kvβ1.3	✓	-	-

✓, investigated; -, not investigated in this work.

The sensitivity of A-type Kv channels to acute RSS and hemin application (as concluded in Table 3) greatly expands their diverse regulatory mechanisms. More extensive studies such as genetic mouse models would help to better understand the specific roles of these

channels regulated by RSS and heme under physiological and pathological conditions.

Bibliography

Abe, K. and Kimura, H. (1996). The possible role of hydrogen sulfide as an endogenous neuromodulator. *J Neurosci*, 16(3):1066–71.

Accili, E. A., Kuryshev, Y. A., Wible, B. A., and Brown, A. M. (1998). Separable effects of human kvbeta1.2 n- and c-termini on inactivation and expression of human kv1.4. *The Journal of Physiology*, 512(2):325–336.

Aidley, D. J. and Stanfield, P. R. (1996). *Ion Channels: Molecules in Action*. Ion Channels: Molecules in Action. Cambridge University Press.

Akaike, T., Ida, T., Wei, F.-Y., Nishida, M., Kumagai, Y., Alam, M. M., Ihara, H., Sawa, T., Matsunaga, T., Kasamatsu, S., Nishimura, A., Morita, M., Tomizawa, K., Nishimura, A., Watanabe, S., Inaba, K., Shima, H., Tanuma, N., Jung, M., Fujii, S., Watanabe, Y., Ohmuraya, M., Nagy, P., Feelisch, M., Fukuto, J. M., and Motohashi, H. (2017). Cysteinyl-tRNA synthetase governs cysteine polysulfidation and mitochondrial bioenergetics. *Nature Communications*, 8(1).

Aldrich, R. W., Corey, D. P., and Stevens, C. F. (1983). A reinterpretation of mammalian sodium channel gating based on single channel recording. *Nature*, 306(5942):436–41.

Amarillo, Y., De Santiago-Castillo, J. A., Dougherty, K., Maffie, J., Kwon, E., Covarrubias, M., and Rudy, B. (2008). Ternary kv4.2 channels recapitulate voltage-dependent inactivation kinetics of a-type k+ channels in cerebellar granule neurons. *J Physiol*, 586(8):2093–106.

Amberg, G. C., Koh, S. D., Imaizumi, Y., Ohya, S., and Sanders, K. M. (2003). A-type potassium currents in smooth muscle. *Am J Physiol Cell Physiol*, 284(3):C583–95.

An, W. F., Bowlby, M. R., Betty, M., Cao, J., Ling, H. P., Mendoza, G., Hinson, J. W., Mattsson, K. I., Strassle, B. W., Trimmer, J. S., and Rhodes, K. J. (2000). Modulation of a-type potassium channels by a family of calcium sensors. *Nature*, 403(6769):553–6.

Antz, C., Bauer, T., Kalbacher, H., Frank, R., Covarrubias, M., Kalbitzer, H. R., Ruppersberg, J. P., Baukrowitz, T., and Fakler, B. (1999). Control of k+ channel gating by

protein phosphorylation: structural switches of the inactivation gate. *Nat Struct Biol*, 6(2):146–50.

Antz, C. and Fakler, B. (1998). Fast inactivation of voltage-gated k(+) channels: From cartoon to structure. *News Physiol Sci*, 13:177–182.

Antz, C., Geyer, M., Fakler, B., Schott, M. K., Guy, H. R., Frank, R., Ruppersberg, J. P., and Kalbitzer, H. R. (1997). Nmr structure of inactivation gates from mammalian voltage-dependent potassium channels. *Nature*, 385(6613):272–5.

Apkon, M. and Nerbonne, J. M. (1991). Characterization of two distinct depolarization-activated k+ currents in isolated adult rat ventricular myocytes. *J Gen Physiol*, 97(5):973–1011.

Ashcroft, F. M. and Rorsman, P. (2013). K(atp) channels and islet hormone secretion: new insights and controversies. *Nat Rev Endocrinol*, 9(11):660–9.

Bahring, R. and Covarrubias, M. (2011). Mechanisms of closed-state inactivation in voltage-gated ion channels. *J Physiol*, 589(Pt 3):461–79.

Bahring, R., Dannenberg, J., Peters, H. C., Leicher, T., Pongs, O., and Isbrandt, D. (2001). Conserved kv4 n-terminal domain critical for effects of kv channel-interacting protein 2.2 on channel expression and gating. *J Biol Chem*, 276(26):23888–94.

Bandell, M., Story, G. M., Hwang, S. W., Viswanath, V., Eid, S. R., Petrus, M. J., Earley, T. J., and Patapoutian, A. (2004). Noxious cold ion channel TRPA1 is activated by pungent compounds and bradykinin. *Neuron*, 41(6):849–857.

Barry, D. M. and Nerbonne, J. M. (1996). Myocardial potassium channels: electrophysiological and molecular diversity. *Annu Rev Physiol*, 58:363–94.

Bautista, D. M., Movahed, P., Hinman, A., Axelsson, H. E., Sterner, O., Hogestatt, E. D., Julius, D., Jordt, S. E., and Zygmunt, P. M. (2005). Pungent products from garlic activate the sensory ion channel trpa1. *Proc Natl Acad Sci U S A*, 102(34):12248–52.

Beck, E. J., Sorensen, R. G., Slater, S. J., and Covarrubias, M. (1998). Interactions between multiple phosphorylation sites in the inactivation particle of a k+ channel. insights into the molecular mechanism of protein kinase c action. *J Gen Physiol*, 112(1):71–84.

Berzofsky, J. A., Peisach, J., and Alben, J. O. (1972a). Sulfheme proteins. 3. carboxy-sulfmyoglobin: the relation between electron withdrawal from iron and ligand binding. *The Journal of biological chemistry*, 247:3774–3782.

Berzofsky, J. A., Peisach, J., and Blumberg, W. E. (1971a). Sulfheme proteins. i. optical and magnetic properties of sulfmyoglobin and its derivatives. *The Journal of biological chemistry*, 246:3367–3377.

Berzofsky, J. A., Peisach, J., and Blumberg, W. E. (1971b). Sulfheme proteins. ii. the reversible oxygenation of ferrous sulfmyoglobin. *The Journal of biological chemistry*, 246:7366–7372.

Berzofsky, J. A., Peisach, J., and Horecker, B. L. (1972b). Sulfheme proteins. iv. the stoichiometry of sulfur incorporation and the isolation of sulfhemin, the prosthetic group of sulfmyoglobin. *The Journal of biological chemistry*, 247:3783–3791.

Birnbaum, S. G., Varga, A. W., Yuan, L. L., Anderson, A. E., Sweatt, J. D., and Schrader, L. A. (2004). Structure and function of kv4-family transient potassium channels. *Physiol Rev*, 84(3):803–33.

Bocksteins, E. and Snyders, D. J. (2012). Electrically silent kv subunits: Their molecular and functional characteristics. *Physiology*, 27(2):73–84.

Bouskila, Y. and Dudek, F. E. (1995). A rapidly activating type of outward rectifier k+ current and a-current in rat suprachiasmatic nucleus neurones. *J Physiol*, 488 (Pt 2):339–50.

Browne, D. L., Gancher, S. T., Nutt, J. G., Brunt, E. R., Smith, E. A., Kramer, P., and Litt, M. (1994). Episodic ataxia/myokymia syndrome is associated with point mutations in the human potassium channel gene, kcna1. *Nat Genet*, 8(2):136–40.

Burton, M. J., Kapetanaki, S. M., Chernova, T., Jamieson, A. G., Dorlet, P., Santolini, J., Moody, P. C., Mitcheson, J. S., Davies, N. W., Schmid, R., Raven, E. L., and Storey, N. M. (2016). A heme-binding domain controls regulation of atp-dependent potassium channels. *Proc Natl Acad Sci U S A*, 113(14):3785–90.

Butler, D. M., Ono, J. K., Chang, T., McCaman, R. E., and Barish, M. E. (1998). Mouse brain potassium channel beta1 subunit mRNA: Cloning and distribution during development. *Journal of Neurobiology*, 34(2):135–150.

Cai, S. Q., Hernandez, L., Wang, Y., Park, K. H., and Sesti, F. (2005). Mps-1 is a k+ channel beta-subunit and a serine/threonine kinase. *Nat Neurosci*, 8(11):1503–9.

Cai, S. Q., Li, W., and Sesti, F. (2007). Multiple modes of a-type potassium current regulation. *Curr Pharm Des*, 13(31):3178–84.

Cao, X. H., Byun, H. S., Chen, S. R., Cai, Y. Q., and Pan, H. L. (2010). Reduction in voltage-gated k+ channel activity in primary sensory neurons in painful diabetic neuropathy: role of brain-derived neurotrophic factor. *J Neurochem*, 114(5):1460–75.

Capera, J., Serrano-Novillo, C., Navarro-Perez, M., Cassinelli, S., and Felipe, A. (2019). The potassium channel odyssey: Mechanisms of traffic and membrane arrangement. *Int J Mol Sci*, 20(3).

Carrasquillo, Y. and Nerbonne, J. M. (2014). Ia channels: diverse regulatory mechanisms. *Neuroscientist*, 20(2):104–11.

Chatfield, M. J. and Mar, G. N. L. (1992). 1h nuclear magnetic resonance study of the prosthetic group in sulfhemoglobin. *Archives of Biochemistry and Biophysics*, 295(2):289–296.

Chen, J., Daggett, H., De Waard, M., Heinemann, S. H., and Hoshi, T. (2002). Nitric oxide augments voltage-gated p/q-type ca(2+) channels constituting a putative positive feedback loop. *Free Radic Biol Med*, 32(7):638–49.

Chen, K. Y. and Morris, J. C. (1972). Kinetics of oxidation of aqueous sulfide by oxygen. *Environmental Science & Technology*, 6(6):529–537.

Chen, W., Fu, L., Chen, C., Xiao, J., Li, W., Zhang, L., Xiao, Q., Huang, C., Sheng, J., and Song, X. (2019). Unexpected reaction patterns enable simultaneous differentiation of h2s, h2sn and biothiols. *Chemical Communications*, 55(56):8130–8133.

Chen, W., Rosser, E. W., Matsunaga, T., Pacheco, A., Akaike, T., and Xian, M. (2015a). The development of fluorescent probes for visualizing intracellular hydrogen polysulfides. *Angewandte Chemie International Edition*, 54(47):13961–13965.

Chen, W., Rosser, E. W., Zhang, D., Shi, W., Li, Y., Dong, W.-J., Ma, H., Hu, D., and Xian, M. (2015b). A specific nucleophilic ring-opening reaction of aziridines as a unique platform for the construction of hydrogen polysulfides sensors. *Organic Letters*, 17(11):2776–2779.

Chien, L. Y., Cheng, J. K., Chu, D., Cheng, C. F., and Tsaur, M. L. (2007). Reduced expression of a-type potassium channels in primary sensory neurons induces mechanical hypersensitivity. *J Neurosci*, 27(37):9855–65.

Clare, J. J. (2010). Targeting ion channels for drug discovery. *Discovery medicine*, 9:253–260.

Coetzee, W. A., Amarillo, Y., Chiu, J., Chow, A., Lau, D., McCormack, T., Moreno, H., Nadal, M. S., Ozaita, A., Pountney, D., Saganich, M., Vega-Saenz de Miera, E., and Rudy, B. (1999). Molecular diversity of k+ channels. *Ann N Y Acad Sci*, 868(1):233–85.

Comes, N., Serrano-Albarras, A., Capera, J., Serrano-Novillo, C., Condom, E., Ramon, Y. C. S., Ferreres, J. C., and Felipe, A. (2015). Involvement of potassium channels in the progression of cancer to a more malignant phenotype. *Biochim Biophys Acta*, 1848(10 Pt B):2477–92.

Connor, J. A. and Stevens, C. F. (1971). Voltage clamp studies of a transient outward membrane current in gastropod neural somata. *J Physiol*, 213(1):21–30.

Cooper, C. E. and Brown, G. C. (2008). The inhibition of mitochondrial cytochrome oxidase by the gases carbon monoxide, nitric oxide, hydrogen cyanide and hydrogen sulfide: chemical mechanism and physiological significance. *Journal of Bioenergetics and Biomembranes*, 40(5):533–539.

Cortese-Krott, M. M., Kuhnle, G. G. C., Dyson, A., Fernandez, B. O., Grman, M., DuMond, J. F., Barrow, M. P., McLeod, G., Nakagawa, H., Ondrias, K., Nagy, P., King, S. B., Saavedra, J. E., Keefer, L. K., Singer, M., Kelm, M., Butler, A. R., and Feelisch, M. (2015). Key bioactive reaction products of the NO/h2s interaction are s/n-hybrid species, polysulfides, and nitroxyl. *Proceedings of the National Academy of Sciences*, 112(34):E4651–E4660.

Covarrubias, M., Bhattacharji, A., De Santiago-Castillo, J. A., Dougherty, K., Kaulin, Y. A., Na-Phuket, T. R., and Wang, G. (2008). The neuronal kv4 channel complex. *Neurochem Res*, 33(8):1558–67.

Covarrubias, M., Wei, A., Salkoff, L., and Vyas, T. B. (1994). Elimination of rapid potassium channel inactivation by phosphorylation of the inactivation gate. *Neuron*, 13(6):1403–12.

Cuevasanta, E., Moller, M. N., and Alvarez, B. (2017). Biological chemistry of hydrogen sulfide and persulfides. *Arch Biochem Biophys*, 617:9–25.

Dallas, M. L., Boyle, J. P., Milligan, C. J., Sayer, R., Kerrigan, T. L., McKinstry, C., Lu, P., Mankouri, J., Harris, M., Scragg, J. L., Pearson, H. A., and Peers, C. (2011). Carbon monoxide protects against oxidant-induced apoptosisviainhibition of kv2.1. *The FASEB Journal*, 25(5):1519–1530.

De Biasi, M., Wang, Z., Accili, E., Wible, B., and Fedida, D. (1997). Open channel block of human heart hkv1.5 by the beta-subunit hkv beta 1.2. *Am J Physiol*, 272(6 Pt 2):H2932–41.

Decher, N., Gonzalez, T., Streit, A. K., Sachse, F. B., Renigunta, V., Soom, M., Heinemann, S. H., Daut, J., and Sanguinetti, M. C. (2008). Structural determinants of kvbeta1.3-induced channel inactivation: a hairpin modulated by pip2. *EMBO J*, 27(23):3164–74.

Dib-Hajj, S. D., Choi, J. S., Macala, L. J., Tyrrell, L., Black, J. A., Cummins, T. R., and Waxman, S. G. (2009). Transfection of rat or mouse neurons by biolistics or electroporation. *Nature Protocols*, 4(8):1118–1127.

Dixon, J. E., Shi, W., Wang, H. S., McDonald, C., Yu, H., Wymore, R. S., Cohen, I. S., and McKinnon, D. (1996). Role of the kv4.3 k+ channel in ventricular muscle. a molecular correlate for the transient outward current. *Circ Res*, 79(4):659–68.

Donegan, R. K., Moore, C. M., Hanna, D. A., and Reddi, A. R. (2019). Handling heme: The mechanisms underlying the movement of heme within and between cells. *Free Radic Biol Med*, 133:88–100.

Dooley, C. T., Dore, T. M., Hanson, G. T., Jackson, W. C., Remington, S. J., and Tsien, R. Y. (2004). Imaging dynamic redox changes in mammalian cells with green fluorescent protein indicators. *J Biol Chem*, 279(21):22284–93.

Dougherty, K. and Covarrubias, M. (2006). A dipeptidyl aminopeptidase-like protein remodels gating charge dynamics in kv4.2 channels. *J Gen Physiol*, 128(6):745–53.

Dougherty, K., De Santiago-Castillo, J. A., and Covarrubias, M. (2008). Gating charge immobilization in kv4.2 channels: the basis of closed-state inactivation. *J Gen Physiol*, 131(3):257–73.

Drain, P., Dubin, A. E., and Aldrich, R. W. (1994). Regulation of shaker k+ channel inactivation gating by the camp-dependent protein kinase. *Neuron*, 12(5):1097–109.

Duan, K. Z., Xu, Q., Zhang, X. M., Zhao, Z. Q., Mei, Y. A., and Zhang, Y. Q. (2012). Targeting a-type k(+) channels in primary sensory neurons for bone cancer pain in a rat model. *Pain*, 153(3):562–74.

Duprat, F., Guillemare, E., Romey, G., Fink, M., Lesage, F., Lazdunski, M., and Honore, E. (1995). Susceptibility of cloned k+ channels to reactive oxygen species. *Proc Natl Acad Sci U S A*, 92(25):11796–800.

Eberhardt, M., Dux, M., Namer, B., Miljkovic, J., Cordasic, N., Will, C., Kichko, T. I., de la Roche, J., Fischer, M., Suárez, S. A., Bikiel, D., Dorsch, K., Leffler, A., Babes, A., Lampert, A., Lennerz, J. K., Jacobi, J., Martí, M. A., Doctorovich, F., Högestätt, E. D., Zygmunt, P. M., Ivanovic-Burmazovic, I., Messlinger, K., Reeh, P., and Filipovic, M. R. (2014). H2s and NO cooperatively regulate vascular tone by activating a neuroendocrine HNO–TRPA1–CGRP signalling pathway. *Nature Communications*, 5(1).

Elrod, J. W., Calvert, J. W., Morrison, J., Doeller, J. E., Kraus, D. W., Tao, L., Jiao, X., Scalia, R., Kiss, L., Szabo, C., Kimura, H., Chow, C. W., and Lefer, D. J. (2007). Hydrogen sulfide attenuates myocardial ischemia-reperfusion injury by preservation of mitochondrial function. *Proc Natl Acad Sci U S A*, 104(39):15560–5.

Elsey, D. J., Fowkes, R. C., and Baxter, G. F. (2010). Regulation of cardiovascular cell function by hydrogen sulfide (h(2)s). *Cell Biochem Funct*, 28(2):95–106.

England, S. K., Uebele, V. N., Shear, H., Kodali, J., Bennett, P. B., and Tamkun, M. M. (1995). Characterization of a voltage-gated k+ channel beta subunit expressed in human heart. *Proc Natl Acad Sci U S A*, 92(14):6309–13.

Eto, K., Asada, T., Arima, K., Makifuchi, T., and Kimura, H. (2002). Brain hydrogen sulfide is severely decreased in alzheimer's disease. *Biochemical and Biophysical Research Communications*, 293(5):1485–1488.

Everill, B. and Kocsis, J. D. (1999). Reduction in potassium currents in identified cutaneous afferent dorsal root ganglion neurons after axotomy. *Journal of Neurophysiology*, 82(2):700–708.

Fedida, D., Wible, B., Wang, Z., Fermini, B., Faust, F., Nattel, S., and Brown, A. M. (1993). Identity of a novel delayed rectifier current from human heart with a cloned k+ channel current. *Circ Res*, 73(1):210–6.

Feng, X., Zhou, Y. L., Meng, X., Qi, F. H., Chen, W., Jiang, X., and Xu, G. Y. (2013). Hydrogen sulfide increases excitability through suppression of sustained potassium channel currents of rat trigeminal ganglion neurons. *Mol Pain*, 9:4.

Filipovic, M. R., Zivanovic, J., Alvarez, B., and Banerjee, R. (2018). Chemical biology of h2s signaling through persulfidation. *Chem Rev*, 118(3):1253–1337.

Firek, L. and Giles, W. R. (1995). Outward currents underlying repolarization in human atrial myocytes. *Cardiovasc Res*, 30(1):31–8.

Furne, J., Saeed, A., and Levitt, M. D. (2008). Whole tissue hydrogen sulfide concentrations are orders of magnitude lower than presently accepted values. *Am J Physiol Regul Integr Comp Physiol*, 295(5):R1479–85.

Gamper, N. and Ooi, L. (2015). Redox and nitric oxide-mediated regulation of sensory neuron ion channel function. *Antioxid Redox Signal*, 22(6):486–504.

Giese, K. P., Storm, J. F., Reuter, D., Fedorov, N. B., Shao, L. R., Leicher, T., Pongs, O., and Silva, A. J. (1998). Reduced k+ channel inactivation, spike broadening, and after-hyperpolarization in kvbeta1.1-deficient mice with impaired learning. *Learning & memory (Cold Spring Harbor, N.Y.)*, 5:257–273.

Giles, G. and Jacob, C. (2002). Reactive sulfur species: An emerging concept in oxidative stress. *Biological Chemistry*, 383(3-4).

Giles, G. I., Tasker, K. M., and Jacob, C. (2001). Hypothesis: the role of reactive sulfur species in oxidative stress. *Free Radical Biology and Medicine*, 31(10):1279–1283.

Giuliani, D., Ottani, A., Zaffe, D., Galantucci, M., Strinati, F., Lodi, R., and Guarini, S. (2013). Hydrogen sulfide slows down progression of experimental alzheimer's disease by targeting multiple pathophysiological mechanisms. *Neurobiol Learn Mem*, 104:82–91.

Gold, M. S., Shuster, M. J., and Levine, J. D. (1996). Characterization of six voltage-gated k+ currents in adult rat sensory neurons. *J Neurophysiol*, 75(6):2629–46.

Goldin, A. L. (1992). [15] maintenance of xenopus laevis and oocyte injection. In *Methods in Enzymology*, pages 266–279. Elsevier.

Goldin, A. L. (2006). Expression of ion channels in xenopus oocytes. In *Expression and Analysis of Recombinant Ion Channels*, pages 1–25. Wiley-VCH Verlag GmbH & Co. KGaA.

Goldin, A. L. and Sumikawa, K. (1992). [16] preparation of RNA for injection into xenopus oocytes. In *Methods in Enzymology*, pages 279–297. Elsevier.

Greiner, R., Palinkas, Z., Basell, K., Becher, D., Antelmann, H., Nagy, P., and Dick, T. P. (2013). Polysulfides link h2s to protein thiol oxidation. *Antioxid Redox Signal*, 19(15):1749–65.

Griffith, O. W. (1999). Biologic and pharmacologic regulation of mammalian glutathione synthesis. *Free Radic Biol Med*, 27(9-10):922–35.

Gruhlke, M. C. and Slusarenko, A. J. (2012). The biology of reactive sulfur species (RSS). *Plant Physiology and Biochemistry*, 59:98–107.

Gulbis, J. M., Mann, S., and MacKinnon, R. (1999). Structure of a voltage-dependent k+ channel beta subunit. *Cell*, 97(7):943–952.

Gulbis, J. M., Zhou, M., Mann, S., and MacKinnon, R. (2000). Structure of the cytoplasmic beta subunit-t1 assembly of voltage-dependent k+ channels. *Science*, 289(5476):123–7.

Gundry, R. L., White, M. Y., Murray, C. I., Kane, L. A., Fu, Q., Stanley, B. A., and Van Eyk, J. E. (2009). Preparation of proteins and peptides for mass spectrometry analysis in a bottom-up proteomics workflow. *Curr Protoc Mol Biol*, Chapter 10(1):Unit10 25.

Gutman, G. A., Chandy, K. G., Grissmer, S., Lazdunski, M., McKinnon, D., Pardo, L. A., Robertson, G. A., Rudy, B., Sanguinetti, M. C., Stuhmer, W., and Wang, X. (2005). International union of pharmacology. liii. nomenclature and molecular relationships of voltage-gated potassium channels. *Pharmacol Rev*, 57(4):473–508.

Hagiwara, S., Kusano, K., and Saito, N. (1961). Membrane changes of onchidium nerve cell in potassium-rich media. *J Physiol*, 155(3):470–89.

Hamill, O. P., Marty, A., Neher, E., Sakmann, B., and Sigworth, F. J. (1981). Improved patch-clamp techniques for high-resolution current recording from cells and cell-free membrane patches. *Pflugers Arch*, 391(2):85–100.

Hammers, M. D., Taormina, M. J., Cerda, M. M., Montoya, L. A., Seidenkranz, D. T., Parthasarathy, R., and Pluth, M. D. (2015). A bright fluorescent probe for h2s enables analyte-responsive, 3d imaging in live zebrafish using light sheet fluorescence microscopy. *Journal of the American Chemical Society*, 137(32):10216–10223.

Hancock, J. T. and Whiteman, M. (2016). Hydrogen sulfide signaling: interactions with nitric oxide and reactive oxygen species. *Ann N Y Acad Sci*, 1365(1):5–14.

Hanna, D. A., Martinez-Guzman, O., and Reddi, A. R. (2017). Heme gazing: Illuminating eukaryotic heme trafficking, dynamics, and signaling with fluorescent heme sensors. *Biochemistry*, 56(13):1815–1823.

Heinemann, S., Rettig, J., Scott, V., Parcej, D. N., Lorra, C., Dolly, J., and Pongs, O. (1994). The inactivation behaviour of voltage-gated k-channels may be determined by association of alpha- and beta-subunits. *J Physiol Paris*, 88(3):173–80.

Heinemann, S. H., Hoshi, T., Westerhausen, M., and Schiller, A. (2014). Carbon monoxide – physiology, detection and controlled release. *Chem. Commun.*, 50(28):3644–3660.

Heinemann, S. H., Rettig, J., Graack, H. R., and Pongs, O. (1996). Functional characterization of kv channel beta-subunits from rat brain. *J Physiol*, 493 (Pt 3):625–33.

Heinemann, S. H., Rettig, J., Wunder, F., and Pongs, O. (1995). Molecular and functional characterization of a rat brain kv beta 3 potassium channel subunit. *FEBS Lett*, 377(3):383–9.

Herson, P. S., Virk, M., Rustay, N. R., Bond, C. T., Crabbe, J. C., Adelman, J. P., and Maylie, J. (2003). A mouse model of episodic ataxia type-1. *Nat Neurosci*, 6(4):378–83.

Hess, D. T., Matsumoto, A., Kim, S.-O., Marshall, H. E., and Stamler, J. S. (2005). Protein s-nitrosylation: purview and parameters. *Nature Reviews Molecular Cell Biology*, 6(2):150–166.

Hille, B. (2001). *Ionic channels of excitable membranes*. Sinauer Associates, 3rd edition edition.

Hodgkin, A. L. and Huxley, A. F. (1952). A quantitative description of membrane current and its application to conduction and excitation in nerve. *J Physiol*, 117(4):500–44.

Hoffman, D. A., Magee, J. C., Colbert, C. M., and Johnston, D. (1997). K+ channel regulation of signal propagation in dendrites of hippocampal pyramidal neurons. *Nature*, 387(6636):869–75.

Hoffmann, M. R. (1977). Kinetics and mechanism of oxidation of hydrogen sulfide by hydrogen peroxide in acidic solution. *Environmental Science & Technology*, 11(1):61–66.

Horrigan, F. T., Heinemann, S. H., and Hoshi, T. (2005). Heme regulates allosteric activation of the slo1 bk channel. *J Gen Physiol*, 126(1):7–21.

Hoshi, T., Zagotta, W. N., and Aldrich, R. W. (1990). Biophysical and molecular mechanisms of shaker potassium channel inactivation. *Science*, 250(4980):533–8.

Hoshi, T., Zagotta, W. N., and Aldrich, R. W. (1991). Two types of inactivation in shaker k+ channels: effects of alterations in the carboxy-terminal region. *Neuron*, 7(4):547–56.

Hsieh, C. P. (2008). Redox modulation of a-type k+ currents in pain-sensing dorsal root ganglion neurons. *Biochem Biophys Res Commun*, 370(3):445–9.

Iciek, M., Kowalczyk-Pachel, D., Bilska-Wilkosz, A., Kwiecien, I., Gorny, M., and Wlodek, L. (2015). S-sulfhydration as a cellular redox regulation. *Biosci Rep*, 36(2).

Imbrici, P., D'Adamo, M. C., Kullmann, D. M., and Pessia, M. (2006). Episodic ataxia type 1 mutations in the kcna1 gene impair the fast inactivation properties of the human potassium channels kv1.4-1.1/kvbeta1.1 and kv1.4-1.1/kvbeta1.2. *Eur J Neurosci*, 24(11):3073–83.

Ishikawa, K., Tanaka, M., Black, J. A., and Waxman, S. G. (1999). Changes in expression of voltage-gated potassium channels in dorsal root ganglion neurons following axotomy. *Muscle Nerve*, 22(4):502–7.

Jaggar, J. H., Li, A., Parfenova, H., Liu, J., Umstot, E. S., Dopico, A. M., and Leffler, C. W. (2005). Heme is a carbon monoxide receptor for large-conductance ca2+-activated k+ channels. *Circ Res*, 97(8):805–12.

Jan, L. Y. and Jan, Y. N. (1990). How might the diversity of potassium channels be generated? *Trends Neurosci*, 13(10):415–9.

Jan, L. Y. and Jan, Y. N. (2012). Voltage-gated potassium channels and the diversity of electrical signalling. *J Physiol*, 590(11):2591–9.

Jeevaratnam, K., Chadda, K. R., Huang, C. L., and Camm, A. J. (2018). Cardiac potassium channels: Physiological insights for targeted therapy. *J Cardiovasc Pharmacol Ther*, 23(2):119–129.

Jerng, H. H., Dougherty, K., Covarrubias, M., and Pfaffinger, P. J. (2009). A novel n-terminal motif of dipeptidyl peptidase-like proteins produces rapid inactivation of kv4.2 channels by a pore-blocking mechanism. *Channels (Austin)*, 3(6):448–61.

Jerng, H. H. and Pfaffinger, P. J. (2014). Modulatory mechanisms and multiple functions of somatodendritic a-type k (+) channel auxiliary subunits. *Front Cell Neurosci*, 8:82.

Jerng, H. H., Pfaffinger, P. J., and Covarrubias, M. (2004a). Molecular physiology and modulation of somatodendritic a-type potassium channels. *Mol Cell Neurosci*, 27(4):343–69.

Jerng, H. H., Qian, Y., and Pfaffinger, P. J. (2004b). Modulation of kv4.2 channel expression and gating by dipeptidyl peptidase 10 (DPP10). *Biophysical Journal*, 87(4):2380–2396.

Jow, F., Zhang, Z.-H., Kopsco, D. C., Carroll, K. C., and Wang, K. (2004). Functional coupling of intracellular calcium and inactivation of voltage-gated kv1.1/kv 1.1 a-type k+ channels. *Proceedings of the National Academy of Sciences*, 101(43):15535–15540.

Kabil, O., Motl, N., and Banerjee, R. (2014). H2s and its role in redox signaling. *Biochim Biophys Acta*, 1844(8):1355–66.

Kaczmarek, L. K. and Zhang, Y. (2017). Kv3 channels: Enablers of rapid firing, neurotransmitter release, and neuronal endurance. *Physiol Rev*, 97(4):1431–1468.

Kandel, E. R., Jessell, T. M., Schwartz, J. H., Siegelbaum, S. A., and Hudspeth, A. J. (2013). *Principles of Neural Science, Fifth Edition*. Principles of Neural Science. McGraw-Hill Education.

Kaulin, Y. A., De Santiago-Castillo, J. A., Rocha, C. A., Nadal, M. S., Rudy, B., and Covarrubias, M. (2009). The dipeptidyl-peptidase-like protein dpp6 determines the unitary conductance of neuronal kv4.2 channels. *J Neurosci*, 29(10):3242–51.

Kawagoe, R., Takashima, I., Uchinomiya, S., and Ojida, A. (2017). Reversible ratiometric detection of highly reactive hydropersulfides using a FRET-based dual emission fluorescent probe. *Chemical Science*, 8(2):1134–1140.

Kim, D. S., Choi, J. O., Rim, H. D., and Cho, H. J. (2002). Downregulation of voltage-gated potassium channel α gene expression in dorsal root ganglia following chronic constriction injury of the rat sciatic nerve. *Molecular Brain Research*, 105(1-2):146–152.

Kimura, H. (2015). Hydrogen sulfide and polysulfides as signaling molecules. *Proc Jpn Acad Ser B Phys Biol Sci*, 91(4):131–59.

Kimura, H. (2019). Signalling by hydrogen sulfide and polysulfides via protein s - sulfuration. *British Journal of Pharmacology*.

Kimura, Y. and Kimura, H. (2004). Hydrogen sulfide protects neurons from oxidative stress. *The FASEB Journal*, 18(10):1165–1167.

Kimura, Y., Koike, S., Shibuya, N., Lefer, D., Ogasawara, Y., and Kimura, H. (2017). 3-mercaptopyruvate sulfurtransferase produces potential redox regulators cysteine- and glutathione-persulfide (cys-SSH and GSSH) together with signaling molecules h2s2, h2s3 and h2s. *Scientific Reports*, 7(1).

Kimura, Y., Mikami, Y., Osumi, K., Tsugane, M., Oka, J., and Kimura, H. (2013). Polysulfides are possible h2s-derived signaling molecules in rat brain. *FASEB J*, 27(6):2451–7.

Kimura, Y., Toyofuku, Y., Koike, S., Shibuya, N., Nagahara, N., Lefer, D., Ogasawara, Y., and Kimura, H. (2015). Identification of h2s3 and h2s produced by 3-mercaptopyruvate sulfurtransferase in the brain. *Scientific Reports*, 5(1).

Kohout, S. C. and Isacoff, E. Y. (2008). To dislodge an enzyme from an ion channel, try steroids. *Nature Chemical Biology*, 4(11):650–651.

Kostyuk, P. G., Veselovsky, N. S., Fedulova, S. A., and Tsyndrenko, A. Y. (1981). Ionic currents in the somatic membrane of rat dorsal root ganglion neurons-iii. potassium currents. *Neuroscience*, 6(12):2439–44.

Krishnan, N., Fu, C., Pappin, D. J., and Tonks, N. K. (2011). H2s-induced sulfhydration of the phosphatase ptp1b and its role in the endoplasmic reticulum stress response. *Sci Signal*, 4(203):ra86.

Kurata, H. T. and Fedida, D. (2006). A structural interpretation of voltage-gated potassium channel inactivation. *Progress in Biophysics and Molecular Biology*, 92(2):185–208.

Kwak, Y. G., Hu, N., Wei, J., George, A. L., J., Grobaski, T. D., Tamkun, M. M., and Murray, K. T. (1999). Protein kinase a phosphorylation alters kvbeta1.3 subunit-mediated inactivation of the kv1.5 potassium channel. *J Biol Chem*, 274(20):13928–32.

Lau, N. and Pluth, M. D. (2019). Reactive sulfur species (RSS): persulfides, polysulfides, potential, and problems. *Current Opinion in Chemical Biology*, 49:1–8.

Lee, S.-R., Yang, K.-S., Kwon, J., Lee, C., Jeong, W., and Rhee, S. G. (2002). Reversible inactivation of the tumor suppressor PTEN by h2o2. *Journal of Biological Chemistry*, 277(23):20336–20342.

Leicher, T., Bahring, R., Isbrandt, D., and Pongs, O. (1998). Coexpression of the kcna3b gene product with kv1.5 leads to a novel a-type potassium channel. *J Biol Chem*, 273(52):35095–101.

Leicher, T., Roeper, J., Weber, K., Wang, X., and Pongs, O. (1996). Structural and functional characterization of human potassium channel subunit β1 (kcna1b). *Neuropharmacology*, 35(7):787–795.

Li, L., Rose, P., and Moore, P. K. (2011). Hydrogen sulfide and cell signaling. *Annu Rev Pharmacol Toxicol*, 51:169–87.

Li, M., Jan, Y. N., and Jan, L. Y. (1992). Specification of subunit assembly by the hydrophilic amino-terminal domain of the shaker potassium channel. *Science*, 257(5074):1225–30.

Li, Q. and Lancaster, J. R. (2013). Chemical foundations of hydrogen sulfide biology. *Nitric Oxide*, 35:21–34.

Lin, V. S., Chen, W., Xian, M., and Chang, C. J. (2015). Chemical probes for molecular imaging and detection of hydrogen sulfide and reactive sulfur species in biological systems. *Chemical Society Reviews*, 44(14):4596–4618.

Lippert, A. R., New, E. J., and Chang, C. J. (2011). Reaction-based fluorescent probes for selective imaging of hydrogen sulfide in living cells. *Journal of the American Chemical Society*, 133(26):10078–10080.

Liss, B., Franz, O., Sewing, S., Bruns, R., Neuhoff, H., and Roeper, J. (2001). Tuning pacemaker frequency of individual dopaminergic neurons by kv4.3l and kchip3.1 transcription. *EMBO J*, 20(20):5715–24.

Liu, C., Chen, W., Shi, W., Peng, B., Zhao, Y., Ma, H., and Xian, M. (2014). Rational design and bioimaging applications of highly selective fluorescence probes for hydrogen polysulfides. *Journal of the American Chemical Society*, 136(20):7257–7260.

Liu, C., Pan, J., Li, S., Zhao, Y., Wu, L. Y., Berkman, C. E., Whorton, A. R., and Xian, M. (2011). Capture and visualization of hydrogen sulfide by a fluorescent probe. *Angewandte Chemie International Edition*, 50(44):10327–10329.

Liu, H., Radford, M. N., tao Yang, C., Chen, W., and Xian, M. (2018). Inorganic hydrogen polysulfides: chemistry, chemical biology and detection. *British Journal of Pharmacology*, 176(4):616–627.

Liu, P. W., Blair, N. T., and Bean, B. P. (2017). Action potential broadening in capsaicin-sensitive drg neurons from frequency-dependent reduction of kv3 current. *J Neurosci*, 37(40):9705–9714.

Llinas, R. R. (1988). The intrinsic electrophysiological properties of mammalian neurons: insights into central nervous system function. *Science*, 242(4886):1654–64.

Long, S. B., Campbell, E. B., and Mackinnon, R. (2005a). Crystal structure of a mammalian voltage-dependent shaker family k+ channel. *Science*, 309(5736):897–903.

Long, S. B., Campbell, E. B., and Mackinnon, R. (2005b). Voltage sensor of kv1.2: structural basis of electromechanical coupling. *Science*, 309(5736):903–8.

Lopez-Barneo, J., Ortega-Saenz, P., Pardal, R., Pascual, A., and Piruat, J. I. (2008). Carotid body oxygen sensing. *European Respiratory Journal*, 32(5):1386–1398.

Lu, M., Hu, L.-F., Hu, G., and Bian, J.-S. (2008). Hydrogen sulfide protects astrocytes against h2o2-induced neural injury via enhancing glutamate uptake. *Free Radical Biology and Medicine*, 45(12):1705–1713.

Maffie, J. and Rudy, B. (2008). Weighing the evidence for a ternary protein complex mediating a-type k+ currents in neurons. *J Physiol*, 586(23):5609–23.

Makarenko, V. V., Nanduri, J., Raghuraman, G., Fox, A. P., Gadalla, M. M., Kumar, G. K., Snyder, S. H., and Prabhakar, N. R. (2012). Endogenous h2s is required for hypoxic sensing by carotid body glomus cells. *American Journal of Physiology-Cell Physiology*, 303(9):C916–C923.

Marino, S. M. and Gladyshev, V. N. (2011). Analysis and functional prediction of reactive cysteine residues. *Journal of Biological Chemistry*, 287(7):4419–4425.

Matsui, T., Sugiyama, R., Sakanashi, K., Tamura, Y., Iida, M., Nambu, Y., Higuchi, T., Suematsu, M., and Ikeda-Saito, M. (2018). Hydrogen sulfide bypasses the rate-limiting oxygen activation of heme oxygenase. *J Biol Chem*, 293(43):16931–16939.

Matsuyoshi, H., Takimoto, K., Yunoki, T., Erickson, V. L., Tyagi, P., Hirao, Y., Wanaka, A., and Yoshimura, N. (2012). Distinct cellular distributions of kv4 pore-forming and auxiliary subunits in rat dorsal root ganglion neurons. *Life Sciences*, 91(7-8):258–263.

McCook, O., Radermacher, P., Volani, C., Asfar, P., Ignatius, A., Kemmler, J., Moller, P., Szabo, C., Whiteman, M., Wood, M. E., Wang, R., Georgieff, M., and Wachter, U. (2014). H2s during circulatory shock: some unresolved questions. *Nitric Oxide*, 41:48–61.

McCormack, K., McCormack, T., Tanouye, M., Rudy, B., and Stühmer, W. (1995). Alternative splicing of the human shaker k+ channel β1 gene and functional expression of the β2 gene product. *FEBS Letters*, 370(1-2):32–36.

McCormack, T. and McCormack, K. (1994). Shaker k+ channel beta subunits belong to an nad(p)h-dependent oxidoreductase superfamily. *Cell*, 79(7):1133–5.

McIntosh, P., Southan, A. P., Akhtar, S., Sidera, C., Ushkaryov, Y., Dolly, J. O., and Robertson, B. (1997). Modification of rat brain kv1.4 channel gating by association with accessory kvbeta1.1 and beta2.1 subunits. *Pflugers Arch*, 435(1):43–54.

Meyer, R. and Heinemann, S. H. (1997). Temperature and pressure dependence of shaker k+ channel n- and c-type inactivation. *European Biophysics Journal*, 26(6):433–445.

Miranda, K. M. and Wink, D. A. (2014). Persulfides and the cellular thiol landscape. *Proc Natl Acad Sci U S A*, 111(21):7505–6.

Mishanina, T. V., Libiad, M., and Banerjee, R. (2015). Biogenesis of reactive sulfur species for signaling by hydrogen sulfide oxidation pathways. *Nat Chem Biol*, 11(7):457–64.

Miyamoto, R., Koike, S., Takano, Y., Shibuya, N., Kimura, Y., Hanaoka, K., Urano, Y., Ogasawara, Y., and Kimura, H. (2017). Polysulfides (h2sn) produced from the interaction of hydrogen sulfide (h2s) and nitric oxide (NO) activate TRPA1 channels. *Scientific Reports*, 7(1).

Monaghan, M. M., Trimmer, J. S., and Rhodes, K. J. (2001). Experimental localization of kv1 family voltage-gated k+ channel alpha and beta subunits in rat hippocampal formation. *J Neurosci*, 21(16):5973–83.

Morales, M. J., Castellino, R. C., Crews, A. L., Rasmusson, R. L., and Strauss, H. C. (1995). A novel beta subunit increases rate of inactivation of specific voltage-gated potassium channel alpha subunits. *J Biol Chem*, 270(11):6272–7.

Muqeem, T., Ghosh, B., Pinto, V., Lepore, A. C., and Covarrubias, M. (2018). Regulation of nociceptive glutamatergic signaling by presynaptic kv3.4 channels in the rat spinal dorsal horn. *J Neurosci*, 38(15):3729–3740.

Mustafa, A. K., Gadalla, M. M., Sen, N., Kim, S., Mu, W., Gazi, S. K., Barrow, R. K., Yang, G., Wang, R., and Snyder, S. H. (2009). H2s signals through protein s-sulfhydration. *Sci Signal*, 2(96):ra72.

Mustafa, A. K., Sikka, G., Gazi, S. K., Steppan, J., Jung, S. M., Bhunia, A. K., Barodka, V. M., Gazi, F. K., Barrow, R. K., Wang, R., Amzel, L. M., Berkowitz, D. E., and Snyder, S. H. (2011). Hydrogen sulfide as endothelium-derived hyperpolarizing factor sulfhydrates potassium channels. *Circ Res*, 109(11):1259–68.

Nadin, B. M. and Pfaffinger, P. J. (2010). Dipeptidyl peptidase-like protein 6 is required for normal electrophysiological properties of cerebellar granule cells. *J Neurosci*, 30(25):8551–65.

Nagaya, N. and Papazian, D. M. (1997). Potassium channel alpha and beta subunits assemble in the endoplasmic reticulum. *J Biol Chem*, 272(5):3022–7.

Nagy, P. and Winterbourn, C. C. (2010). Rapid reaction of hydrogen sulfide with the neutrophil oxidant hypochlorous acid to generate polysulfides. *Chem Res Toxicol*, 23(10):1541–3.

Need, A. C., Irvine, E. E., and Giese, K. P. (2003). Learning and memory impairments in kvbeta1.1-null mutants are rescued by environmental enrichment or ageing. *European Journal of Neuroscience*, 18(6):1640–1644.

Neher, E. (1971). Two fast transient current components during voltage clamp on snail neurons. *J Gen Physiol*, 58(1):36–53.

Neher, E. (1992). [6] correction for liquid junction potentials in patch clamp experiments. In *Methods in Enzymology*, volume 207, pages 123–131. Academic Press.

Neher, E. and Sakmann, B. (1976). Single-channel currents recorded from membrane of denervated frog muscle fibres. *Nature*, 260(5554):799–802.

Nerbonne, J. M. (2000). Molecular basis of functional voltage-gated k+ channel diversity in the mammalian myocardium. *J Physiol*, 525 Pt 2:285–98.

Nielsen, N. H., Winkel, B. G., Kanters, J. K., Schmitt, N., Hofman-Bang, J., Jensen, H. S., Bentzen, B. H., Sigurd, B., Larsen, L. A., Andersen, P. S., Haunso, S., Kjeldsen, K., Grunnet, M., Christiansen, M., and Olesen, S. P. (2007). Mutations in the kv1.5 channel gene kcna5 in cardiac arrest patients. *Biochem Biophys Res Commun*, 354(3):776–82.

Nilius, B., Appendino, G., and Owsianik, G. (2012). The transient receptor potential channel trpa1: from gene to pathophysiology. *Pflugers Arch*, 464(5):425–58.

Ogawa, H., Takahashi, K., Miura, S., Imagawa, T., Saito, S., Tominaga, M., and Ohta, T. (2012). H(2)s functions as a nociceptive messenger through transient receptor potential ankyrin 1 (trpa1) activation. *Neuroscience*, 218:335–43.

Oliver, D., Lien, C. C., Soom, M., Baukrowitz, T., Jonas, P., and Fakler, B. (2004). Functional conversion between a-type and delayed rectifier k+ channels by membrane lipids. *Science*, 304(5668):265–70.

Olson, K. R., Gao, Y., Arif, F., Arora, K., Patel, S., DeLeon, E. R., Sutton, T. R., Feelisch, M., Cortese-Krott, M. M., and Straub, K. D. (2018). Metabolism of hydrogen sulfide (h 2 s) and production of reactive sulfur species (RSS) by superoxide dismutase. *Redox Biology*, 15:74–85.

Olson, T. M., Alekseev, A. E., Liu, X. K., Park, S., Zingman, L. V., Bienengraeber, M., Sattiraju, S., Ballew, J. D., Jahangir, A., and Terzic, A. (2006). Kv1.5 channelopathy due to kcna5 loss-of-function mutation causes human atrial fibrillation. *Hum Mol Genet*, 15(14):2185–91.

Ono, K., Akaike, T., Sawa, T., Kumagai, Y., Wink, D. A., Tantillo, D. J., Hobbs, A. J., Nagy, P., Xian, M., Lin, J., and Fukuto, J. M. (2014). Redox chemistry and chemical biology of h2s, hydropersulfides, and derived species: Implications of their possible biological activity and utility. *Free Radical Biology and Medicine*, 77:82–94.

Ovsepian, S. V., LeBerre, M., Steuber, V., O'Leary, V. B., Leibold, C., and Oliver Dolly, J. (2016). Distinctive role of kv1.1 subunit in the biology and functions of low threshold k(+) channels with implications for neurological disease. *Pharmacol Ther*, 159:93–101.

Padanilam, B. J., Lu, T., Hoshi, T., Padanilam, B. A., Shibata, E. F., and Lee, H. C. (2002). Molecular determinants of intracellular ph modulation of human kv1.4 n-type inactivation. *Mol Pharmacol*, 62(1):127–34.

Pan, Y., Levin, E. J., Quick, M., and Zhou, M. (2012). Potentiation of the kv1 family k(+) channel by cortisone analogues. *ACS Chem Biol*, 7(10):1641–6.

Pan, Y., Weng, J., Cao, Y., Bhosle, R. C., and Zhou, M. (2008a). Functional coupling between the kv1.1 channel and aldoketoreductase kvβ1. *Journal of Biological Chemistry*, 283(13):8634–8642.

Pan, Y., Weng, J., Kabaleeswaran, V., Li, H., Cao, Y., Bhosle, R. C., and Zhou, M. (2008b). Cortisone dissociates the shaker family k+ channels from their β subunits. *Nature Chemical Biology*, 4:708.

Pan, Y., Weng, J., Levin, E. J., and Zhou, M. (2011). Oxidation of nadph on kvbeta1 inhibits ball-and-chain type inactivation by restraining the chain. *Proc Natl Acad Sci U S A*, 108(14):5885–90.

Papazian, D. M., Schwarz, T. L., Tempel, B. L., Jan, Y. N., and Jan, L. Y. (1987). Cloning of genomic and complementary dna from shaker, a putative potassium channel gene from drosophila. *Science*, 237(4816):749–53.

Parcej, D. N. and Eckhardt-Strelau, L. (2003). Structural characterisation of neuronal voltage-sensitive k+ channels heterologously expressed in pichia pastoris. *J Mol Biol*, 333(1):103–16.

Parcej, D. N., Scott, V. E., and Dolly, J. O. (1992). Oligomeric properties of alpha-dendrotoxin-sensitive potassium ion channels purified from bovine brain. *Biochemistry*, 31(45):11084–8.

Paul, B. D., Sbodio, J. I., Xu, R., Vandiver, M. S., Cha, J. Y., Snowman, A. M., and Snyder, S. H. (2014). Cystathionine gamma-lyase deficiency mediates neurodegeneration in huntington's disease. *Nature*, 509(7498):96–100.

Paul, B. D. and Snyder, S. H. (2012). H2s signalling through protein sulfhydration and beyond. *Nat Rev Mol Cell Biol*, 13(8):499–507.

Paulsen, C. E. and Carroll, K. S. (2013). Cysteine-mediated redox signaling: Chemistry, biology, and tools for discovery. *Chemical Reviews*, 113(7):4633–4679.

Pearce, R. J. and Duchen, M. R. (1994). Differential expression of membrane currents in dissociated mouse primary sensory neurons. *Neuroscience*, 63(4):1041–56.

Peers, C., Bauer, C. C., Boyle, J. P., Scragg, J. L., and Dallas, M. L. (2012). Modulation of ion channels by hydrogen sulfide. *Antioxid Redox Signal*, 17(1):95–105.

Peng, H., Cheng, Y., Dai, C., King, A. L., Predmore, B. L., Lefer, D. J., and Wang, B. (2011). A fluorescent probe for fast and quantitative detection of hydrogen sulfide in blood. *Angewandte Chemie International Edition*, 50(41):9672–9675.

Peng, Y.-J., Makarenko, V. V., Nanduri, J., Vasavda, C., Raghuraman, G., Yuan, G., Gadalla, M. M., Kumar, G. K., Snyder, S. H., and Prabhakar, N. R. (2014). Inherent variations in CO-h2s-mediated carotid body o2 sensing mediate hypertension and pulmonary edema. *Proceedings of the National Academy of Sciences*, 111(3):1174–1179.

Peng, Y.-J., Nanduri, J., Raghuraman, G., Souvannakitti, D., Gadalla, M. M., Kumar, G. K., Snyder, S. H., and Prabhakar, N. R. (2010). H2s mediates o2 sensing in the carotid body. *Proceedings of the National Academy of Sciences*, 107(23):10719–10724.

Phuket, T. R. N. (2009). Kv4 channels underlie the subthreshold-operating a-type k+-current in nociceptive dorsal root ganglion neurons. *Frontiers in Molecular Neuroscience*, 2.

Pietri, R., Roman-Morales, E., and Lopez-Garriga, J. (2011). Hydrogen sulfide and hemeproteins: knowledge and mysteries. *Antioxid Redox Signal*, 15(2):393–404.

Pioletti, M., Findeisen, F., Hura, G. L., and Minor, D. L., J. (2006). Three-dimensional structure of the kchip1-kv4.3 t1 complex reveals a cross-shaped octamer. *Nat Struct Mol Biol*, 13(11):987–95.

Pongs, O. (1992). Molecular biology of voltage-dependent potassium channels. *Physiol Rev*, 72(4 Suppl):S69–88.

Pongs, O. and Schwarz, J. R. (2010). Ancillary subunits associated with voltage-dependent k+ channels. *Physiol Rev*, 90(2):755–96.

Predmore, B. L. and Lefer, D. J. (2010). Development of hydrogen sulfide-based therapeutics for cardiovascular disease. *J Cardiovasc Transl Res*, 3(5):487–98.

Pérez-García, M. T., López-López, J. R., and González, C. (1999). Kvβ1.2 subunit coexpression in hek293 cells confers o(2)sensitivity to kv4.2 but not to shaker channels. *The Journal of General Physiology*, 113(6):897–907.

Qian, A. H., Liu, X. Q., Yao, W. Y., Wang, H. Y., Sun, J., Zhou, L., and Yuan, Y. Z. (2009). Voltage-gated potassium channels in ib4-positive colonic sensory neurons mediate visceral hypersensitivity in the rat. *Am J Gastroenterol*, 104(8):2014–27.

Ranjan, R., Logette, E., Marani, M., Herzog, M., Tâche, V., Scantamburlo, E., Buchillier, V., and Markram, H. (2019). A kinetic map of the homomeric voltage-gated potassium channel (kv) family. *Frontiers in Cellular Neuroscience*, 13.

Rasband, M. N., Park, E. W., Vanderah, T. W., Lai, J., Porreca, F., and Trimmer, J. S. (2001). Distinct potassium channels on pain-sensing neurons. *Proc Natl Acad Sci U S A*, 98(23):13373–8.

Rasmusson, R. L., Wang, S., Castellino, R. C., Morales, M. J., and Strauss, H. C. (1997). The beta subunit, kv beta 1.2, acts as a rapid open channel blocker of nh2-terminal deleted kv1.4 alpha-subunits. *Adv Exp Med Biol*, 430:29–37.

Reddie, K. G. and Carroll, K. S. (2008). Expanding the functional diversity of proteins through cysteine oxidation. *Current Opinion in Chemical Biology*, 12(6):746–754.

Rettig, J., Heinemann, S. H., Wunder, F., Lorra, C., Parcej, D. N., Dolly, J. O., and Pongs, O. (1994). Inactivation properties of voltage-gated k+ channels altered by presence of beta-subunit. *Nature*, 369(6478):289–94.

Rhodes, K. J., Monaghan, M. M., Barrezueta, N. X., Nawoschik, S., Bekele-Arcuri, Z., Matos, M. F., Nakahira, K., Schechter, L. E., and Trimmer, J. S. (1996). Voltage-gated k+ channel beta subunits: Expression and distribution of kvbeta1 and kvbeta2 in adult rat brain. *The Journal of Neuroscience*, 16(16):4846–4860.

Rhodes, K. J., Strassle, B. W., Monaghan, M. M., Bekele-Arcuri, Z., Matos, M. F., and Trimmer, J. S. (1997). Association and colocalization of the kvbeta1 and kvbeta2 beta-subunits with kv1 alpha-subunits in mammalian brain k+ channel complexes. *J Neurosci*, 17(21):8246–58.

Ritter, D. M., Ho, C., O'Leary, M. E., and Covarrubias, M. (2012). Modulation of kv3.4 channel n-type inactivation by protein kinase c shapes the action potential in dorsal root ganglion neurons. *J Physiol*, 590(1):145–61.

Ritter, D. M., Zemel, B. M., Hala, T. J., O'Leary, M. E., Lepore, A. C., and Covarrubias, M. (2015a). Dysregulation of kv3.4 channels in dorsal root ganglia following spinal cord injury. *J Neurosci*, 35(3):1260–73.

Ritter, D. M., Zemel, B. M., Lepore, A. C., and Covarrubias, M. (2015b). Kv3.4 channel function and dysfunction in nociceptors. *Channels (Austin)*, 9(4):209–17.

Roeper, J., Lorra, C., and Pongs, O. (1997). Frequency-dependent inactivation of mammalian a-type k+ channel kv1.4 regulated by ca2+/calmodulin-dependent protein kinase. *J Neurosci*, 17(10):3379–91.

Rudy, B. (1988). Diversity and ubiquity of k channels. *Neuroscience*, 25(3):729–49.

Ruppersberg, J. P., Frank, R., Pongs, O., and Stocker, M. (1991a). Cloned neuronal ik(a) channels reopen during recovery from inactivation. *Nature*, 353(6345):657–60.

Ruppersberg, J. P., Stocker, M., Pongs, O., Heinemann, S. H., Frank, R., and Koenen, M. (1991b). Regulation of fast inactivation of cloned mammalian ik(a) channels by cysteine oxidation. *Nature*, 352(6337):711–4.

Sahoo, N., Goradia, N., Ohlenschlager, O., Schonherr, R., Friedrich, M., Plass, W., Kappl, R., Hoshi, T., and Heinemann, S. H. (2013). Heme impairs the ball-and-chain inactivation of potassium channels. *Proc Natl Acad Sci U S A*, 110(42):E4036–44.

Sahoo, N., Hoshi, T., and Heinemann, S. H. (2014). Oxidative modulation of voltage-gated potassium channels. *Antioxid Redox Signal*, 21(6):933–52.

Sakmann, B. and Neher, E. (1984). Patch clamp techniques for studying ionic channels in excitable membranes. *Annual Review of Physiology*, 46(1):455–472.

Salzer, I., Ray, S., Schicker, K., and Boehm, S. (2019). Nociceptor signalling through ion channel regulation via GPCRs. *International Journal of Molecular Sciences*, 20(10):2488.

Santacruz-Toloza, L., Huang, Y., John, S. A., and Papazian, D. M. (1994). Glycosylation of shaker potassium channel protein in insect cell culture and in xenopus oocytes. *Biochemistry*, 33(18):5607–13.

Sbodio, J. I., Snyder, S. H., and Paul, B. D. (2016). Transcriptional control of amino acid homeostasis is disrupted in huntington's disease. *Proc Natl Acad Sci U S A*, 113(31):8843–8.

Schreurs, B. G., Gusev, P. A., Tomsic, D., Alkon, D. L., and Shi, T. (1998). Intracellular correlates of acquisition and long-term memory of classical conditioning in purkinje cell dendrites in slices of rabbit cerebellar lobule HVI. *The Journal of Neuroscience*, 18(14):5498–5507.

Schulteis, C. T., Nagaya, N., and Papazian, D. M. (1996). Intersubunit interaction between amino- and carboxyl-terminal cysteine residues in tetrameric shaker k+ channels. *Biochemistry*, 35(37):12133–40.

Scott, V. E., Parcej, D. N., Keen, J. N., Findlay, J. B., and Dolly, J. O. (1990). Alpha-dendrotoxin acceptor from bovine brain is a k+ channel protein. evidence from the n-terminal sequence of its larger subunit. *Journal of Biological Chemistry*, 265(33):20094–20097.

Scott, V. E., Rettig, J., Parcej, D. N., Keen, J. N., Findlay, J. B., Pongs, O., and Dolly, J. O. (1994). Primary structure of a beta subunit of alpha-dendrotoxin-sensitive k+ channels from bovine brain. *Proc Natl Acad Sci U S A*, 91(5):1637–41.

Sculptoreanu, A., Yoshimura, N., and de Groat, W. C. (2004). KW-7158 [(2s)-(+)-3,3,3-trifluoro-2-hydroxy-2-methyl-n-(5,5,10-trioxo-4,10-dihydrothieno[3,2-c][1]benzothiepin-9-yl)propanamide] enhances a-type k(+) currents in neurons of the dorsal root ganglion of the adult rat. *Journal of Pharmacology and Experimental Therapeutics*, 310(1):159–168.

Sewing, S., Roeper, J., and Pongs, O. (1996). Kv beta 1 subunit binding specific for shaker-related potassium channel alpha subunits. *Neuron*, 16(2):455–63.

Shah, M. M., Hammond, R. S., and Hoffman, D. A. (2010). Dendritic ion channel trafficking and plasticity. *Trends Neurosci*, 33(7):307–16.

Shen, N. V., Chen, X., Boyer, M. M., and Pfaffinger, P. J. (1993). Deletion analysis of k+ channel assembly. *Neuron*, 11(1):67–76.

Shen, X., Peter, E. A., Bir, S., Wang, R., and Kevil, C. G. (2012). Analytical measurement of discrete hydrogen sulfide pools in biological specimens. *Free Radic Biol Med*, 52(11-12):2276–83.

Shen, Y., Shen, Z., Luo, S., Guo, W., and Zhu, Y. Z. (2015). The cardioprotective effects of hydrogen sulfide in heart diseases: From molecular mechanisms to therapeutic potential. *Oxid Med Cell Longev*, 2015:925167.

Shi, G., Nakahira, K., Hammond, S., Rhodes, K. J., Schechter, L. E., and Trimmer, J. S. (1996). β subunits promote k+ channel surface expression through effects early in biosynthesis. *Neuron*, 16(4):843–852.

Shieh, C. C., Coghlan, M., Sullivan, J. P., and Gopalakrishnan, M. (2000). Potassium channels: molecular defects, diseases, and therapeutic opportunities. *Pharmacol Rev*, 52(4):557–94.

Shin, T. M., Smith, R. D., Toro, L., and Goldin, A. L. (1998). [29] high-level expression and detection of ion channels in xenopus oocytes. In *Methods in Enzymology*, pages 529–556. Elsevier.

Sokolova, O., Accardi, A., Gutierrez, D., Lau, A., Rigney, M., and Grigorieff, N. (2003). Conformational changes in the c terminus of shaker k+ channel bound to the rat kvbeta2-subunit. *Proc Natl Acad Sci U S A*, 100(22):12607–12.

Spassov, S. G., Donus, R., Ihle, P. M., Engelstaedter, H., Hoetzel, A., and Faller, S. (2017). Hydrogen sulfide prevents formation of reactive oxygen species through pi3k/akt signaling and limits ventilator-induced lung injury. *Oxid Med Cell Longev*, 2017:3715037.

Stephens, G. J., Owen, D. G., Opalko, A., Pisano, M. R., MacGregor, W. H., and Robertson, B. (1996a). Studies on the blocking action of human kv3.4 inactivation peptide variants in the mouse cloned kv1.1 k+ channel. *J Physiol*, 496 (Pt 1):145–54.

Stephens, G. J., Owen, D. G., and Robertson, B. (1996b). Cysteine-modifying reagents alter the gating of the rat cloned potassium channel kv1.4. *Pflugers Arch*, 431(3):435–42.

Stephens, G. J. and Robertson, B. (1995). Inactivation of the cloned potassium channel mouse kv1.1 by the human kv3.4 'ball' peptide and its chemical modification. *J Physiol*, 484 (Pt 1)(1):1–13.

Stewart, T., Beyak, M. J., and Vanner, S. (2003). Ileitis modulates potassium and sodium currents in guinea pig dorsal root ganglia sensory neurons. *The Journal of Physiology*, 552(3):797–807.

Streng, T., Axelsson, H. E., Hedlund, P., Andersson, D. A., Jordt, S. E., Bevan, S., Andersson, K. E., Hogestatt, E. D., and Zygmunt, P. M. (2008). Distribution and function of the hydrogen sulfide-sensitive trpa1 ion channel in rat urinary bladder. *Eur Urol*, 53(2):391–9.

Suh, B.-C. and Hille, B. (2008). PIP2is a necessary cofactor for ion channel function:howand why? *Annual Review of Biophysics*, 37(1):175–195.

Sun, W. H., Liu, F., Chen, Y., and Zhu, Y. C. (2012). Hydrogen sulfide decreases the levels of ros by inhibiting mitochondrial complex iv and increasing sod activities in cardiomyocytes under ischemia/reperfusion. *Biochem Biophys Res Commun*, 421(2):164–9.

Suo, R., Zhao, Z. Z., Tang, Z. H., Ren, Z., Liu, X., Liu, L. S., Wang, Z., Tang, C. K., Wei, D. H., and Jiang, Z. S. (2013). Hydrogen sulfide prevents h(2)o(2)-induced senescence in human umbilical vein endothelial cells through sirt1 activation. *Mol Med Rep*, 7(6):1865–70.

Swain, S. M., Sahoo, N., Dennhardt, S., Schonherr, R., and Heinemann, S. H. (2015). Ca(2+)/calmodulin regulates kvbeta1.1-mediated inactivation of voltage-gated k(+) channels. *Sci Rep*, 5:15509.

Szabó, C. (2007). Hydrogen sulphide and its therapeutic potential. *Nature Reviews Drug Discovery*, 6(11):917–935.

Szabo, C. and Papapetropoulos, A. (2011). Hydrogen sulphide and angiogenesis: mechanisms and applications. *Br J Pharmacol*, 164(3):853–65.

Szabo, I., Zoratti, M., and Gulbins, E. (2010). Contribution of voltage-gated potassium channels to the regulation of apoptosis. *FEBS Lett*, 584(10):2049–56.

Takeda, M., Tanimoto, T., Ikeda, M., Nasu, M., Kadoi, J., Yoshida, S., and Matsumoto, S. (2006). Enhanced excitability of rat trigeminal root ganglion neurons via decrease in a-type potassium currents following temporomandibular joint inflammation. *Neuroscience*, 138(2):621–630.

Takimoto, K., Yang, E. K., and Conforti, L. (2002). Palmitoylation of kchip splicing variants is required for efficient cell surface expression of kv4.3 channels. *J Biol Chem*, 277(30):26904–11.

Tang, G., Wu, L., and Wang, R. (2010). Interaction of hydrogen sulfide with ion channels. *Clin Exp Pharmacol Physiol*, 37(7):753–63.

Tang, X. D., Xu, R., Reynolds, M. F., Garcia, M. L., Heinemann, S. H., and Hoshi, T. (2003). Haem can bind to and inhibit mammalian calcium-dependent slo1 bk channels. *Nature*, 425(6957):531–5.

Tao, B.-B., Liu, S.-Y., Zhang, C.-C., Fu, W., Cai, W.-J., Wang, Y., Shen, Q., Wang, M.-J., Chen, Y., Zhang, L.-J., Zhu, Y.-Z., and Zhu, Y.-C. (2013). VEGFR2 functions as an h2s-targeting receptor protein kinase with its novel cys1045–cys1024 disulfide bond serving as a specific molecular switch for hydrogen sulfide actions in vascular endothelial cells. *Antioxidants & Redox Signaling*, 19(5):448–464.

Tapper, A. R. and George, A. L. (2003). Heterologous expression of ion channels. In *Neurogenetics*, pages 285–294. Humana Press.

Thomas, P. and Smart, T. G. (2005). Hek293 cell line: A vehicle for the expression of recombinant proteins. *Journal of Pharmacological and Toxicological Methods*, 51(3):187–200.

Thompson, S. H. (1977). Three pharmacologically distinct potassium channels in molluscan neurones. *J Physiol*, 265(2):465–88.

Tierney, A. J. and Harris-Warrick, R. M. (1992). Physiological role of the transient potassium current in the pyloric circuit of the lobster stomatogastric ganglion. *J Neurophysiol*, 67(3):599–609.

Tipparaju, S. M., Barski, O. A., Srivastava, S., and Bhatnagar, A. (2008). Catalytic mechanism and substrate specificity of the beta-subunit of the voltage-gated potassium channel. *Biochemistry*, 47(34):8840–54.

Toohey, J. I. (2011). Sulfur signaling: is the agent sulfide or sulfane? *Anal Biochem*, 413(1):1–7.

Trimmer, J. S. and Rhodes, K. J. (2004). Localization of voltage-gated ion channels in mammalian brain. *Annu Rev Physiol*, 66:477–519.

Tsiftsoglou, A. S., Tsamadou, A. I., and Papadopoulou, L. C. (2006). Heme as key regulator of major mammalian cellular functions: molecular, cellular, and pharmacological aspects. *Pharmacol Ther*, 111(2):327–45.

Vacher, H., Mohapatra, D. P., and Trimmer, J. S. (2008). Localization and targeting of voltage-dependent ion channels in mammalian central neurons. *Physiol Rev*, 88(4):1407–47.

van der Wijst, J., Konrad, M., Verkaart, S. A. J., Tkaczyk, M., Latta, F., Altmuller, J., Thiele, H., Beck, B., Schlingmann, K. P., and de Baaij, J. H. F. (2018). A de novo kcna1 mutation in a patient with tetany and hypomagnesemia. *Nephron*, 139(4):359–366.

Vandini, E., Ottani, A., Zaffe, D., Calevro, A., Canalini, F., Cavallini, G. M., Rossi, R., Guarini, S., and Giuliani, D. (2018). Mechanisms of hydrogen sulfide against the progression of severe alzheimer's disease in transgenic mice at different ages. *Pharmacology*, 103(1-2):50–60.

Wallace, J. L. and Wang, R. (2015). Hydrogen sulfide-based therapeutics: exploiting a unique but ubiquitous gasotransmitter. *Nat Rev Drug Discov*, 14(5):329–45.

Wang, H., Yan, Y., Liu, Q., Huang, Y., Shen, Y., Chen, L., Chen, Y., Yang, Q., Hao, Q., Wang, K., and Chai, J. (2007). Structural basis for modulation of kv4 k+ channels by auxiliary kchip subunits. *Nat Neurosci*, 10(1):32–9.

Wang, R. (2002). Two's company, three's a crowd: can h2s be the third endogenous gaseous transmitter? *FASEB J*, 16(13):1792–8.

Wang, R. (2003). The gasotransmitter role of hydrogen sulfide. *Antioxid Redox Signal*, 5(4):493–501.

Wang, R. (2012). Physiological implications of hydrogen sulfide: a whiff exploration that blossomed. *Physiol Rev*, 92(2):791–896.

Wang, R. (2014). Gasotransmitters: growing pains and joys. *Trends Biochem Sci*, 39(5):227–32.

Wang, S., Publicover, S., and Gu, Y. (2009). An oxygen-sensitive mechanism in regulation of epithelial sodium channel. *Proc Natl Acad Sci U S A*, 106(8):2957–62.

Wang, Z., Fermini, B., and Nattel, S. (1993). Sustained depolarization-induced outward current in human atrial myocytes. evidence for a novel delayed rectifier k+ current similar to kv1.5 cloned channel currents. *Circ Res*, 73(6):1061–76.

Wells, J. A. and McClendon, C. L. (2007). Reaching for high-hanging fruit in drug discovery at protein-protein interfaces. *Nature*, 450(7172):1001–9.

Weng, J., Cao, Y., Moss, N., and Zhou, M. (2006). Modulation of voltage-dependent shaker family potassium channels by an aldo-keto reductase. *J Biol Chem*, 281(22):15194–200.

Wettwer, E., Hala, O., Christ, T., Heubach, J. F., Dobrev, D., Knaut, M., Varro, A., and Ravens, U. (2004). Role of ikur in controlling action potential shape and contractility in the human atrium: influence of chronic atrial fibrillation. *Circulation*, 110(16):2299–306.

Wilkinson, W. J. and Kemp, P. J. (2011). Carbon monoxide: an emerging regulator of ion channels. *J Physiol*, 589(Pt 13):3055–62.

Willis, M., Leitner, I., Seppi, K., Trieb, M., Wietzorrek, G., Marksteiner, J., and Knaus, H. G. (2018). Shaker-related voltage-gated potassium channels kv1 in human hippocampus. *Brain Struct Funct*, 223(6):2663–2671.

Winkelman, D. L. B. (2005). Inhibition of the a-type k+ channels of dorsal root ganglion neurons by the long-duration anesthetic butamben. *Journal of Pharmacology and Experimental Therapeutics*, 314(3):1177–1186.

Wulff, H., Castle, N. A., and Pardo, L. A. (2009). Voltage-gated potassium channels as therapeutic targets. *Nat Rev Drug Discov*, 8(12):982–1001.

Xu, G.-Y., Winston, J. H., Shenoy, M., Yin, H., and Pasricha, P. J. (2006). Enhanced excitability and suppression of a-type k+ current of pancreas-specific afferent neurons in a rat model of chronic pancreatitis. *American Journal of Physiology-Gastrointestinal and Liver Physiology*, 291(3):G424–G431.

Xuan, A., Long, D., Li, J., Ji, W., Zhang, M., Hong, L., and Liu, J. (2012a). Hydrogen sulfide attenuates spatial memory impairment and hippocampal neuroinflammation in beta-amyloid rat model of alzheimer's disease. *J Neuroinflammation*, 9(1):202.

Xuan, A., Long, D., Li, J., Ji, W., Zhang, M., Hong, L., and Liu, J. (2012b). Hydrogen sulfide attenuates spatial memory impairment and hippocampal neuroinflammation in beta-amyloid rat model of alzheimer's disease. *Journal of Neuroinflammation*, 9(1).

Xuan, W., Sheng, C., Cao, Y., He, W., and Wang, W. (2012c). Fluorescent probes for the detection of hydrogen sulfide in biological systems. *Angewandte Chemie International Edition*, 51(10):2282–2284.

Yang, C., Chen, L., Xu, S., Day, J. J., Li, X., and Xian, M. (2017). Recent development of hydrogen sulfide releasing/stimulating reagents and their potential applications in cancer and glycometabolic disorders. *Frontiers in Pharmacology*, 8.

Yang, E. K., Takimoto, K., Hayashi, Y., de Groat, W. C., and Yoshimura, N. (2004). Altered expression of potassium channel subunit mrna and alpha-dendrotoxin sensitivity of potassium currents in rat dorsal root ganglion neurons after axotomy. *Neuroscience*, 123(4):867–74.

Yang, F., Gao, H., Li, S.-S., An, R.-B., Sun, X.-Y., Kang, B., Xu, J.-J., and Chen, H.-Y. (2018). A fluorescent tau-probe: quantitative imaging of ultra-trace endogenous hydrogen polysulfide in cells and in vivo. *Chemical Science*, 9(25):5556–5563.

Yang, G., Wu, L., Jiang, B., Yang, W., Qi, J., Cao, K., Meng, Q., Mustafa, A. K., Mu, W., Zhang, S., Snyder, S. H., and Wang, R. (2008). H2s as a physiologic vasorelaxant: Hypertension in mice with deletion of cystathionine γ-lyase. *Science*, 322(5901):587–590.

Yang, K., Coburger, I., Langner, J. M., Peter, N., Hoshi, T., Schonherr, R., and Heinemann, S. H. (2019). Modulation of k(+) channel n-type inactivation by sulfhydration through hydrogen sulfide and polysulfides. *Pflugers Arch*, 471(4):557–571.

Yu, F. H. and Catterall, W. A. (2004). The vgl-chanome: a protein superfamily specialized for electrical signaling and ionic homeostasis. *Sci STKE*, 2004(253):re15.

Yuan, G., Vasavda, C., Peng, Y.-J., Makarenko, V. V., Raghuraman, G., Nanduri, J., Gadalla, M. M., Semenza, G. L., Kumar, G. K., Snyder, S. H., and Prabhakar, N. R. (2015). Protein kinase g-regulated production of h2s governs oxygen sensing. *Science Signaling*, 8(373):ra37–ra37.

Yunoki, T., Takimoto, K., Kita, K., Funahashi, Y., Takahashi, R., Matsuyoshi, H., Naito, S., and Yoshimura, N. (2014). Differential contribution of kv4-containing channels to a-type, voltage-gated potassium currents in somatic and visceral dorsal root ganglion neurons. *Journal of Neurophysiology*, 112(10):2492–2504.

Zemel, B. M., Muqeem, T., Brown, E. V., Goulao, M., Urban, M. W., Tymanskyj, S. R., Lepore, A. C., and Covarrubias, M. (2017). Calcineurin dysregulation underlies spinal cord injury-induced k(+) channel dysfunction in drg neurons. *J Neurosci*, 37(34):8256–8272.

Zemel, B. M., Ritter, D. M., Covarrubias, M., and Muqeem, T. (2018). A-type kv channels in dorsal root ganglion neurons: Diversity, function, and dysfunction. *Front Mol Neurosci*, 11:253.

Zhang, J., Chen, S., Liu, H., Zhang, B., Zhao, Y., Ma, K., Zhao, D., Wang, Q., Ma, H., and Zhang, Z. (2013). Hydrogen sulfide prevents hydrogen peroxide-induced activation of epithelial sodium channel through a pten/pi(3,4,5)p3 dependent pathway. *PLoS One*, 8(5):e64304.

Zhang, L., Li, S., Hong, M., Xu, Y., Wang, S., Liu, Y., Qian, Y., and Zhao, J. (2014). A colorimetric and ratiometric fluorescent probe for the imaging of endogenous hydrogen sulphide in living cells and sulphide determination in mouse hippocampus. *Org Biomol Chem*, 12(28):5115–25.

Zhang, Y., Cai, G., Ni, X., and Sun, J. (2007a). The role of ERK activation in the neuronal excitability in the chronically compressed dorsal root ganglia. *Neuroscience Letters*, 419(2):153–157.

Zhang, Y., Jiang, D., Li, H., Sun, Y., Jiang, X., Gong, S., Qian, Z., and Tao, J. (2019). Melanocortin type 4 receptor-mediated inhibition of a-type k(+) current enhances sensory neuronal excitability and mechanical pain sensitivity in rats. *J Biol Chem*, 294(14):5496–5507.

Zhang, Z., Huang, H., Liu, P., Tang, C., and Wang, J. (2007b). Hydrogen sulfide contributes to cardioprotection during ischemia-reperfusion injury by opening k atp channels. *Can J Physiol Pharmacol*, 85(12):1248–53.

Zhao, W., Zhang, J., Lu, Y., and Wang, R. (2001). The vasorelaxant effect of h2s as a novel endogenous gaseous katp channel opener. *EMBO J*, 20(21):6008–16.

Zhou, M., Morais-Cabral, J. H., Mann, S., and MacKinnon, R. (2001). Potassium channel receptor site for the inactivation gate and quaternary amine inhibitors. *Nature*, 411(6838):657–61.

Zhu, Y., Colak, T., Shenoy, M., Liu, L., Mehta, K., Pai, R., Zou, B., Xie, X. S., and Pasricha, P. J. (2012). Transforming growth factor beta induces sensory neuronal hy-

perexcitability, and contributes to pancreatic pain and hyperalgesia in rats with chronic pancreatitis. *Mol Pain*, 8:65.

Appendices

A Declaration

I hereby declare that:

I am aware of the doctoral regulations of the Faculty of Medicine of the Friedrich Schiller University of Jena.

I have researched and written the presented thesis myself, no passages of text have been taken from third parties without having been identified. All tools, personal notifications, and sources used by me have been indicated in the thesis.

My doctoral supervisor, Prof. Dr. Stefan H. Heinemann has supported me in selecting and analyzing the material, as well as in the preparation of the manuscript. Part of the presented thesis has already published in *Pflügers Archiv - European Journal of Physiology*.

The assistance of any doctoral consultant has not been utilized, and no third parties have either directly or indirectly received monetary benefits from me for the work related to the content of the thesis submitted.

I have not submitted the thesis as an examination paper for a state or other academic examination.

I have not submitted the same, a substantially similar or another thesis to another university as a dissertation.

Kefan Yang

B Ehrenwörtliche Erklärung

Hiermit erkläre ich, dass mir die Promotionsordnung der Medizinischen Fakultät der Friedrich-Schiller-Universität bekannt ist,

ich die Dissertation selbst angefertigt habe und alle von mir benutzten Hilfsmittel, persönlichen Mitteilungen und Quellen in meiner Arbeit angegeben sind,

mich folgende Personen bei der Auswahl und Auswertung des Materials sowie bei der Herstellung des Manuskripts unterstützt haben: Prof. Dr. Stefan H. Heinemann,

die Hilfe eines Promotionsberaters nicht in Anspruch genommen wurde und dass Dritte weder unmittelbar noch mittelbar geldwerte Leistungen von mir für Arbeiten erhalten haben, die im Zusammenhang mit dem Inhalt der vorgelegten Dissertation stehen,

dass ich die Dissertation noch nicht als Prüfungsarbeit für eine staatliche oder andere wissenschaftliche Prüfung eingereicht habe und

dass ich die gleiche, eine in wesentlichen Teilen ähnliche oder eine andere Abhandlung nicht bei einer anderen Hochschule als Dissertation eingereicht habe.

_____

Kefan Yang

C Acknowledgements

First and foremost, I would like to express the deepest appreciation to my doctoral supervisor, Prof. Dr. Stefan H. Heinemann. I am very grateful to him for giving me this opportunity to continue my doctoral thesis under his supervision. He has always been supportive of me, from the early stage of my research project until my thesis defense.

I am thankful to PD Dr. Roland Schönherr, Prof. Dr. Toshi Hoshi (University of Pennsylvania), Dr. Ina Coburger, Prof. Dr. Enrico Leipold, and Dr. Guido Gessner for their interest in my research works, valuable suggestions, and help in preparing this thesis and the manuscript for publication.

In addition, I would like to thank the funding support by grants of the German Research Foundation Research Training Groups 1715 and Joint Sino-German Research Project.

My sincere gratitude to Mrs. Dorith Schmidt, Dr. Franziska Jahn and Mrs. Elke Müller, for their unconditional help in accomplishing administrative and official work. Many thanks to Mrs. Angela Roßner, Mr. Holger Sack, and Mrs. Pia Stier for their technical and lab assistances.

Special thanks to our lunch group Philipp Rühl, Nicole Peter and Alisa Bernert, and Dr. Navin Kumar Ojha, Johanna Maria Langner and Nikita Kuldyushev, for their nice, valuable and lively discussions both scientific and non-scientific.

Finally, I would like to thank my father and mother for their support, love and affection. Last but never the least, I would like to thank my wife Wanqi, for her love, help and understanding throughout my Ph.D. thesis and giving me a cute son Alan.

Kefan Yang